# Durham E-Theses

*Hydrogen plasma reduction of supported metal salts*

Byrne, M.E.

**How to cite:**

Byrne, M.E. (1995) *Hydrogen plasma reduction of supported metal salts*, Durham theses, Durham University. Available at Durham E-Theses Online: http://etheses.dur.ac.uk/5155/

**Use policy**

# The Hydrogen Plasma Reduction

# of Supported Metal Salts

**Submitted By:**  *Ms. M.E. Byrne B.Sc. hons*
**University of Durham, England.**

# Hydrogen Plasma Reduction of Supported Metal Salts

## Submitted by Ms. M.E. Byrne B. Sc. hons

### Abstract

During the last thirty years, in the electronics industry, there has been increasing interest in the use of partially ionised plasmas for the processing of surfaces. A large amount of work has been carried out on plasma etching using halogen plasmas. However, halogen plasmas cause both environmental and handling problems and as a reuslt hydrogen plasmas are often used as a substitute.

Gold films are very important in the electronics industry. Several techniques have been proposed for the deposition of conducting gold films, including CVD, PVD, and Sol-gel techniques.

In the work outlined in this thesis, a hydrogen plasma was generated at 0.1 torr using an RF power supply, in order to modify the surfaces of gold (III) chloride films, spin coated onto either a glass or nylon substrate. It has been postulated that if hydrogen atoms will react with a material in a plasma to form a volatile compound (eg. HCl), then the surface will be modified. The aim of this work was to create a conducting gold film, by removal of chlorine species from the original spin coated film, through use of a hydrogen plasma.

The results of this work demonstrate that chlorine removal from the original film, by use of a hydrogen plasma, is a function of the concentration of the spin coated $AuCl_3$; the plasma treatment time; and the plasma power. The substrate onto which the $AuCl_3$ is deposited also appears to play an important role. The deposition method proposed in this thesis is a quick, cheap and easy way to deposit thin gold films.

*To the Celts*

# Hydrogen Plasma Reduction of Supported Metal Salts

# Contents

Submitted by Ms. M. E. Byrne B.Sc. hons

# 1. Plasmas

## 1.1 General Introduction

### 1.1.1 Types of Plasmas

### 1.1.2 Glow Discharge Plasmas

*1.1.2.1 Electron and Ion Temperatures*

*1.1.2.2 Plasma Potential*

*1.1.2.3 Floating Potential*

## 1.2 Types of Electric Field

### 1.2.1 DC Discharges

### 1.2.2 AC Discharges

### 1.2.3 RF Discharges

## 1.3 Surface Modification Using Partially Ionised Plasmas

## 1.4 Surface Modification Using Hydrogen Plasmas

### 1.4.1 Introduction

### 1.4.2 Reactions of Hydrogen

### 1.4.3 Hydrogen Plasmas

*1.4.3.1 Introduction*

*1.43.2 Applications Using Hydrogen Plasmas*

## 1.5 Conclusion

## 1.6 References

## 1.1 General Introduction:

A plasma is a partially ionised gas consisting of an equal number of positive and negative charges[1] (quasi neutral) and a different number of un-ionised gas atoms or molecules or any higher form of excitation as well as light quanta.[2]

It has been suggested[3] that 99% of the matter in the universe is in the plasma state. This estimate may not be very accurate, but it is certainly reasonable in view of the fact that stellar interiors and atmospheres, gaseous nebulae, and much of interstellar hydrogen are plasmas.

As one leaves the earth's atmosphere, one encounters the plasmas comprising the Van Allen radiation belts and the solar winds. On the other hand, one encounters a flash of lightning, the soft glow of the Aurora Borealis, the conducting gas inside a fluorescent or neon sign and the slight amount of ionisation in a rocket exhaust. It would seem that we live in the 1% of the universe where plasmas do not occur naturally.

The plasmas in nature[4] differ mainly in their electron concentrations $n_e$ and in their average electron energy $kT_e$. Figure 1.1 below depicts characteristic electron densities and electron energies of a number of plasmas.
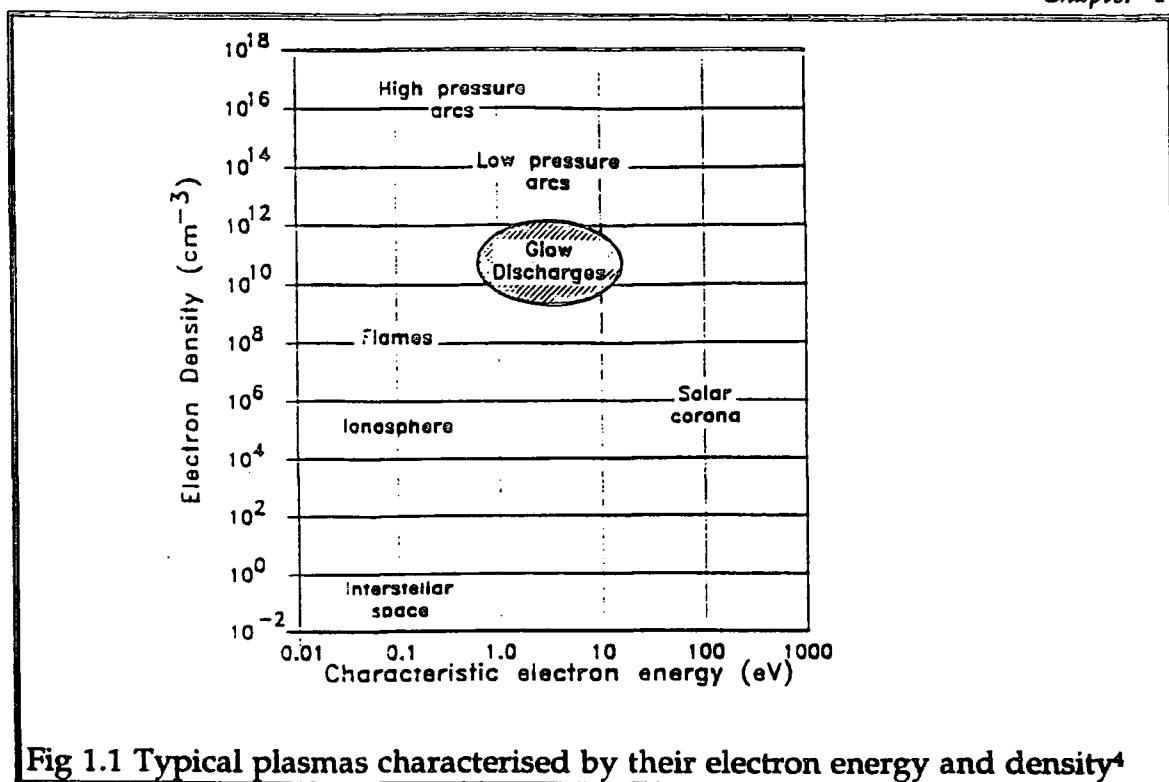
Fig 1.1 Typical plasmas characterised by their electron energy and density[4]

## 1.1.1 Types of Plasmas

There are two classes of plasmas[5], equilibrium and non-equilibrium plasmas. An *equilibrium plasma* (or "hot plasma") occurs if the pressure is so high that the charged particles cannot move very far before the next collision, or if the field is so low, that the kinetic energy of the charged particles may tend toward the energy of the neutral particles. Very often a plasma in equilibrium is a plasma at a very high temperature. At high temperatures, the number of collisions between all particles increases to such an extent that the energy is equally distributed among all particles and degrees of freedom.

A *non-equilibrium plasma* has a low degree of ionisation, i.e., the total number density of charged particles is much less than the total number density of neutral particles. The plasmas are also quasi neutral, i.e., the density of positive charge carriers is equal to the density of the negative charge carriers. If energy is supplied and a potential difference applied

3

across this type of plasma, the electric field will act on the charged particles and impart energy to them. Therefore, the neutral particles are not directly affected by the field, but the electrons due to their light mass, are immediately accelerated to higher velocities than the heavier ions in the time available for collisions. These plasmas are also termed "cold plasmas", and are often used where the substrate is a polymer. Many types of electric discharge have been described in the literature. One of the regions of greatest interest to plasma chemistry is that of the glow discharge plasmas.

### 1.1.2 Glow Discharge Plasmas

A glow discharge plasma is a type of non-equilibrium plasma,[1] because the electron temperature is much higher than the ion or gas temperature ($T_e/T_i$=10-100). Glow discharge plasmas are weakly ionised and the ratio of ionised to neutral molecules is of the order $10^{-6}$ to $10^{-4}$, so the gas consists mainly of neutral species. Glow discharge plasmas are typically formed by partially ionising a gas, through use of an electric field, at a pressure well below atmospheric.

When a glow discharge is established, it becomes visible by a characteristic glow. The actual distribution of light in the glow discharge is significant and dependent on the voltage-current characteristics of the discharge. The relationship between the applied voltage and the current of gaseous discharges, generated through use of a dc discharge, for pressures in the range of 0.1-10 torr, is shown in figure 1.2.
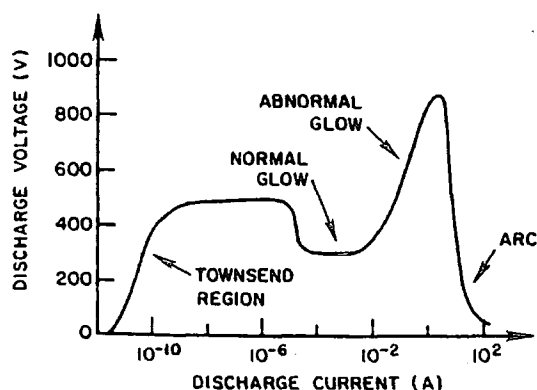
Fig 1.2 The voltage-current relationship of a dc discharge.[9]

In the glow discharge region, initially very low currents are observed, followed at a certain voltage by a sharp rise in the current. This voltage is known as the breakdown potential of the gas. The breakdown potential is dependant on the inter-electrode distance and the gas pressure.

### 1.1.2.1 Electron and Ion Temperatures in the Glow Discharge Plasma

Assume that the charged particles are singly charged positive ions and electrons. The processes occurring in the plasma are excitation, relaxation, ionisation and recombination.[1] An external energy source (generally an electric field) can act directly on the charged particles only. Let $m_e$ and $m_i$ be the masses of the electrons and ions respectively. As $m_i \gg m_e$, the action of the field is generally to give energy to the electrons.

In general, collisions are plentiful in plasmas. Electrons collide with neutral atoms and ions, but only a small energy transfer to the heavy particle can occur. In turn, the neutral atoms and ions share their energy efficiently in collision processes and likewise lose energy to the walls of the chamber. The result is that the electrons have a higher net kinetic energy (2-8eV typically). The ions, gaining little energy from the electric field, have an average kinetic energy similar to the neutrals; the neutrals gain their energy

from collisions with ions (effective) and with electrons (ineffective) and remain essentially at room temperature.

If we assume that there are a large number of electron-electron collisions and other interactions and that energy sharing is very efficient among the electrons, then from a Maxwell-Boltzmann distribution, the average electron energy is around 2 eV which corresponds to an electron temperature of 23,200K. However, as the heat capacity of the electrons is so small, and the ions receive some energy from the electric field then the overall temperature of the reaction vessel is roughly 500K.[1]

O Neutral Atoms
− Negative Electrons
÷ Positive Ions

Neutrals $\quad m = 6.6 \ 10^{-23}g$

$T = 20^{\circ}C = 293K \equiv 1/40eV$

$\bar{c} = 4.0 \ 10^4 \ cm/sec$

Ions $\quad m_i = 6.6 \ 10^{-23}g$

$T_i = 500K \equiv 0.04eV$

$\bar{c}_i = 5.2 \ 10^4 \ cm/sec$

Electrons $\quad m_e = 9.1 \ 10^{-28}g$

$T_e = 23\ 200K \equiv 2eV$

$\bar{c}_e = 9.5 \ 10^7 \ cm/sec$

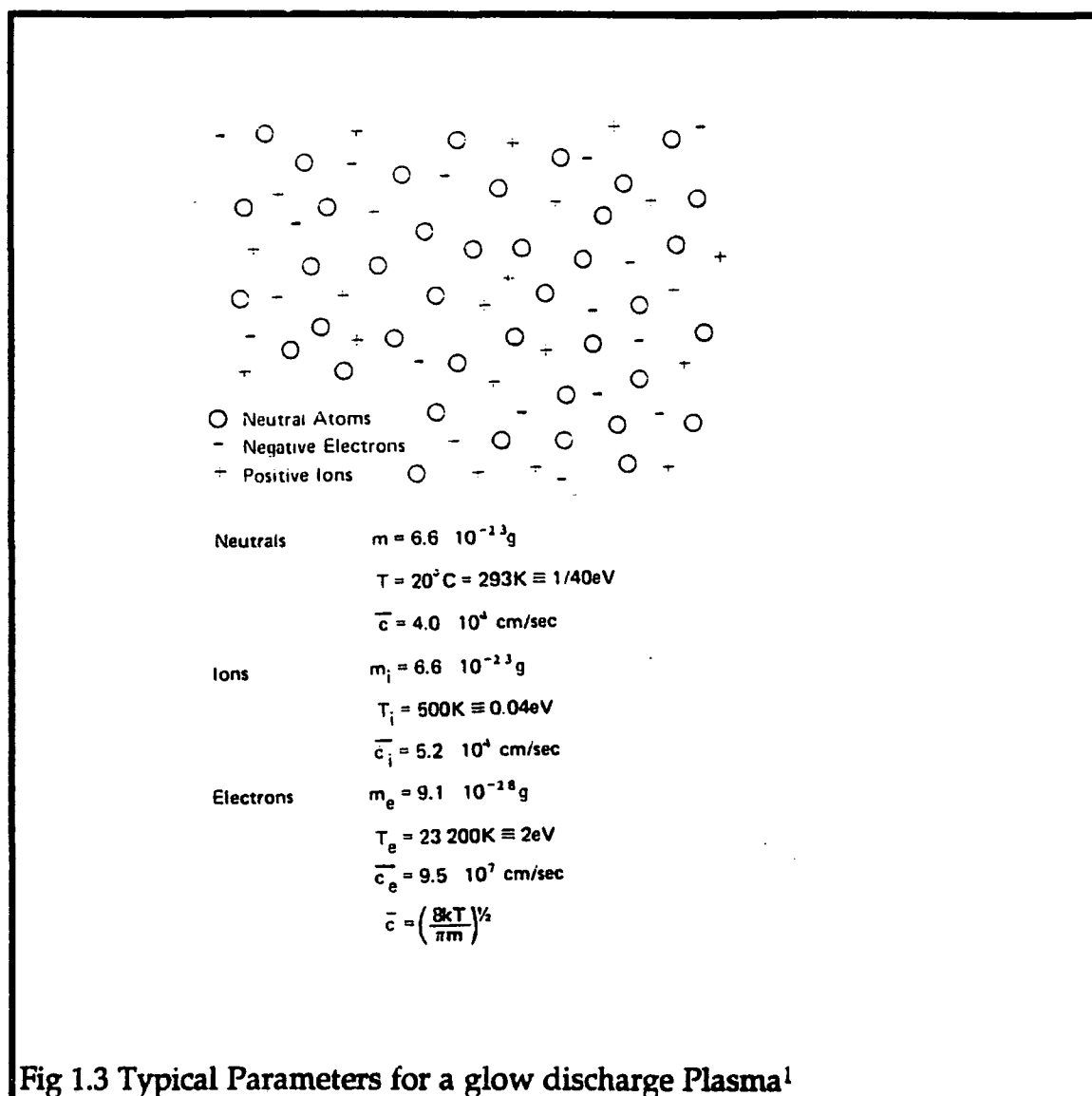$\bar{c} = \left(\frac{8kT}{\pi m}\right)^{1/2}$

Fig 1.3 Typical Parameters for a glow discharge Plasma[1]

### 1.1.2.2 *Plasma Potential:*

If a small electrically isolated substrate is placed into the plasma, it will be struck by both electrons and ions, which both have charge flux densities ($j_x$). As $j_e >> j_i$ the substrate starts to build up a negative charge and hence a negative potential with respect to the plasma.[1] Immediately the quasi-random motion of the ions and electrons is disturbed in the region of our object. Since the substrate is negatively charged, it attracts ions and repels electrons. The electron flux near the substrate still charges negatively until the electron flux is reduced by repulsion so as to balance the ion flux. The plasma is now virtually electric field free and is equipotential. This potential is referred to as the *plasma potential*, $V_p$.

### 1.1.2.3 *Floating Potential*

The isolated substrate has a *floating potential*, $V_f$, associated with it. As $V_f$ repels electrons, then $V_f < V_p$. This means that the isolated substrate will acquire a net positive charge around it, and in glow discharge plasmas a sheath forms. A sheath is a region of the plasma over which there is a significant voltage drop, and as a result, there is an extremely low electron density. The plasma is a region of uniform potential, and virtually all of the voltage change from the plasma to the surface in contact with the plasma, occurs in the sheath.[9] One of the obvious features of the discharge is that it glows, due to relaxation of atoms excited by electron impact. The glow intensity is therefore dependent on the number density and energy of exciting electrons. Since the electron density is lower in the sheath it does not glow as much and this area of lower luminosity around the substrate is referred to as a "dark space".

Note that the plasma is positive with respect to the isolated substrate. Because the electrons can move rapidly relative to the ions, they can move rapidly away from the plasma. This in turn makes the plasma even more

positive and is thus a self-limiting process. As the substrate repels electrons, it attracts ions. It does effect the energy with which the ion strikes the substrate. The ion enters the sheath with a low energy, it is then accelerated by the sheath voltage, and in the absence of collisions in the sheath, would strike the substrate with a kinetic energy equivalent to that of the sheath voltage. In practise the sheath above an electrically isolated substrate varies from one or two volts upwards. The resulting kinetic energies are comparable to interatomic binding energies in a thin film (1-10eV) so a growing thin film on an electrically isolated substrate in the plasma is much affected by such an impact.

## 1.2 Types of Electric field

Glow discharge processes are almost always driven by RF high frequency power supplies, usually in the megahertz range. In the work described in this thesis, radio frequency (RF) was used as a source of high frequency power. In this system there is no cathode or anode since the net flow of charge to either electrode is zero.

### 1.2.1 DC Discharge

One of the most elementary means of forming a plasma is through the use of a dc diode discharge. The dc diode discharge consists of two electrodes within a vacuum chamber and an external high voltage power supply.[9] An electric field is created between the electrodes. The applications of dc diode plasmas are typically either sputter etching of samples placed on the cathode surface or else sputter deposition of cathode materials onto samples placed onto the anode or elsewhere in the system. However, dc plasmas are rarely used due to their low plasma density and high discharge voltage. In addition, the electrodes in a dc discharge must be conducting to allow flow

of the current. If an insulating sample is placed on the electrode, and the glow discharge is initiated, the negatively biased target is bombarded with ions and begins to lose electrons. Thus the insulator charges positively with respect to the plasma[1] and the levels of ion bombardment will be of relatively low energy.[9]

### 1.2.2 AC Discharge

A system incorporating an AC discharge was proposed to deal with the above mentioned problem of dc discharges, so that the positive charge accumulated during one half of the cycle could be neutralised by electron bombardment during the next half cycle. However, using conventional mains frequency (50Hz), the insulator takes most of the half cycle to charge up so most of the time, the discharge is off. To produce a discharge almost continuously, a frequency of ca. 1 MHz is required. These high frequencies can be supplied by RF.

### 1.2.3 Radio Frequency Discharges

When a high frequency electric field is applied across the charged particles in the volume, the direction of the field changes, and the direction of force on the electron will oscillate within the volume of the gas,[6] provided that the walls of the chamber are sufficiently far apart. When frequencies are low (e.g.. ac) the reversal of direction of acceleration does not occur before the electron strikes the wall of the container. At high frequencies, if there were only electrons and no gas atoms then the electrons would oscillate out of phase with the field and no energy would be transferred. In the presence of the gas, electron-atom collisions occur and the electrons are accelerated by the field after each collision, sometimes losing, sometimes gaining energy, but on average, a net transfer of the field to the electrons will occur.

9

RF discharges are also known as electrodeless discharges as the electrodes are not in direct contact with the species in the plasma. Depending on the type of electrode geometry used, the energy is transferred to the gas via inductive or capacitive coupling. For electrode configurations shown in figure 1.4, a) and b) employ capacitive coupling and c) uses inductive coupling and the plasma is generated in the magnetic field of the induction coil.[4]
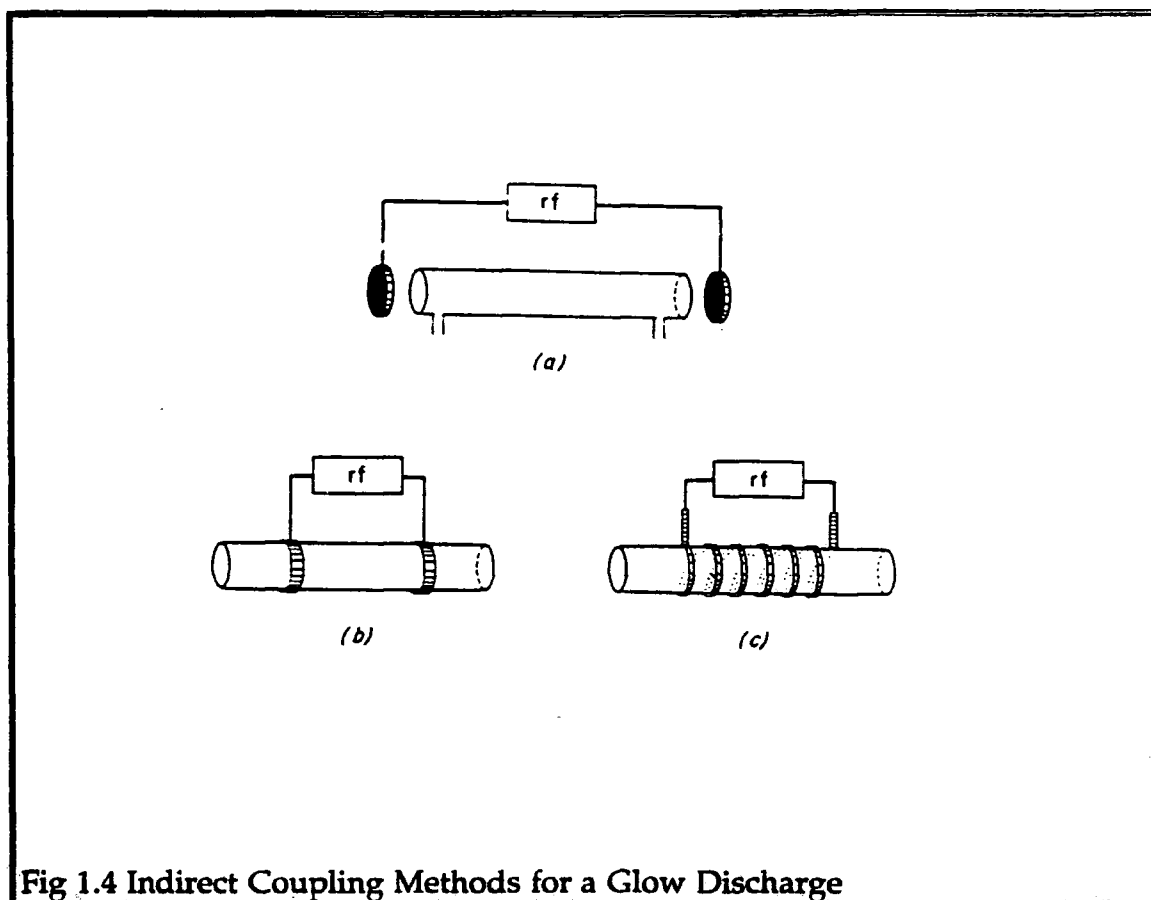


Fig 1.4 Indirect Coupling Methods for a Glow Discharge

Generally RF plasmas are preferred for the following reasons[7]:

* Electrons can pick up sufficient energy during their oscillations in an RF field to cause further ionisation. Therefore, the discharge can be sustained independently of the yield of secondary electrons from the walls and electrodes.

* RF discharges can be excited from outside the reaction chamber by inductive or capacitive coupling.

\* The efficiency of electron collisions is enhanced by electron oscillations which means that RF discharges can be operated at pressures as low as 1mTorr, with mean free paths of a few centimetres. This leads to higher etch rates from enhanced yields of atoms and radicals.

## 1.3 Surface Modification Using Partially Ionised Plasmas.

### 1.3.1 Introduction

During the last 30 years, there has been enormous growth in the use of partially ionised plasmas for the processing of surfaces. Surface processing in this context can be divided into three major categories: deposition, etching, and surface modification. "Surface Modification" is used to describe those processes which alter the physical and/or the chemical properties of a pre-existing solid surface, in which this modification is limited to a region relatively near the surface of a solid.[6] Examples of surface modification are plasma oxidation and reduction, plasma nitriding, and surface texturing.[28] Some areas of technology in which partially ionised plasma play a major part are in microelectronics, magnetic and optical recording technologies, and machine tool fabrication.

There are two characteristics of plasmas which make them so attractive for these purposes: one is the ability of certain kinds of plasmas to deliver a uniform flux of energetic positive ions to a surface with controllable energy and flux. The second is their ability to deliver spatially uniform, relatively large fluxes of atoms or molecular radicals to surfaces. In both cases the surfaces can be near room temperature and electrically insulating surfaces can therefore be processed with no great difficulty. In some applications, only the energetic ion bombardment is required, whilst in others, only radical fluxes are important. However, in more and more cases, it is a combination of energetic ions and reactive radicals or atoms which are

11

responsible for the unique surface processing capabilities of some partially ionised plasmas. In this case, i.e., when both reactive radicals and energetic ions are required, it is difficult to find a more superior approach than the partially ionised plasma.[6]

A major focus of surface modification is on semiconductor processing in halogen plasmas created in a dual-electrode system.[7]

## 1.4 Hydrogen Plasmas for Surface Modification

In the work outlined in this thesis, a glow discharge was generated in the presence of only hydrogen over a gold (III) chloride film. Hydrogen is the simplest of the elements with its one valence orbital and single electron. It can react only by gaining or sharing another electron. Hydrogen combines with almost all other elements.[10]

### 1.4.1 Introduction

Some of the important properties of hydrogen are listed below.[11]

| | | |
|---|---|---|
| Heat of dissociation | $H_2(g) = 2H(g)$ | $\Delta H = 435.9$ kJ/mol |
| Ionisation Potential | $H(g) = H^+ + e^-$ | $I = 13.595$ eV |
| Electron Affinity | $H(g) + e^- = H^-(g)$ | $E = 68.99$ kJ/mol |

As the hydrogen molecule bond energy, 435.9 kJ/mol, is high, molecular hydrogen is fairly unreactive at ordinary temperatures. However, at high temperatures, it combines, either directly or with the aid of a catalyst, with most elements.

Covalent hydrides are formed with almost all the elements with electronegativities up to about 1.5. As hydrogen has an electronegativity of

2.1, it follows that bond polarities in the hydrogen halides are strongly positive towards the hydrogen end i.e. $H^{\delta+} - X^{\delta-}$.

Hydrogen undergoes several reactions including recombination[28] and transfer[28] reactions. It reacts with unsaturated hydrocarbons[29] and with compounds of C, H, and O.[12, 30] Hydrogen atoms, being highly reactive, are strong reducing agents. The reducing effects of hydrogen have been observed on oxides of metals, inorganic halides and on several other compounds which are described in reference 10.

### 1.4.2 Hydrogen plasmas:

*1.4.2.1 Introduction*

Since 1922, when Wood[12] obtained more than 50% dissociation of hydrogen gas into atoms using a low frequency electrode discharge, at 0.2-1.0 mm Hg pressure, electrical discharges have been widely employed using hydrogen.

In a microwave plasma, 90% dissociation was obtained at 0.5mm Hg and 100 watts of power. At low pressures, hydrogen does not appear in a highly reactive state, but at high pressure (30-300mm Hg) three body recombination of the atoms appear to give rise to unstable molecules which retain the greater part of the energy of recombination and survive as many as $10^8$ collisions in the gas phase.[15]

A plasma is used as an efficient means of generating active hydrogen atoms.[13] In recent years plasma etching has become an increasingly important processing technique for the semiconductor industry. Gases containing the halogens and their compounds are extensively used to etch semiconductors, metals and insulators.[7] These are very useful but do give rise to problems with regard to handling and atmospheric pollution.

Hydrogen can be used as an alternative for some plasma processes.[14] Although hydrogen does not etch such a wide range of materials as the halogens and their compounds, it can often be used as a substitute. Atomic hydrogen can be formed by dissociating hydrogen molecules using electrons or photons. The threshold energy for dissociation of $H_2$ into H atoms is 8.8 eV and this is discussed extensively in references 26 and 27. The rate of H production is proportional to the hydrogen gas density, the average electron velocity and electron density. Generally, using a RF plasma of density greater than 2-10 $W/cm^3$ gives rise to roughly 60% hydrogen atoms.[26, 27]

Hydrogen plasmas only affect the top few layers (ca. 100Å) of a solid surface, so there is no overall change in either the appearance or the bulk properties of the material.[21]

### 1.4.2.2 *Some Applications Using Hydrogen Plasmas:*

A plasma is an efficient means of generating active hydrogen atoms. If the hydrogen atoms will react with the material placed in the plasma to form a volatile compound then the surface properties of the material will be changed.[16]

It has been shown that hydrogen atoms created in an RF plasma rapidly etch silicon, gallium-arsenide and gallium-antimony semiconductors[16, 17] as well as some other materials. In agreement with previous work,[18] Chang & co-workers suggested that the mechanism was that the hydrogen atoms reacted with solid materials to form volatile hydrides. Further, it was proposed that any material which forms a volatile hydride will be etched by hydrogen atoms. Based on these postulations, Chou and Phillips reconstructed a tin foil in a hydrogen plasma, as tin forms a volatile hydride which is unstable above 220 K,[19] but can be transported over atomic scale distances.

The influence of an admixture of hydrogen to a styrene monomer, on films, prepared by RF plasma polymerisation, was studied and compared to the films resulting from the RF plasma polymerised styrene monomer only. The admixture of the hydrogen changes the electronic and atomic structure of a polystyrene film drastically. This is probably due to an increase in hydrogen ion impingement on the surface of the growing film.[20]

Silver oxide can be reduced to silver metal with $Ar/H_2$ plasmas. $H_2$ replaces F or O in surfaces and can also remove organics on materials that are sensitive to oxidation. The contamination is converted to volatile low molecular weight species that do not polymerise or re-deposit on adjacent surfaces.[21]

A $N_2/H_2$ dc pulsed plasma was used to obtain iron-nitride layers on the pure iron substrates. The $H_2$ increased the excitation of iron atoms and of nitrogen molecules and therefore assisted the nitriding process.[22]

$H_2$ was also introduced to a titanium nitriding process and it is postulated that the hydrogen is responsible for the reliable metallurgical results that are obtained.[22]

Use was made of the 'pulsing' concept where the gases in the discharge can be changed between the RF pulses to obtain aluminium metal films. After carbide was deposited in the first RF pulse, the gas was changed to hydrogen and several RF pulses were used to remove the carbon as methane. Thus the technique used consisted of successive depositions of the carbide and subsequent etching of the carbon by hydrogen to leave the aluminium film.[23]

There are many examples of situations in which a surface was exposed to a glow discharge and a change was noted in some macroscopic surface property with little or no understanding of the microscopic details. Hydrogen plasmas seem to be used in this way more often than discharges of other gases and this is often termed 'plasma annealing'.[19]

A $H_2$ plasma radiates at a shorter wavelength than $O_2$ (121.5nm and 130.2nm respectively photon energies of 235 Kcal/mol and 220 Kcal/ mol[21]). The $H_2$ radiation is absorbed by the surface of PTFE and can break ist surface bonds. Also, the H can abstract the surface fluorine to form HF and expose carbon free radicals to further attack by other species in the boundary layer.[25]

## 1.5 Conclusion

Plasmas, which are also referred to as the fourth state of matter, find more and more applications in everyday usage. The electronics revolution of the past thirty years would not have occurred without the development of plasma processes. Plasmas can be used in biomedical applications,[8] permselective membranes, and protective coatings.[4, 9]

One of the regions of greatest interest to plasma chemistry is that of glow discharge plasmas. One of the biggest advantages of this technique is that these plasmas can be used to modify temperature sensitive substrates.

During the past thirty years, there has been increasing interest in the use of partially ionised plasmas for the processing of surfaces. A large amount of work has been done on plasma etching using halogen plasmas. However, halogen plasmas cause both handling and environmental problems and as a result hydrogen plasmas are often used as a substitute.

In the work outlined in this thesis, a hydrogen plasma was generated at 0.1 torr, by using an RF power supply, to modify the surfaces of gold (III) chloride films. It has been postulated that if hydrogen atoms will react with a material in a plasma to form a volatile compound (HCl), then the surface will be modified. The aim of this work was to create a conducting gold film, by removal of the chlorine species from the original film, through use of a hydrogen plasma.

References:

1. Chapman, B., *Glow Discharge Processes*, Wiley 1980 Chapter 3 & 5

2. Eliasson, B., *IEEE Transactions on Plasma Science*, 19 (6) (1991) 1603

3. Chen, F.F. *Introduction to Plasma Physics*, Plenum Press, 1976, Chapter 1

4. Hollahan, J.R., Bell, A.T., *Techniques and Applications of Plasma Chemistry*, Wiley 1974, Chapter 1

5. Walls, J.M., *Methods of Surface Analysis, Techniques and Applications* Cambridge University Press, 1989 Chapter 1

6. Hirsch, M.N., Oskam, H.J.,*Gaseous Electronics, Electrical Discharges*, Academic Press, 1978

7. Manos, D.M., Flamm, D.L., *Plasma Etching, An Introduction*, Academic Press, NY, 1989, Chapter 1

8. Yasuda, H., *Plasma Polymerisation*, Academic Press, 1985

9. Vossen, J.L., Kern, W., *Thin Film Processes II*, Academic Press, 1991

10. Greenwood and Earnshaw

11. MacKay, K.M., MacKay, R.A., *Introduction to Modern Inorganic Chemistry*, Blackie, 4th Ed., 1989

12. McTaggart, F.K., *Plasma Chemistry in Electrical Discharges*, Elsevier, 1967

13. Chang, R.P.H., Chang, C.C., Darack, S.J., *J.Vac. Sci. Technol..*, B2 675 (1984)

14. Chang, R.P.H., Chang, C.C., Darack, S. *J. Vac. Sci. Technol.*, 20 (1) 490 (1982)

15. Villermaux, J., *J. Chem.*, 61 (1964) 1023-1033

16. Chang, R.P.H., Chang, C.C., Darack, S., *J. Vac. Sci. Technol.* , 20 45 (1982)

17. Friedel, P., Larsen, P.K., Gourrier, S., Cabannie, J.P., *J. Vac.Sci. Technol.*, B2, 675 (1984).

18. Coburn, J.W., Winters, H.F., *J. Vac.Sci. Technol.*, 16 391 (1979)

19. *CRC Handbook of Chemistry and Physics* 63 rd Edition

20. Schelz, S., Eitle, J., Steiner, R., Oelhafen, P., *Appl. Surf. Sci.* 91 301-306 (1991)

**21.** Liston, E.M., *J. Adhesion,* **30** 199-218 (1989)

**22.** Boughdira, J., Henrion, G., *J. Phys.,D. Appl. Phys.,* **24** 1076 (1991)

**23.** Llewellyn, L.P., Rimmer, W., Scarsbrook, G.A., *Thin Solid Films,* **191** 135 (1990)

**24.** Robb, F.Y., *J. Electrochem. Soc.,* **131** 1670 (1984)

**25.** Akorali, G., *The Interfacial Interactions in Polymeric Composites, Plasmas and Surfaces,* pp.223-268 1993

**26.** Goodyear, C.C., Van Engel, A., *Proc Phys. Soc.,* **79** 732 (1962)

**27.** Khare, S.P., Moiseiwitsch, B.L., *Proc. Phys. Soc.,* **88** 605 (1966)

**28.** Smith, W.V., *J. Chem. Phys.,* **11** 110 (1943)

**29.** Allen, P.E., Melville, H.W., Robb, J.C., *Proc. Royal Soc.,* **A218** 311 (1958)

**30.** Trost, W.R., Darwent, B., Steacie, E.W.R., *J. Chem. Phys.,* **13** 554 (1945)
**31.** Major, S., Kumar, S., Bhatnager, M., Chopra, K., *Appl. Phys. Letters,* **49** (7) 394 (1986)
**32.** Grünze, M., Hirschwald, W., Hofmann, D., *J. Cryst. Growth,* **52** 241 (1981)

# 2. Surface Analysis

## 2.1 Analysis of Surfaces and Interfaces

## 2.2 XPS

### 2.2.1 Introduction

### 2.2.2 Instrumentation

*2.2.2.1 Introduction*

*2.2.2.2 UHV*

*2.2.2.3 Photon Sources*

*2.2.2.4 Electron Analysers*

### 2.2.3 Spectral Interpretation

*2.2.3.1 The Photoelectron Spectrum*

## 2.3 XP Spectra of Elements Analysed for this Work

### 2.3.1 Au (4f)

### 2.3.2 Cl (2p)

### 2.3.3 Si (2p)

### 2.3.4 C (1s)

### 2.3.5 O (1s)

### 2.3.6 N (1s)

## 2.1 Analysis of Surfaces and Interfaces

Surface analysis is used to obtain the elemental composition of the outermost atomic layer of a solid.[1] There are several surface sensitive techniques available, some of which are shown below:

|          | *Electrons* | *Incident Ions* | *Radiation Neutrals* | *X-Rays* |
|----------|-------------|-----------------|----------------------|----------|
| Electrons | AES         | INS             |                      | UPS      |
|          | LEED        |                 |                      | XPS      |
|          | HREELS      |                 |                      |          |
| Ions     | ESD         | SIMS            | FABMS                |          |
|          |             | ISS             |                      |          |
|          |             | RBS             |                      |          |
| Neutrals |             | SNMS            |                      |          |
| X-Rays   | EPMA        | PIXE            |                      | SEXAFS   |

where the electrons, ions, neutrals and X-rays are the radiation detected and the *electrons, ions, neutrals* and *X-rays* are the input radiation.

AES: Auger Electron Spectroscopy

LEED: Low Energy Electron Diffraction

HRLEELS: High Resolution Low Energy Electron Loss Spectroscopy

ESD: Electron Stimulated Desorption

EPMA : Electron Probe X-Ray Microanalyser

INS: Ion Neutralisation Spectroscopy

21

SIMS: Secondary Ion Mass Spectrometry

ISS: Ion Scattering Spectroscopy

RBS: Rutherford Back Scattering

SNMS: Secondary Neutral Mass Spectroscopy

PIXE: Particle-Induced X-Ray Emission

FABMS: Fast Atom Bombardment Mass Spectrometry

UPS: Ultraviolet Photoelectron Spectroscopy

XPS: X-Ray Photoelectron Spectroscopy

S-EXAFS: Surface-Extended X-Ray Absorption Fine-Structure Spectroscopy


Each of the many surface analysis techniques approaches one or more of the many aspects of surfaces , so that, in principle each has a particular advantage.


AES and XPS dominate the surface analysis field.[2] These can be used as analysis tools in microelectronics, metallurgy, catalysis, polymer technology and surface corrosion.


## 2.2 X-Ray Photoelectron Spectroscopy


### 2.2.1 Introduction

XPS has evolved into a powerful surface analytical tool.  Photoelectron spectroscopy involves the ejection of electrons from atoms or molecules following monochromatic irradiation.[1, 2, 7]  The electron which is ejected is called the photoelectron.  XPS involves irradiating the sample with photons from the X-ray region of the electromagnetic spectrum, to eject electrons form core orbitals.


$$M + h\nu = M^+ + e^- \qquad (2.2.1.1)$$

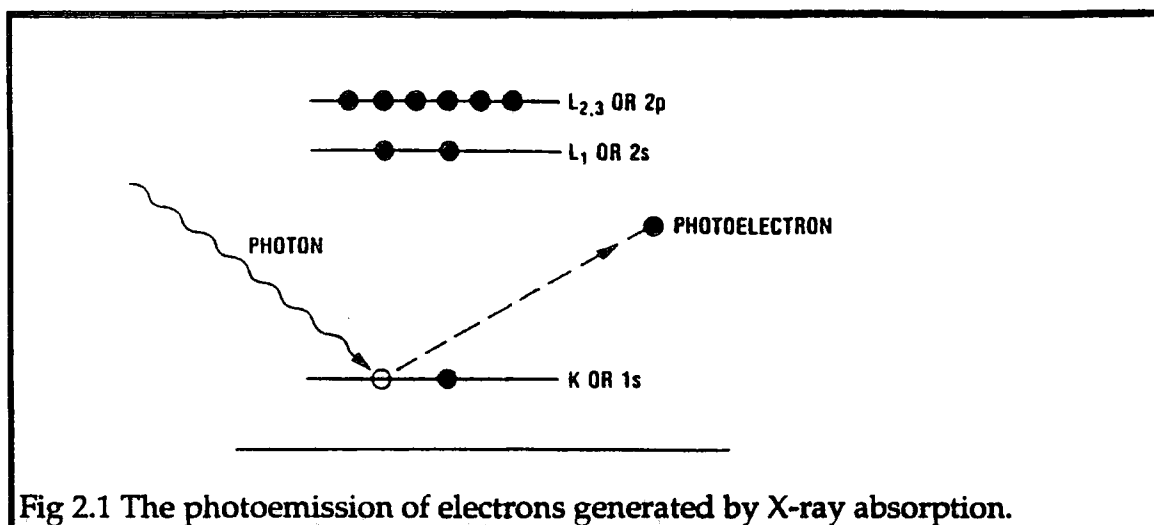The photoemission of electrons is shown schematically in figure 2.1.



Fig 2.1 The photoemission of electrons generated by X-ray absorption.

Using the basic equation of photoelectron spectroscopy (equation 2.2.1.2), the binding energies of the electrons in the original atom can be calculated.

$$K.E. = hv - B.E. - \phi \qquad (2.2.1.2)$$

where K.E. is the kinetic energy of the photoemitted electron, h is Plancks constant, $v$ is the frequncy of the photon source, $\phi$ is the work function of the spectrometer, and B.E. is the binding energy of the electron in the atom. Since the energy of the incident photon and the work function are both known, and if the K.E.'s are measured, then the binding energy of the electron in the original atom can be calculated and its chemical environment can be identified. The B.E. peaks are well catalogued and provide a quick means of identifying the chemical constituents in the specimen. Since B.E.'s are sensitive to local charge environment, XPS peaks shift significantly as the chemical environment changes.[4]

XPS involves the detection of photoelectrons in the energy range of 5-2000eV which are emitted or scattered from the surface. This technique derives its surface sensitivity from the fact that electrons in this energy range have a high

probability of inelastic scattering,[2] (the mean free path of an electron is of the order of, or less than, a few tens of angstroms (Å), and in the energy range of 5-2000eV, is typically less than 10Å), so that if electrons are detected at an energy which is known to be unchanged by passage through a surface region of the solid, then they have passed through a very thin surface layer.

### 2.2.2. Instrumentation

*2.2.2.1 Introduction*

All X-ray photoelectron spectrometers must incorporate the following:

1. A UHV environment

2. A photon source

3. An electron energy analyser

The important components of a photoelectron spectrometer are shown in figure 2.2. The sample is inserted into the target chamber via an insertion lock. The sample is then irradiated with X-ray photons causing photoelectrons to be ejected in all directions. Some of these pass through the slit into the electron energy analyser and then on to the electron detector. The spectrum is then recorded as the number of electrons per unit time as a function of the kinetic energy of the photoelectrons.
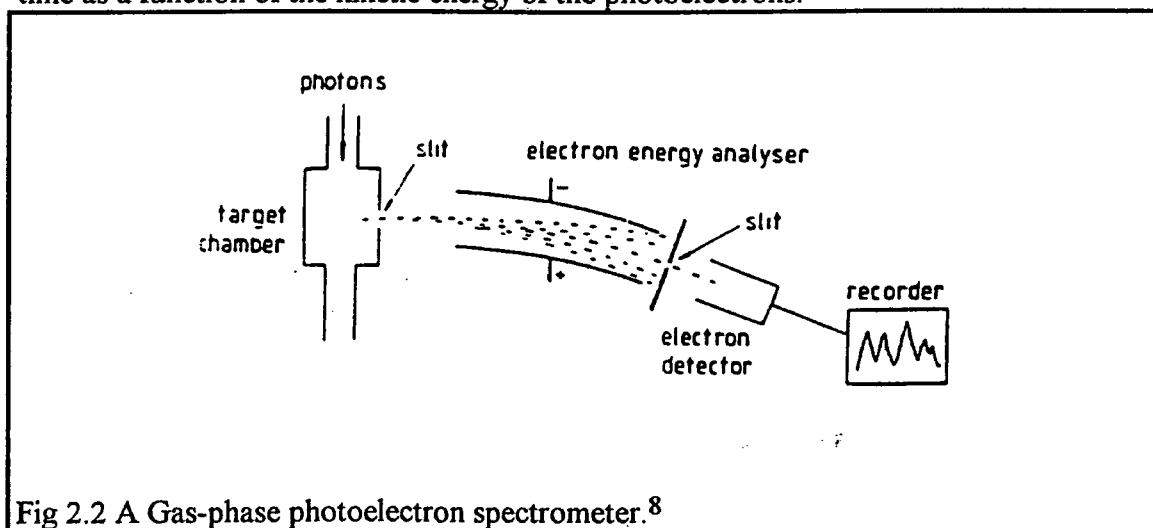


Fig 2.2 A Gas-phase photoelectron spectrometer.[8]

The important aspects of XPS are discussed in detail in the following sections.

*2.2.2.2 Ultra High Vacuum Environment*

In order to characterise the properties of a surface at an atomic level, the composition of the surface must remain constant over the duration of the analysis.[2] Thus the rate of arrival of reactive species from the gas phase must be low. In XPS, as in most surface analysis techniques, a UHV environment of $10^{-8}$ to $10^{-10}$ torr is required. Assuming unit sticking probability, a monolayer forms on the surface of a sample in $3 \times 10^{-6}$ seconds at a pressure of 1 torr, in 3 seconds at $10^{-6}$ torr, and in ca. 1 hour at a pressure of $10^{-9}$ torr. UHV is also required to allow the electrons to reach the analyser without colliding with a gas phase particle. The spectrometers are maintained at $10^{-8}$ to $10^{-10}$ torr constantly as when they are allowed up to ambient pressures, it is necessary to "bake" the spectrometer in order to achieve UHV conditions again.

*2.2.2.3 Photon Sources.*

A photon source must have several specific properties. Conventional XPS sources are created by bombarding a solid target with high energy electrons; the emission from this target consists of characteristic line emissions associated with the filling of core holes created by the incident beam, superimposed on a continuum background up to the incident electron energy due to bremsstrahlung.In order to gain useful information by energy analysing the photoemitted electrons from the occupied energy levels on the surface, the photon source should be as monochromatised as is possible. This means that the X-ray source material should have a low bremsstrahlung background and a narrow characteristic line emission, dominated by a single line.

As considerable energy is supplied to the target by the incident beam, it is usually necessary to cool the target, which is a relatively simple process if the target is a good conductor of heat. Therefore a metallic target is preferred. In

UHV analysis chamber vacuum systems, outgassing of the target can lead to pressure rises thus making a cool target a requirement.

Aluminium and magnesium are the most commonly used XPS photon sources, as these possess all the above named required properties. Magnesium has a linewidth of 0.7 eV and generates photons of energy 1253.6 eV. Aluminium has a linewidth of 0.85 eV and generates photons of energy 1486.6 eV.[2] In both cases a K$\alpha_{1,2}$ (i.e. 2p -> 1s) transition may be used and the spectrum is an unresolved doublet, with several satellite peaks and a low bremsstrahlung background. The emission spectrum of magnesium is shown in figure 2.3. It is possible to remove the bremsstrahlung background and satellite peaks by using a monochromator (eg. a quartz single crystal). This also reduces the dominant K$\alpha_{1,2}$ line width to ca. 0.2 eV.
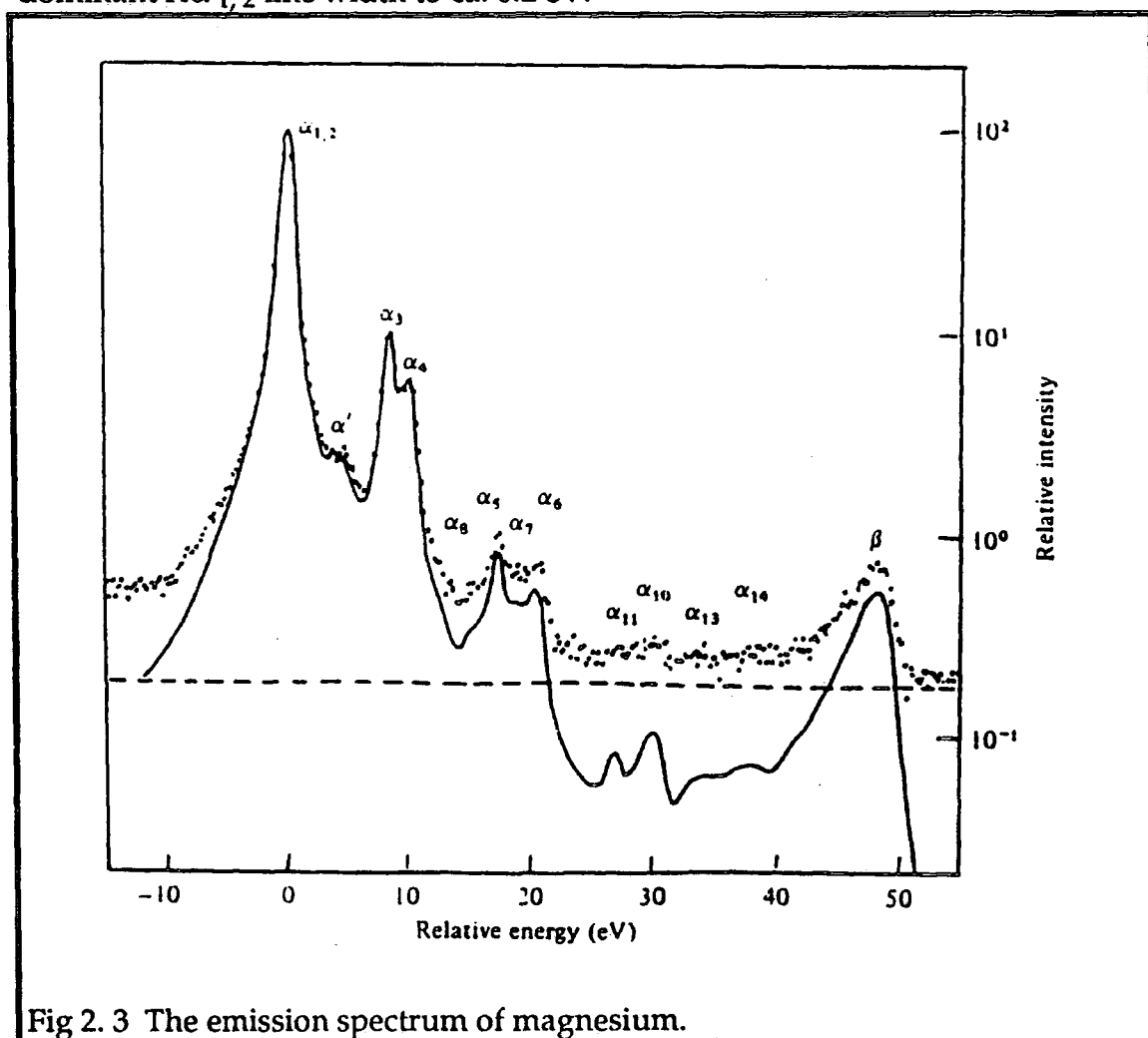
Fig 2. 3 The emission spectrum of magnesium.

## 2.2.2.4 Electron Analysers

The surface specificity of XPS is derived from a knowledge of the electrons, therefore some form of electron analyser is required. The basic purpose of any electron spectrometer is to separate out from electrons with a wide range of energies entering the spectrometer, only those electrons in a certain narrow band of energies. Ideally, this should be achieved with some kind of energy band pass filter but can be done with a simpler high pass filter followed by some sort of signalling processing.[2] The two principal analysers are the cylindrical mirror analyser (CMA), and the concentric hemispherical analyser (CHA), which are both dispersive, i.e., the electrons are dispersed by the field, and for any other given field only those electrons with energies in a certain narrow range are measured. The CHA is generally used for XPS because, with the addition of a lens, it can maintain higher luminosity at high energy resolution.[3] In the work completed in this thesis, an XPS with a CHA was used and this is discussed in detail below.

### Concentric Hemispherical Analyser

The CHA, established in ca. 1969 by Siegbahn, is the energy analyser mainly used for XPS.[1] This is shown schematically in figure 2.4.
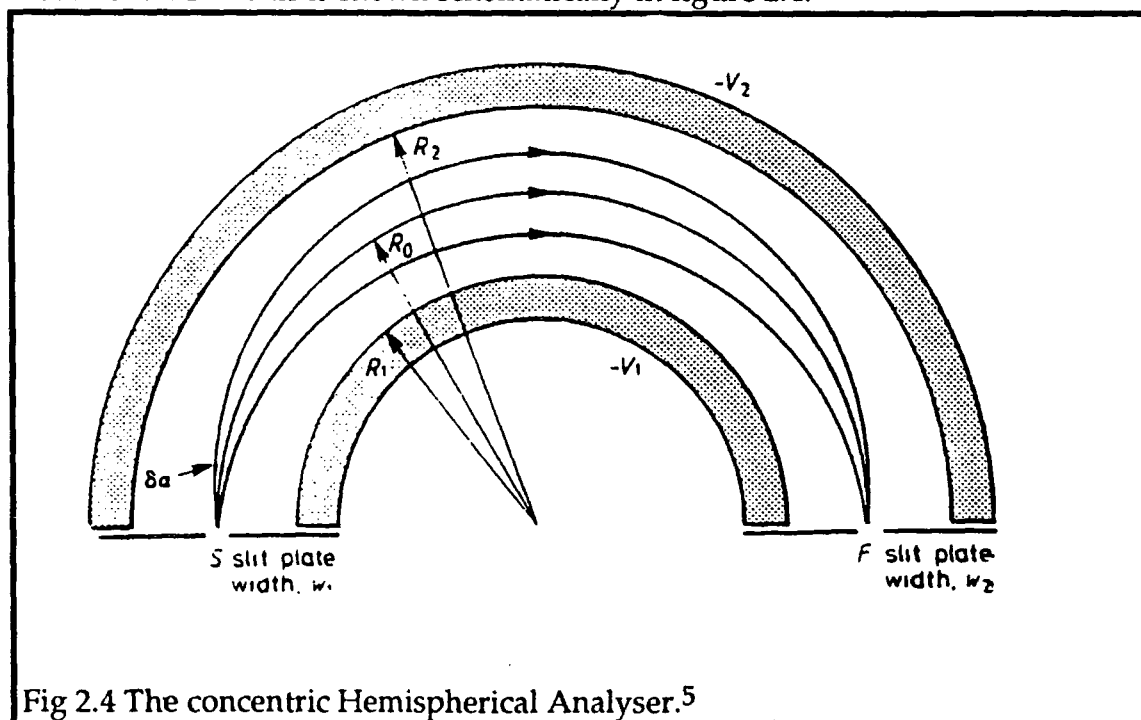


Fig 2.4 The concentric Hemispherical Analyser.[5]

Two hemispherical surfaces of inner radius $R_1$ and outer radius $R_2$ are positioned concentrically. A potential $\Delta V$ is applied between the surfaces so that the outer sphere is negative and the inner positive, with respect to $\Delta V$. A median equipotential surface of radius $R_0$ exists between the two hemispheres, and if the concentric hemispheres are are geometrically perfect then $R_0 = (R_1 + R_2)/2$. The entrance and exit slits of the CHA are both centred on $R_0$. In general, electrons entering the analyser at an angle a with respect to the normal at the centre of the slit will travel in elliptical orbits in the CHA. If an electron of kinetic energy E enters the analyser at the centre of the slit at $a = 0^0$, and travels in a circular orbit of $R_0$, then the following relationship must hold:

$$(e)\,(\Delta V)\ = E\,(R_2/R_1 - R_1/R_2) \qquad (2.2.2.4.1)$$

where e is the electron charge and $\Delta V$ is the reflecting potential in volts. This gives the ideal pass energy. During the measurement, the entire CHA is isolated from ground and floats at a varying potential which scans through the desired range of energy, while $\Delta V$ is maintained at a fixed value with respect to the floating potential.[3]

There are two retarding modes in which CHA's are currently used. The CRR (or FRR) mode decelerates the electrons by a constant factor or ratio from their initial kinetic energies, giving a constant (or fixed) relative resolution. The CAT (or FAT) mode decelerates the electrons to a constant pass energy which leads to a constant (or fixed) absolute resolution. The FAT mode is easier to quantify than the FRR mode, as the absolute resolution is the same for all parts of the spectrum, but the signal to noise ratio gets worse at high kinetic energies. These peaks at low kinetic energy are easier to detect in the FRR made but quantification is generally poor.

### 2.2.3 Spectral Interpretation

The orbiting paths of electrons around atomic nuclei have momenta associated with them. An electron has orbital angular momentum, l, which can take the values 0, 1, 2..etc., and spin momentum s, which can have the values ± 1/2. The total electronic angular momentum is a combination of both of these and is referred to as j-j coupling.[6] Total angular momentum is characterised by the quantum number, j, where j = l + s and this therefore can take the value 1/2, 3/2, 5/2 etc.

### *2.2.3.1 The Photoelectron Spectrum*

A series of peaks are observed on the background which generally increase to a low kinetic energy (K.E.) but which also show step-like increases on the low K.E. side of each significant peak. If the X-ray source is non-monochromatic then the output consists of a broad continuous distribution upon which are superimposed lines characteristic of the target material. There are two types of peaks observed on the photoelectron spectrum: the peaks due to photoemission from core-levels and those due to X-ray excited Auger emission from valence-levels. The work outlined in this thesis focussed on the peaks from photoemission from core levels. Core levels have variable intensities and widths. Non s-levels are doublets, which arise through spin-orbit (j-j) coupling. Two possible states arise when l > 0 and these are characterised by the quantum number j. The difference in the energy states, $\Delta E_j$, reflects the parallel or anti-parallel nature of the spin and orbital angular momentum vectors of the remaning electron. The magnitude of this energy separation is expected to increase as Z increases for a given subshell. The relative intensities of the doublet peaks are given by the ratio of their respective degeneracies (2j+1). The area ratios of the spin-orbit doublets are given below:

| Subshell | j values | Area ratio |
|----------|----------|------------|
| s | 1/2 | -- |
| p | 1/2, 3/2 | 1:2 |
| d | 3/2, 5/2 | 2:3 |
| f | 5/2, 7/2 | 3:4 |

## 2.3 XP spectra of the elements analysed in this work

In the work discussed in this thesis, $AuCl_3$ in IPA, on both glass and nylon substrates, was reduced using a hydrogen plasma, and examined by XPS. The XPS peaks analysed were therefore Au(4f), Cl(2p), C(1s), O(1s), Si(2p), and N(1s). The literature values for these are discussed in this section.

### 2.3.1 Au (4f)

Figure 2.5 shows the XPS spectrum of gold. Gold shows one set of spin orbit split doublets in the Au (4f) core region. This doublet results from the removal of a 4f electron leaving $4f_{7/2}$ and $_{5/2}$ core states for which l=3, s=1/2, and j= 5/2 or 7/2. The 4f 7/2 peak has a maximum at 84.0 eV,[9] but other values have been cited. Some of these are listed below:

**Au 4f $_{7/2}$**

$83.7 \pm 0.2$ [10, 11]

84.0 [12,13]

$84.0 \pm 0.2$ [14, 15]

84.1 [16, 17]

For the work described in this thesis, an ES 200 X-ray photoelectron spectrometer was used and this was calibrated to the Au 4f $_{7/2}$ peak at 83.9 eV, full width at half maximum 1.2 eV.
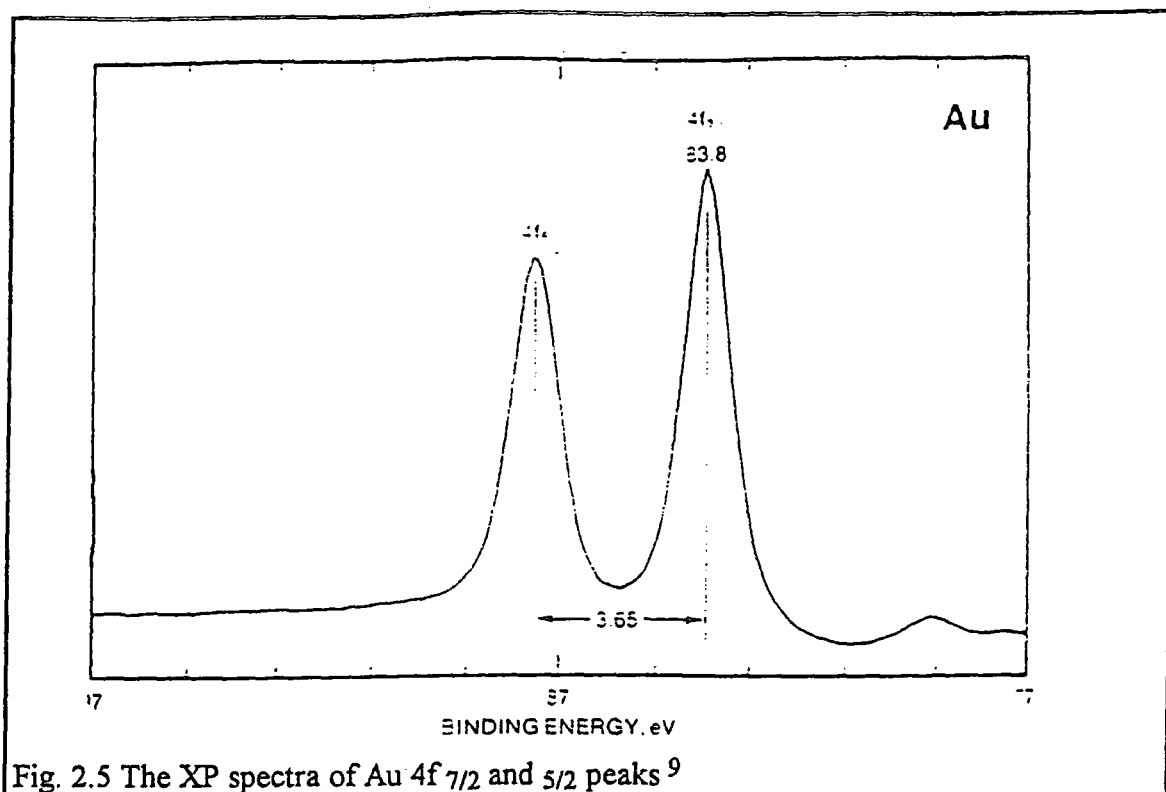
Fig. 2.5 The XP spectra of Au 4f $_{7/2}$ and $_{5/2}$ peaks [9]

## 2.3.2 Cl (2p)

The XPS Cl (2p) peak has a maximum at 199 eV for the element, and at 199.9 eV in PVC. The XP spectra of the Cl (2p) peak is shown for PVC in fig. 2.6
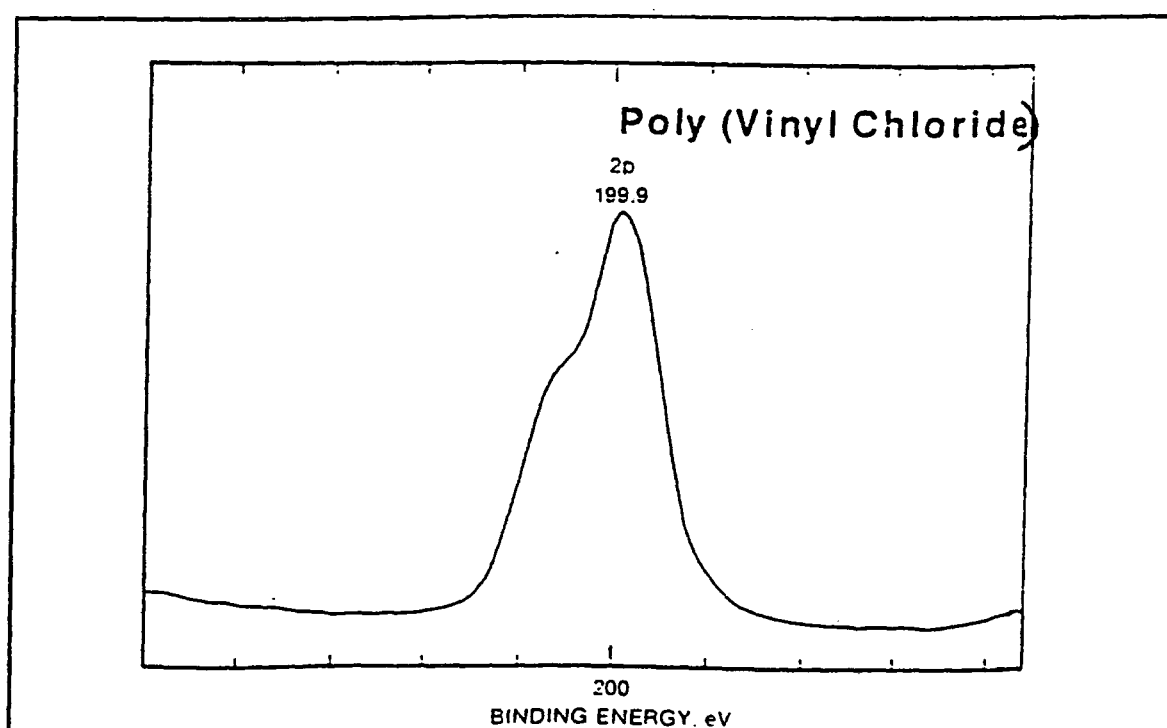


Fig 2.6 XP spectra of Cl (2p) in PVC[9]

### 2.3.3 Si (2p)

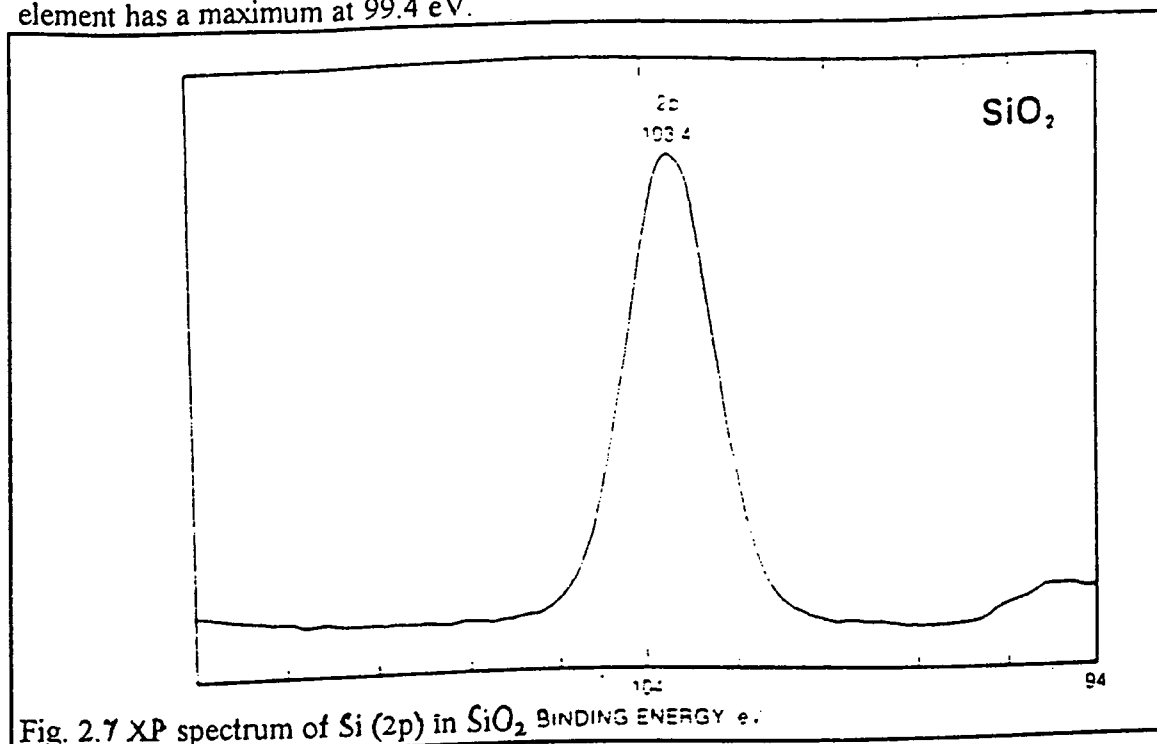In $SiO_2$, the XP Si (2p) peak has a maximum at 103.4 eV (shown in fig. 2.7), and the element has a maximum at 99.4 eV.



Fig. 2.7 XP spectrum of Si (2p) in $SiO_2$ BINDING ENERGY e.

### 2.3.4 C (1s)

The XPS peak for C (1s) has a maximum at 284 eV, and in polyethylene has a maximum at 284.6. C (1s) in PC is shown in fig. 2.8.
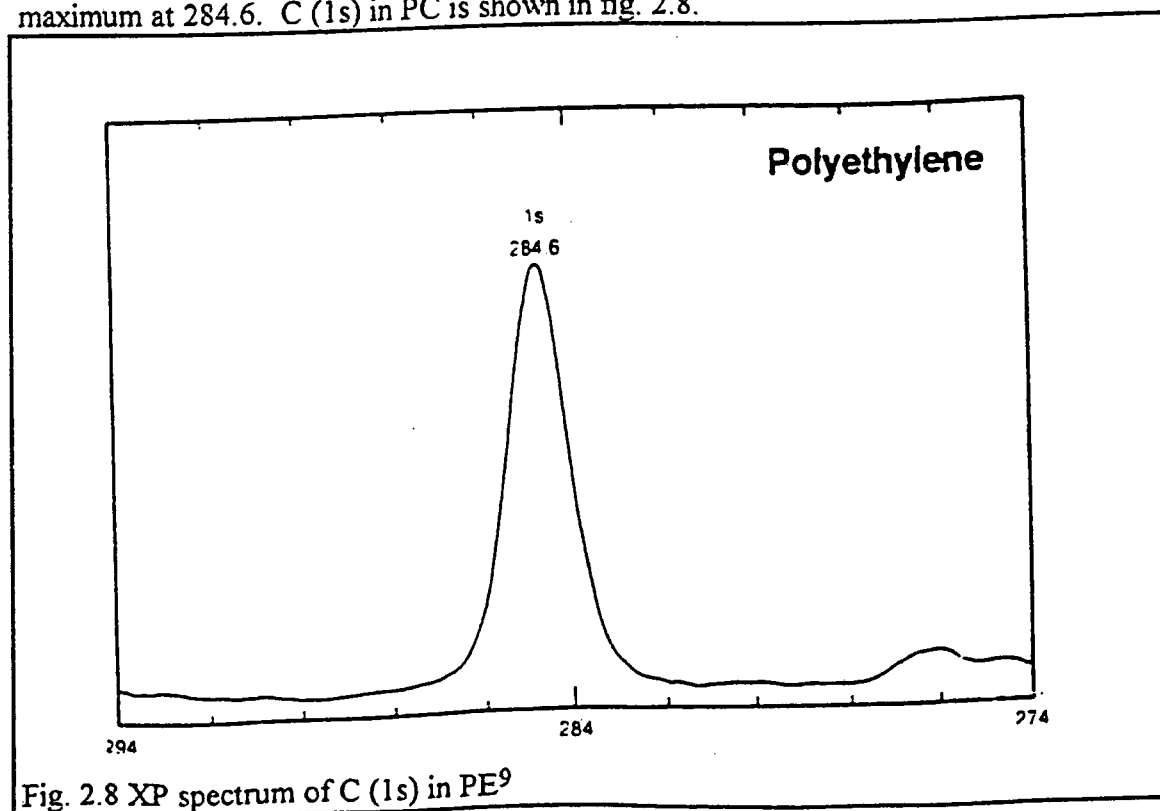


Fig. 2.8 XP spectrum of C (1s) in PE[9]

## 2.3.5 O (1s)

The element has a maximum at 531 eV, and in $Al_2O_3$ has a maximum at 531.6 eV (see fig. 2.9).
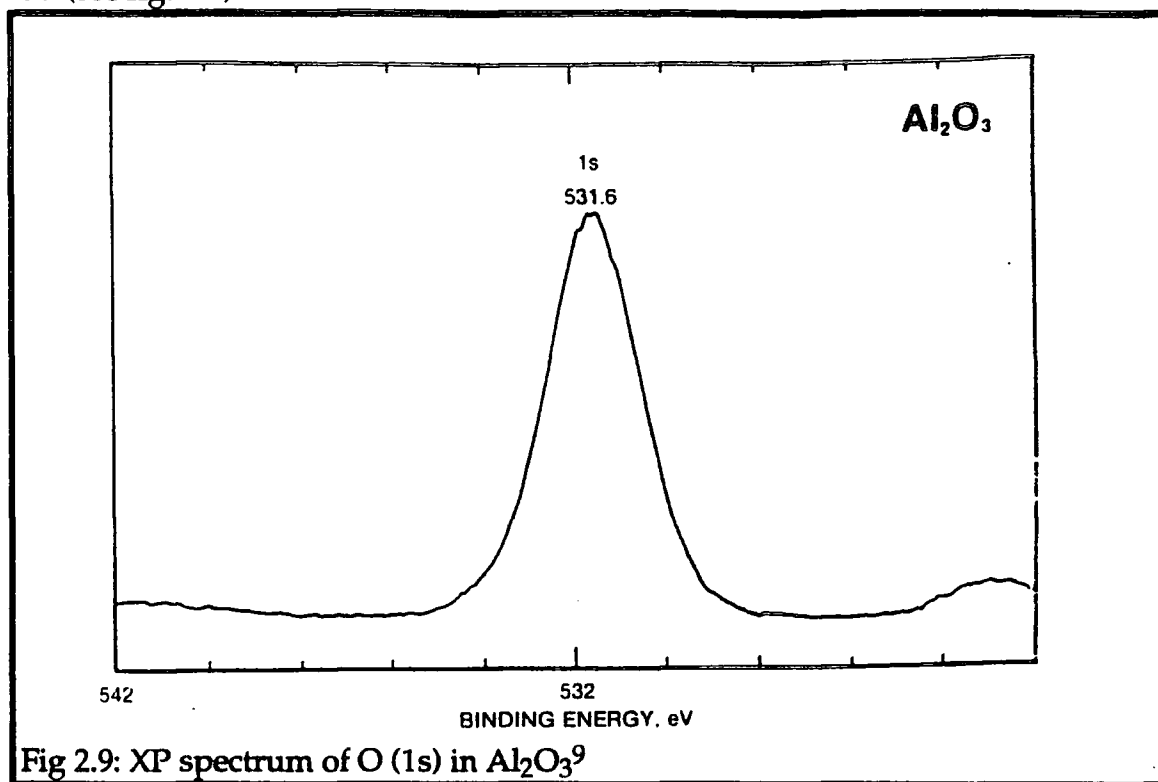


Fig 2.9: XP spectrum of O (1s) in $Al_2O_3$[9]

## 2.3.6 N (1s)

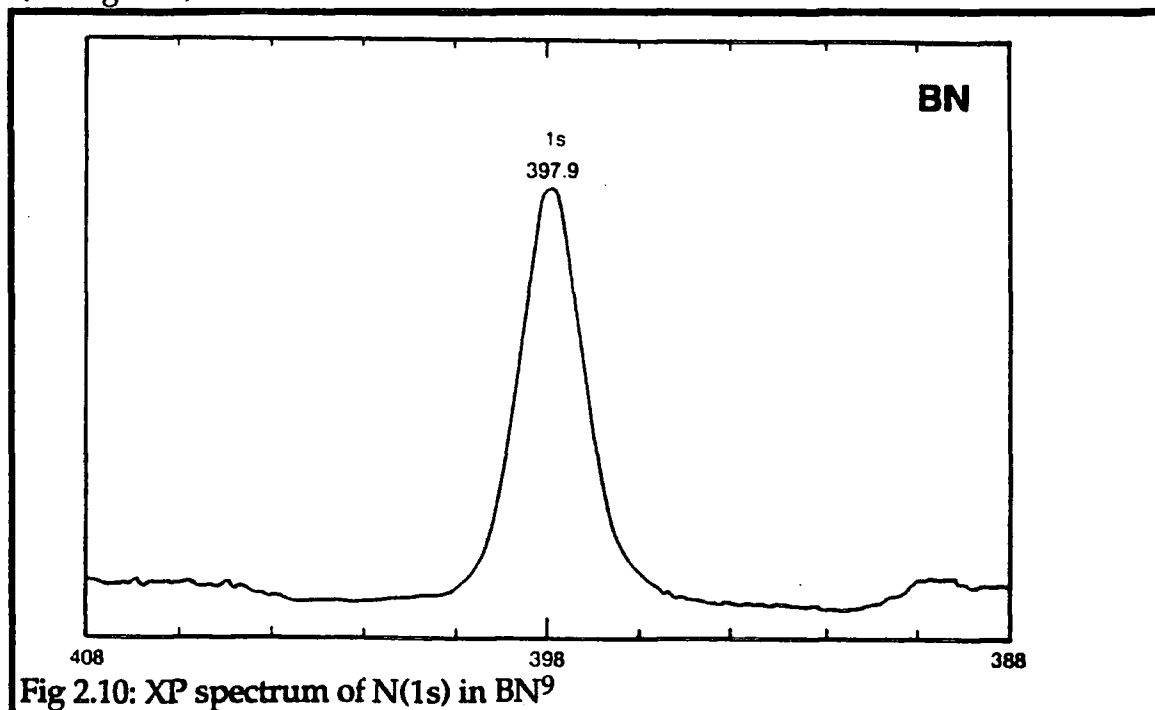The element has a maximum at 402 eV, and in BN has a maximum at 397.9eV (see fig 2.10).



Fig 2.10: XP spectrum of N(1s) in BN[9]

References

1 Briggs, D., Seah, M.P., *Practical Surface Analysis*, Wiley 1983 Chapter 1

2. Woodruff, D.P., Delchar, T.A., *Modern Techniques of Surface Science*, Cambridge University Press, 1992, Chapter3

3. Tong, H-M., Nguyen, L.T., *New Characterisation Techniques for Thin Polmer Films*, Wiley 1990 Chapter 11

4. Clark, D.T., Feast, W.J., *Polymer Surfaces*, Wiley, 1978, Chapter 16

5. Briggs, D., Seah, M.P., *Practical Surface Analysis*, Wiley, 1983, Chapter 2

6. Briggs, D., Seah, M.P., *Practical Surface Analysis*, Wiley, 1983, Chapter 3.

7. Walls, J.M., *Methods of Surface Analysis: Techniques and Applications*, Cambridge University Press, (1989)

8. Hollas, J.M., *Modern Spectroscopy*, Wiley (1987)

9. Perkin Elmer *Handbook of Photoelectron Spectroscopy* ,1989

10. Fuggle, J.C., Källne, E., Watson, L.M., *Phys. Rev.* **B16**, 750 (1977)

11. Anderson, C.R., Lee, R.N., Morar, J.F., *J. Vac. Sci. Technol.*, **20** 617 (1982)

12. Schön, G., *J. Electron. Spectros.*, **1** 377(1972)

13. Bird, R.J., Swift, P.J., *J. Electron Spectros.*, Relat. Phenom., **21** 227 (1980)

14. Abel, M.F., *J. Electron Spectros.*, **8** 213 (1976)

15. Lindau, I., Planetta, P., Yu, K.Y., Spicer, W.E., *Phys. Rev.* , B13 492 (1976)

16. Asami, K., *J. Electron Spectros. Relat. Phenom.*, **9**469 (1976)

17. Powell, C.J., Erickson, N.E., J. *Vac. Sci. Technol.*, **20** 625 (1981)

# 3. Thin Metallic Films:

# 3.1. Methods of Deposition of Thin Metallic Films:

### 3.1.1 Chemical Vapour Deposition (CVD):

Chemical Vapour Deposition (CVD)[1] is the process of chemically reacting a volatile compound of a material to be deposited with other gases, to produce a nonvolatile solid that deposits on a suitably placed substrate.

CVD methods have the ability to produce a large variety of films and coatings of metals, semiconductors, and compounds in either a crystalline or vitreous form. The equipment required is relatively inexpensive and CVD is suitable for batch and semi-continuous operation. Due to its popularity, many variants of CVD processing have been developed, including low pressure CVD (LPCVD), plasma enhanced CVD (PECVD), and laser enhanced CVD (LECVD).

The various types of chemical reactions that have been employed to deposit films and coatings are:

- Pyrolysis:        thermal decomposition of such gaseous species as hydrides, carbonyls, and organometallic compounds on hot substrates.

- Reduction        these reactions commonly employ hydrogen gas as the reducing agent to effect the reduction of such gaseous species as halides, carbonyl halides, oxyhalides or other oxygen containing compounds. Refractory metals such as W and Mo have been deposited by reducing the corresponding hexafluorides eg.

$$WF_6 + 3H_2 \rightarrow W + 6HF \ (300°C)$$

· Oxidation

An important oxidation reaction is:

$$SiH_4 + O_2 \rightarrow SiO_2 + 2H_2$$
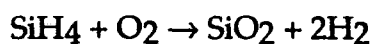
The oxidation of $SiH_4$, which leads to the deposition of $SiO_2$, is carried out during the processing of integrated circuits where higher substrate temperatures could not be tolerated.

· Disproportionation

These reactions are possible when a non-volatile metal can form volatile compounds with different degrees of stability depending on the temperature. This is especially noticeable in halide compounds, where the metal can exist in two valence states, such that the lower valent state is more stable at higher temperatures. The metal can be transported into the vapour phase by reacting it with its volatile, higher valent halide to produce a more stable lower valent form.

· Reversible transfer

Chemical transfer is characterised by a reversal in the reaction equilibrium at source and deposition regions maintained at different temperatures within a single reactor. An important example of this type of reaction is the deposition of single crystal GaAs films by the chloride process according to the reaction

$$As_4 + As_2 + 6GaCl + 3H_2 \rightarrow 6GaAs + 6HCl$$

37
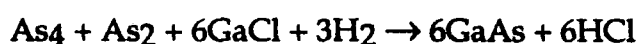
The previous examples are a small sample of the CVD film and coating deposition reactions. A table is presented below of CVD processes for depositing elemental and compound semiconductors and other assorted compounds.

| Deposited Material | Substrate | Input Reactants | Deposition Temperature (°C) |
|---|---|---|---|
| Si | Single crystal Si | Either $SiCl_2H_2$, $SiCl_3H$ or $SiCl_4$ + $H_2$ | 1050-1200 |
| ZnS | GaAs, GaP | Zn, $H_2S$, $H_2$ | 825 |
| CdS | GaAs, sapphire | Cd, $H_2S$, $H_2$ | 690 |
| $Al_2O_3$ | Si | $Al(CH_3)_3$ + $O_2$ | 275-475 |
| $TiO_2$ | Quartz | $Ti(OC_2H_5)_4$ + $O_2$ | 450 |
| TiN | Steel | $TiCl_4$,$N_2$, $H_2$ | 1000 |
| BN | Steel | $BCl_3$, $NH_3$, $H_2$ | 1000 |

Table 1: CVD Processes for Deposition

## 3.1.2 Physical Vapour Deposition (PVD):

The two main types of PVD are evaporation and sputtering.[1] In evaporation, atoms are removed from the source by thermal means, whereas in sputtering the atoms are dislodged from solid target surfaces through impact of gaseous ions.

Some factors that distinguish PVD from CVD are:
- Reliance on solid or molten sources
- Physical mechanisms (evaporation and collisional impact) by which source atoms enter the gas phase.

- Reduced pressure environment through which gaseous species are transported.

- General absence of chemical reactions in the gas phase and at the substrate surface

Metals evaporate generally as atoms and occasionally as clusters. Solid evaporation rate is controlled by the temperature of the source, which in turn governs the vapour pressure. Gold has a minimum evaporation temperature of 1132°C, and can be evaporated from a W or Fe basket. Metal films can be deposited at high rates and with excellent control of structure and properties.

### 3.1.3 Sol Gel

The sol-gel process is the name given to any one of a number of processes involving a solution or sol that undergoes a sol-gel transition[2]. A solution is a truly single phase liquid, while a sol is a stable suspension of colloidal particles. At the transition, the solution (or sol) becomes a rigid porous mass by destabilisation, precipitation or supersaturation.[3]

Most of the coatings are true one-phase solutions which go through a sol-gel transition to a rigid two-phase system of solid and solvent filled pores. The sol-gel transition in this case is not reversible.

The advantages of this method include the facts that material use is efficient, the films formed are of high purity and are homogeneous, and it can be used to make films that, using other techniques, separate into two phases. A disadvantage is that the raw materials are often expensive.[2]

### 3.1.4 Techniques for Depositing Gold:

*3.1.4.1 In Situ Techniques for Preparing Thin Gold Films:*

Research into *in situ* production of metal bearing compounds and particles in the gas phase[4] has been prompted by continuing interest in alternative methods of thin film production. These *in situ* approaches eliminate the need to synthesise, store and handle metal compounds used in chemical vapour deposition (CVD) techniques and solution based techniques, which are often toxic and sensitive to air and moisture.

Gold films are of particular interest for the electronics industry, and several CVD methods have been utilised.[5] It has been proposed[4] that a combination of several proven techniques could result in the development of a new technique for the production of gold compound/ composite particles.

Some of the *in situ* methods of preparing thin gold films are discussed below:
1. Industrial techniques often use plasmas to provide the reactive environment into which evaporated or sputtered metal atoms are introduced. The *in situ* formation of gold oxides and halides has been reported using this approach.[6]

Several groups have reported the incorporation of large amounts of Au particles (10-20 nm diam) into plasma polymerised films by sputtering Au into radio frequency (RF) stimulated halocarbon plasmas.[7,8,9]

2. Small amounts of gold oxide[10] and gold carbonyl[11] complexes have been formed in cryogenic matrices for spectroscopic analyses by co-deposition of Au vapour with $O_2$, CO, $C_2H_2$ or $C_2H_6$.

3. Evaporation of gold into a gaseous environment at concentrations high enough to promote homogeneous or heterogeneous nucleation is another

method of thin film formation. The resultant ultrafine particles are then used to form thin films. Gold blacks and gold smokes have historically been prepared by evaporating Au into a hydrogen, nitrogen or inert gas at pressures of 100-1300 Pa.[12, 13] Gold films prepared from these materials are composed of loose networks of 1-25nm diameter gold particles and have low electrical conductivity and optical reflectivity. Harris et al[14] could increase particle size by increasing the nitrogen pressure between 50-400 Pa. McKenzie[15] altered the optical properties of gold blacks by incorporating tungsten oxides. However, gold black films collapse at temperatures greater than 385K.

4. Some techniques producing ultrafine particles (showing bulk metal properties) include neutral and ionised cluster beams formed in supersonic jets emitted from a heated crucible through a nozzle (gas pressure =1300Pa).[16] However, the disadvantage with this method is that low yields (1-2%) are obtained.

5. Owing to contamination from container materials, another method using lasers was employed to deposit thin gold films. [17, 18] For example a low energy (<10mJ/pulse) Na: Yttrium-Aluminium-Garnett (YAG) laser followed by supersonic expansion and then direct pulsed vaporisation of gold[19] has been used to form small amounts of gold clusters.

6. Using a solid gold target and various carbonaceous/diluent gas mixtures at 600-1400 Pa pressure, in a high power pulsed laser stimulated plasma, superfine gold has been produced. These films have 82-99% Au by mass.[20]

7. Etching of a metal (gold) by energetic ion enhanced chemical plasma and injection of this volatile species into a plasma containing a polymer (fluorocarbon) film matrix, achieves a highly crosslinked fluorocarbon polymer film with zero valent gold clusters. This technique can be used to control metal

content, metal cluster size, and crystallographic structure of the resultant films. In comparison with other techniques, the rate of deposition is very much slower and the metal clusters are formed by metal atom migration onto a fluorocarbon surface which is subject to low energy ion bombardment.

### 13.2.2 CVD Techniques

Thin gold coatings have been prepared by CVD on heated substrates, using $AuCl_2^-$ or $AuCl(PPh_3)$ complexes as starting materials,[22] but uniform gold films were difficult to obtain.[24]

Laser CVD[25] and laser photolysis[26] of dimethyl(2,4-pentane-dionato) gold(III) ($Me_2Au(acac)$), have also been employed as CVD gold deposition techniques.

A metal doped system can be obtained by combined techniques like the evaporation of gold from an external source during plasma polymerisation of organic compounds[27] or plasma polymerisation with simultaneous sputtering of the metal.[9]

Growing pure films of PECVD of $Me_2Au(acac)$ has also been studied.[23] An advantage of this method is that high substrate temperature is avoided and the deposition of thin films can be carried out at room temperature or at slighly elevated temperatures.

### 3.1.2.3 PVD Techniques

Photodeposition[29] of gold is difficult owing to the scarcity of precursors. Alkyl molecules are not volatile and the carbonyls are either unavailable or do not exist. Gold can be photo-deposited from the vapour phase using a simple optical projection system to produce metal line widths as small as $2\mu m$. $Me_2Au(acac)$ was photo dissociated by pulsed excimer radiation at 193nm (ArF). Films 2000-3000Å thick were produced. No deposition occured if the

wavelength was 351nm which demonstrated that the film growth processes are photochemical in nature.

Sputtering of gold from dimethylgold hexafluoracetylacetonate (DMG) can be carried out at room temperature by ion beam irradiation, to form an Au film. These films exhibit roughly 30% C contamination, poor resistivity and large void areas in the deposited film. Heating the substrate to 100°C during deposition resulted in a decrease in carbon contamination, near bulk resistivity and higher density polycrystalline deposits.[31]

### 3.1.4.4 Sol-Gel

A nanocomposite of clusters of gold atoms in a silica gel matrix has been prepared by the sol-gel technique through reduction of gold chloride. Using tetramethoxysilane (TMOS), $SiO_2$ was extracted by hydrolysis.[28] Citric acid was used to reduce $AuCl_3$ and Au was dispersed in the silica gel insulating matrix. This method was used to achieve a film of high dielectric strength. The gold islands amid the silica gel are materials which are designed to utilise the percolation phenomenon, which is to create a peak in the dielectric constant, as a function of optimal topology.

## 3.2 Optical Properties of Metallic Discontinuous Films.

### 3.2.1 General Introduction

If one assumes the small metal particles to be clusters of 1-100Å, a large percentage of the atoms are on the surface.[30] The existence of this vast interface between the cluster and the surrounding medium can have a vast effect on the cluster properties. Typically these clusters are surrounded by dielectrics such as air, solvents, polymers, or glasses, which have much lower

refractive indices than the inorganic metal clusters themselves. Because of this refractive index boundary, the field intensity near, at and inside the cluster surface can be enhanced considerably to the incident intensity. This enhancement in local field may be considered to be a result of the "dielectric confinement effect" and can be an important factor in describing the spectroscopy, photochemistry and non-linear optical properties of metal clusters.

In the case of small metal particles dispersed in a host matrix, an anomalous optical absorption arising from optical resonance is typical.[30] The position of the absorption maximum in the spectrum and its intensity are functions of the starting materials, metal volume fraction $f$ , the size and shape of the metal grains, and the effect of disorder.

For example, in a matrix containing plasma polymers and gold, the absorbance of the metal free plasma polymerised layers is small in the visible and infra red (ir) regions. When a small amount of gold is incorporated into the polymer, a minimum in transmission occurs near $0.55\mu m$ and intensifies with increasing $f$. For higher values of $f$ the transmittance on the ir side decreases due to an increase in film reflectance and intrinsic absorbance of gold (fig. 3.1)

Fig. 3.1:
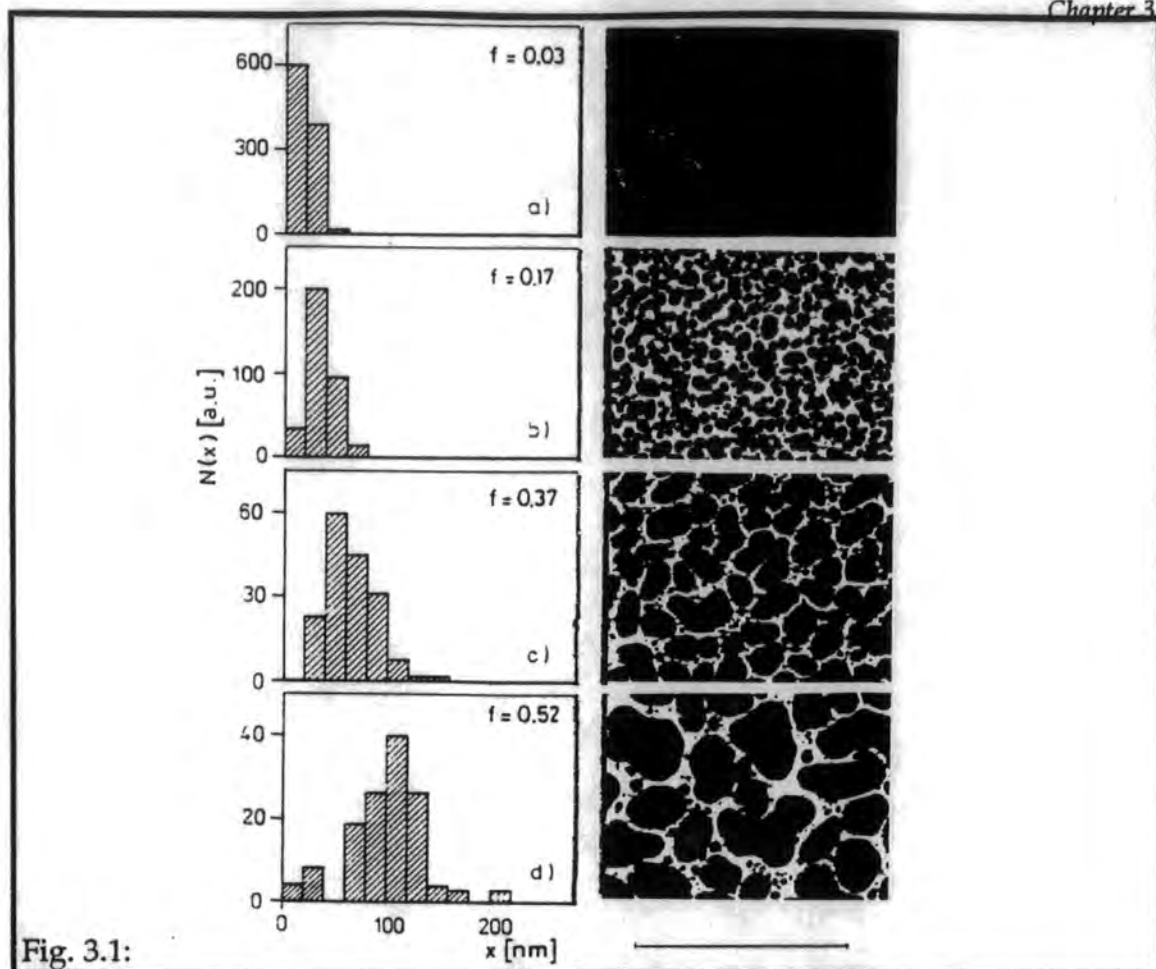
A pronounced absorption maximum develops in the visible region from optical resonance when the metallic grains are large enough, i.e. more than a few nanometers in size.[32]

However, when a carbon matrix is used (and not a plasma polymer and incorporated metal), there is a higher absorption in the visible region. When metal grains are dispersed in a carbon matrix the development of the optical selectivity is masked by the overall absorption of the carbon matrix itself.

There are models to explain the optical properties of metallic films and these are discussed in detail below.

### 3.2.2 Effective Medium Theory

The effective medium theory assumes a micro structural representation in the form of unit cells that are embedded in the effective medium (EM).[32] This EM is described as a macroscopically homogeneous material with properties such that the random unit cell embedded into it is not detectable by electromagnetic radiation of the given wavelength. This means that the replacement of some of the EM by the unit cell does not change the electrical field in the surroundings of the cell and the propagating wave is not scattered by the cell in the EM.

A homogeneous system may be described by:

$$\varepsilon(\omega) = \varepsilon_r - i\,\sigma/\omega \qquad (3.2.2.1)$$

where $\varepsilon(\omega)$ is the complex dielectric relative permittivity, $\varepsilon_r$ is the real part, i is imaginary, $\sigma$ is the conductivity and $\omega$ is the circular frequency.

The behaviour of a two phase composite material may be described by an effective dielectric function $\varepsilon$:

$$\varepsilon(\lambda) = N^2(\lambda) = [n(\lambda) + ik(\lambda)]^2 \qquad (3.2.2.1)$$

where N is the complex refractive index, n the refractive index and k is the extinction coefficient. The effective dielectric function is dependent on the permittivities $\varepsilon_a(\lambda)$ and $\varepsilon_b(\lambda)$ of the constituents a and b, the respective filling factors $f_a$ and $f_b$ and a variety of structural factors.

ie $\qquad \varepsilon = \varepsilon(\varepsilon_a, \varepsilon_b, f_a, f_b, \text{microstructure}) \qquad (3.2.2.3)$

Heterogeneous materials exhibit various types of microstructure but the most frequent ones are:[33]

a)  cermet structure, particles of component b are dispersed in a continuous medium a (fig. 3.2a)

and

b)  aggregate structure where both components a and b are randomly mixed (fig 3.2b).

It is usually accepted that both constituents completely fill the volume of the composite i.e., $(fa + fb = 1)$.

Several models have been proposed to characterise the optical response of heterogeneous sytems. Maxwell and Garnett proposed that a cermet structure is a unit cell formed by a coated sphere consisting of a nucleus with permittivity $\varepsilon_b$ and the coating shell with permittivity $\varepsilon_a$ (fig 3.2c).

The ratio between the dimension of the nucleus and coating thickness is given by the respective volume fraction $f$.. This yields the effective dielectric function[34] $\varepsilon_{mg}$ as

$$\frac{\varepsilon_{mg}-\varepsilon_a}{\varepsilon_{mg}+2\varepsilon_a} = f \frac{\varepsilon_b-\varepsilon_a}{\varepsilon_b+2\varepsilon_a} \qquad (3.2.2.4)$$

where $f = fb = 1 - f.a$

This is limited to a low $f$ region (usually $f < 0.3$) for topologically assymmetric systems when one component considerably dominates. The Maxwell Garnett (MG) model describes the optical responses.

47

The structural equivalence of the components in the aggregate structures results in a unit cell filled by material b with probability $f$ and by material a with probability $1-f$. (fig 3.2d) This yields the Bruggeman Self Consistent[35] expression for the effective permittivity, $\varepsilon_{BSC}$ as

$$\frac{3f}{2+\varepsilon b/\varepsilon_{BSC}} + \frac{3(1-f)}{2+\varepsilon a/\varepsilon_{BSC}} = 1 \qquad (3.2.2.5)$$

The BSC model predicts the percolation threshold value for the electrical conductivity but it fails when predicting the optical behaviour. Therefore further models have been proposed. For example the probabilistic growth model which incorporates both of the above theories: (Sheng[36, 37]).

The model is based on the probability of nucleation during thin film growth and the theory of an EM. The medium is supposed to be formed by particles of two types: a metal grain surrounded by an insulator or a dielectric grain covered by a metal (fig 3.2e). The dielectric responses from a simplified version of this model[36] are defined by
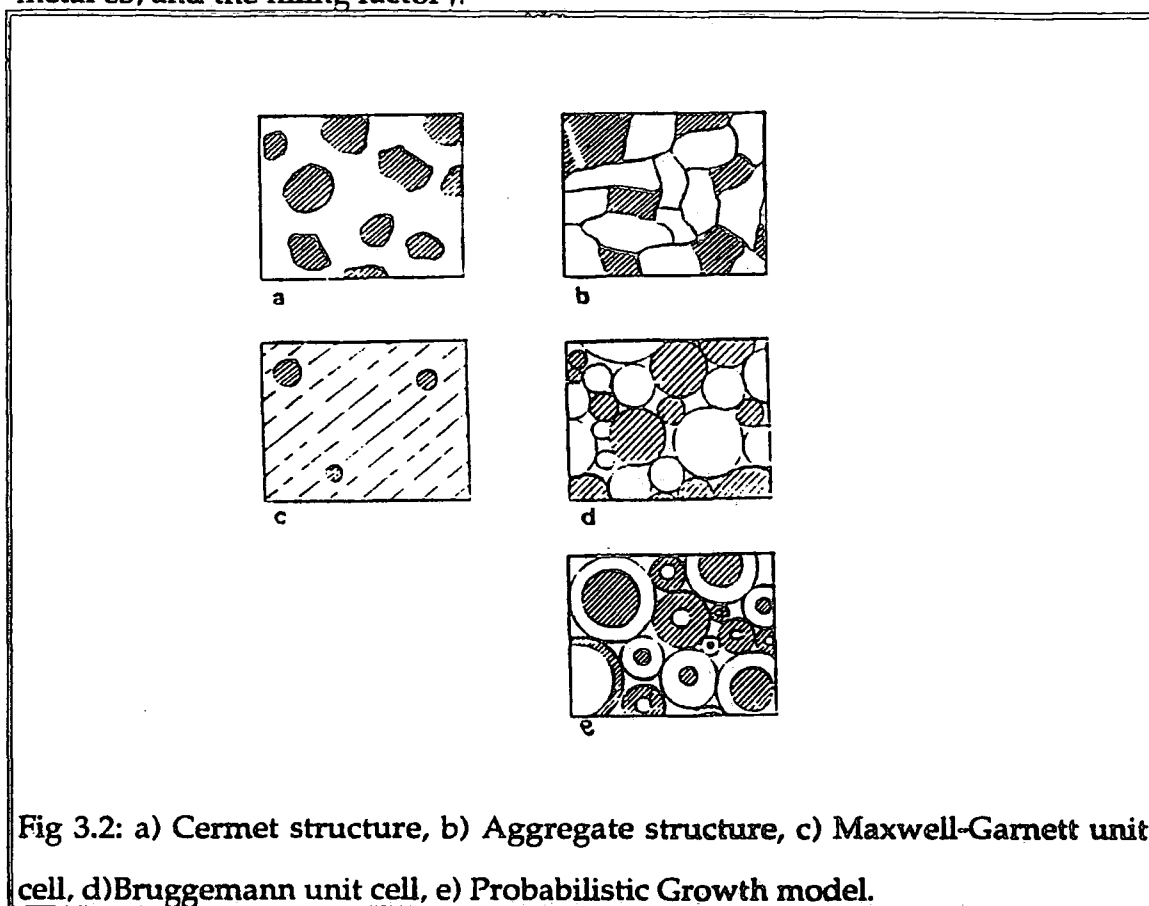
$$\varepsilon_1 = \varepsilon_a \frac{2f(\varepsilon_b-\varepsilon_a) + (2\varepsilon_a+\varepsilon_b)}{(2\varepsilon_a+\varepsilon_b) - f(\varepsilon_b-\varepsilon_a)} \qquad (3.2.2.6)$$

and

$$\varepsilon_2 = \varepsilon_b \frac{2(1-f)(\varepsilon_a-\varepsilon_b) + (2\varepsilon_b+\varepsilon_a)}{(2\varepsilon_b+\varepsilon_a) - (1-f)(\varepsilon_a-\varepsilon_b)} \qquad (3.2.2.7)$$

where subscript 1 signifies the grains with the metal in the centre and 2 signifies the dielectric grains covered by the metal.

48

The dielectric response depends on the permittivity of the dielectric $\varepsilon a$, of the metal $\varepsilon b$, and the filling factor $f$.

Fig 3.2: a) Cermet structure, b) Aggregate structure, c) Maxwell-Garnett unit cell, d)Bruggemann unit cell, e) Probabilistic Growth model.

As the properties of metals in the form of small grains substantially differ from the bulk properties, the size effect must be considered. It is therefore necessary to change the permittivity of the metal by changing the relaxation times of the electrons according to the actual grain diameters.[38, 39]

### 3.2.3 Optical Properties of Thin Semicontinuous Gold Films over a Wavelength Range of 2.5 to 500μm

For metal/insulator composites, an anomalous absorption peak is found in the visible or near infra-red (IR) regime.[40] Several effective medium theories have been used to calculate the optical properties of such materials (Maxwell Garnett, Bruggemann and modifications of these two approaches).

It has been found that these theories are applicable if the samples are not too close to the metal-insulator transition and the optical wavelength is long enough i.e. as long as the optical wavelength is much larger than the metallic grains.[41]

Recently a new scaling model has been proposed[42] to calculate the optical properties of two dimensional composites near the percolation threshold (the metallisation transition).

The anomalous diffusion length $L(\omega)$[43] on the time scale $1/\omega$ is the relevant length scale, and is much shorter than the optical wavelength. As long as the percolation length $\xi$ is larger than $L(\omega)$ the film is inhomogeneous and the effective medium approach is not applicable, as the theory assumes film homogeneity. Only when $L(\omega)$ is much more larger than $\xi$ can the film be treated as homogeneous.

Following the above arguments, films close to the percolation threshold may appear to be inhomogeneous even in the far IR regime, where $\xi$ is shorter than the optical wavelength but longer than $L(\omega)$.

*In situ* optical measurements[44] have shown that such films should be considered as inhomogeneous over a wide range above and below the percolation threshold at 2.2$\mu$m.

Much longer wavelengths (2.5-500$\mu$m) should be used therefore to detect the crossover between the homogeneous and the inhomogeneous behaviour. Both the ME theory and the scaling model were compared and the scaling model proved more accurate.

## 3.3. Electrical Properties:

### 3.3.1 Introduction to Microelectronics Processing:

Microelectronics processing is a question of surfaces. Processing techniques are concerned with modifying properties no more than a few microns below or above the surface of a working material. The flat macroscopic object on which processing occurs is the substrate.[45]

A substrate can be transformed into a set of electrical devices. These devices must be connected with each other and the outside world to form a useful circuit. To form these connections two types of materials are required; conductors and insulators. The conductors form the electrical connections and the insulators separate the conductors from each other, the substrate and the external contaminants. These materials are deposited on the surface of the substrate as films, a micrometer or less in thickness, and then are patterned photolithographically. Hence thin film deposition is a branch of microelectronics technology.[45]

The principal reason for depositing metal films onto microelectronics substrates is to fabricate conductive interconnections between circuit elements. The substrate is first covered with an insulating film through which windows are then etched to allow the metal to contact the substrate. The metal is then deposited and photolithographically patterned into strips connecting the desired elements. From an electrical point of view these strips must be adequate current carriers and make good electrical contact where they touch the substrate.

Chemically the film must be stable, adhere well to the substrate and allow photolithography and etching.[45]

### 3.3.2 The Conduction Mechanism in Thin Discontinuous Metal Films

The conduction mechanism in discontinuous metal films has never been satisfactorily explained. The electrical properties of metallic discontinuous films can be treated in terms of theoretical concept derived for granular metals.[46, 47]

From the point of view of the electrical properties three structural regimes are distinguishable:[48]

1) The metallic regime: the filling factor is large i.e. the metallic content is high.

2) The dielectric regime: isolated metal particles are dispersed in a metallic continuum i.e.. the filling factor is small.

3) The transition regime

In the metallic regime, the magnitude of the electrical conductivity may be several orders lower than its bulk metal value due to strong electron scattering from dielectric grain inclusions and grain boundaries, which both decrease the electron mean free path.

By decreasing the metal content, the dielectric inclusions form a maze structure and the metal exists as individual grains or islands. The changeover from metallic to dielectric regime occurs via a transition regime and both electron percolation (see section 3.2.2.2) along the metallic maze and tunnelling (see section 3.2.2.1) between metal islands gives rise to conductivity in a three dimensional path. The conductivity drops by many orders of magnitude. This abrupt transition can be referred to as the percolation threshold characterised by a critical metal volume fraction $fc$.

Finally, in the dielectric regime the dominating conductivity mechanism is the charge transport of electrons and holes by tunnelling from one isolated grain to the other.

The electrical conduction in polymer systems is predominantly governed by the amount of metal and its micro structural arrangement.[49] This can generally be analysed by the EM approach where the islands are assumed to be oblate spheroids.
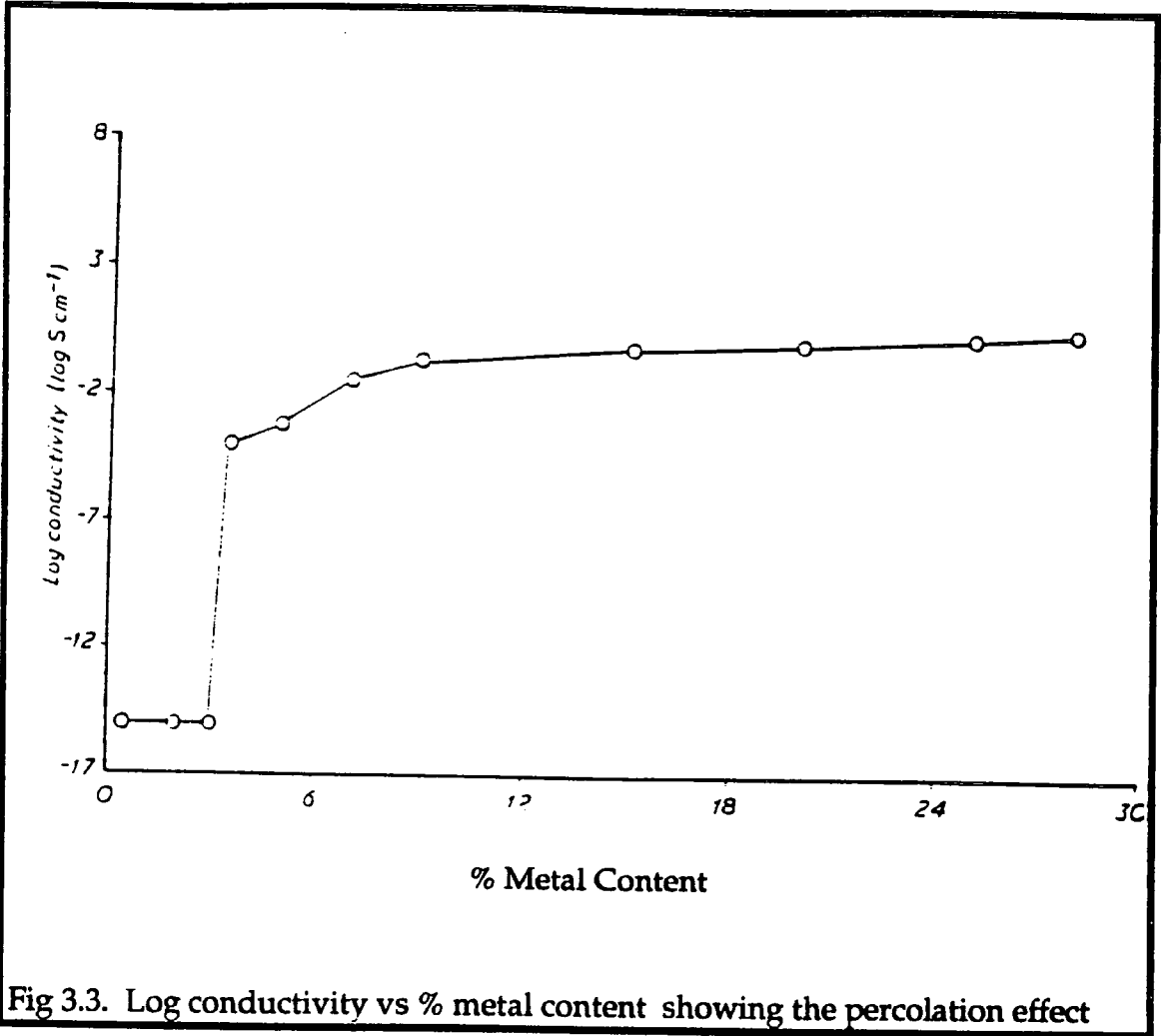
### 3.3.2.1 Tunnelling

If two metals separated by an insulator, the insulator normally acts as a barrier to the flow of conduction electrons from one metal to the other. If the barrier is sufficiently thin (<10-20Å) there is a significant probability that an electron which impinges on the barrier will pass from one metal to the other.[50] This phenomenom is known as tunnelling.

### 3.3.2.2 Percolation

In the region of low metal concentrations, the metal is in the form of small particles and is distributed in the insulating host. There are no contacts between the adjacent metal particles. As the metal content is increased, agglomerates of the metal begin to form, and these metal particles are in contact with one another. At a certain metal content, the growing agglomerates of the metal begin to touch each other, and as a consequence, a metal network is formed and the conductivity shows a drastic increase to the high value of the conductive network. After this, conductivity shows a slight increase with increasing metal content and eventually reaches a plateau (see fig 3).[51]

The critical point is referred to as the percolation threshold and percolation is conduction along touching metal particles.



Fig 3.3. Log conductivity vs % metal content showing the percolation effect

### 3.3.3 Theory of Conduction

Neugebauer and Webb[53] proposed the tunnelling model which states that the transfer of an electron between two initially neutral islands results in an increase in the systems electrostatic energy (charge density). The equilibrium density of charged islands is related to the total density, N, of islands by the Boltzmann distribution:[52]

$$n=N \exp (-\partial E/kt) \qquad (3.3.3.1)$$

$\partial E$ is the activation energy and is given by:

$$\frac{e^2}{4\Pi\, E_r} \qquad (3.3.3.2)$$

i.e. the electrostatic energy of an isolated charged island of radius r (the work required to remove an electron to infinity).

$\partial E$ is also:

$$\frac{e^2}{4\Pi\, E} \left( \frac{1}{r} - \frac{1}{2r+s} \right) \qquad (3.3.3.3)$$

when the distance between the islands is s. i.e. the energy required to remove the electron to the next island situated a distance s away.

Later Abeles and Dryer[54] proposed that there were two types of tunnelling transition:

1. Neutral-neutral transfers (charge carrier generation)

2. Neutral charged tunnelling (non-activated mobility term)

This implies that along a given percolation path through the films, activated charge separation clearly requires a greater gap potential than non-activated charge transfer to pass the same average current.

Swanson[55] proposed that the tunnelling was due to three types of tunnelling transition:

1)    Neutral-neutral tunnelling (charge separation)

2)    Positive-negative (recombination)

3)    Charged-neutral

In this case there is no mobility concept.

Hill, Kiernan, Stops, Barr & Finney[56] assumed a fundamentally different approach. They calculated the tunnelling between two initially neutral islands with respect to the requirement that the tunnelling excess must be able to provide the electrostatic energy.

Barr & Finney' s[56] result is considered to be the most accurate. The current density is evaluated at one point along its path (the point of charge carrier generation) and the mobility concept is unnecessary.

### 3.3.4 The Conduction Mechanism in Thin Gold Films

The most widely studied granular or island metal film has been gold because of its chemical stability and freedom from multilayer oxidation.[53]

Neugebauer and Webb[53] proposed that the charge transport mechanism in gold island films is thermally activated electron tunnelling between the islands which are separated by a few nanometers. However, this has never proved very reliable as tunnel currents exist for a simple metal-insulator-metal (MIM) structure and are critically dependant on the gap width. This and other parameters are generally not precisely known, so even for the simplest tunnel junction this theory is not reliable.[57]

In gold granular films, a statistical size distribution is assumed, for island and interisland gap. The tunnelling theory considers only one or two potential barriers and these are assumed to be identical[57] Due to this statistical size distribution a different approach was considered, by Morris & Coutts, based on the percolation theory.[52] This is limited to considering a distribution of linear resistors or diodes which predicts a power-law dependence of conductivity with potential.[60]

Another method proposed[57] as a modification to the latter is to look for the sharp rise in current which occurs at the $P_c$, the percolation threshold, to identify tunnelling as a transport mechanism at MIM (Metal-Insulator-Metal) junctions. The results can be interpreted as arising from a network of non-linear tunnel junctions and it is proposed that a resonant tunnelling process occurs between localised states a few meV below the insulator conduction-band edge.

### 3.3.4.1 Gold-Temperature dependance

It is assumed[59,60] that the main conduction mechanism in gold granular films is a direct tunnelling of electrons between metal islands within the insulator through a barrier potential which changes with the temperature.

The corresponding potential drop shifts the position of the Fermi level with respect to the bottom of the conduction band of the insulator and changes the height of the tunnelling barrier.

The conduction process is generated by four different types of mechanisms:[58]

1) Direct tunnelling of electrons between metal islands, which is responsible for the main conductivity process at low temperatures.

2) Thermionic current, which is responsible for the conductivity process at high temperatures.

3) Tunnelling of electrons from surface states of the insulator to the metal islands, which is necessary to obtain thermal equilibrium of the electrons at the metal-insulator interface.

4) A thermal injection of electrons from the metal to the conduction band of the insulator, which contributes to the balance of dispatched charge and becomes important at the highest temperatures.

Both the direct tunnelling and the thermionic effect occur between metal islands within the insulator and are limited to a very thin layer of the insulator itself (20Å) below the surface. Therefore, the conductance between two metal islands can easily be calculated, at each temperature, once the potential barrier is found.

A study [58] was done on discontinuous gold films on different substrates; sapphire, fused silica, quartz and mica. A typical structure of the film is represented by large islands separated by gaps, which are also generally large,

but become small in critical points where electrical conduction from one island to another takes place. The smallest distance of the islands must be of the order of few tens of angstroms to account for the observed conductivity of these films by tunnelling.
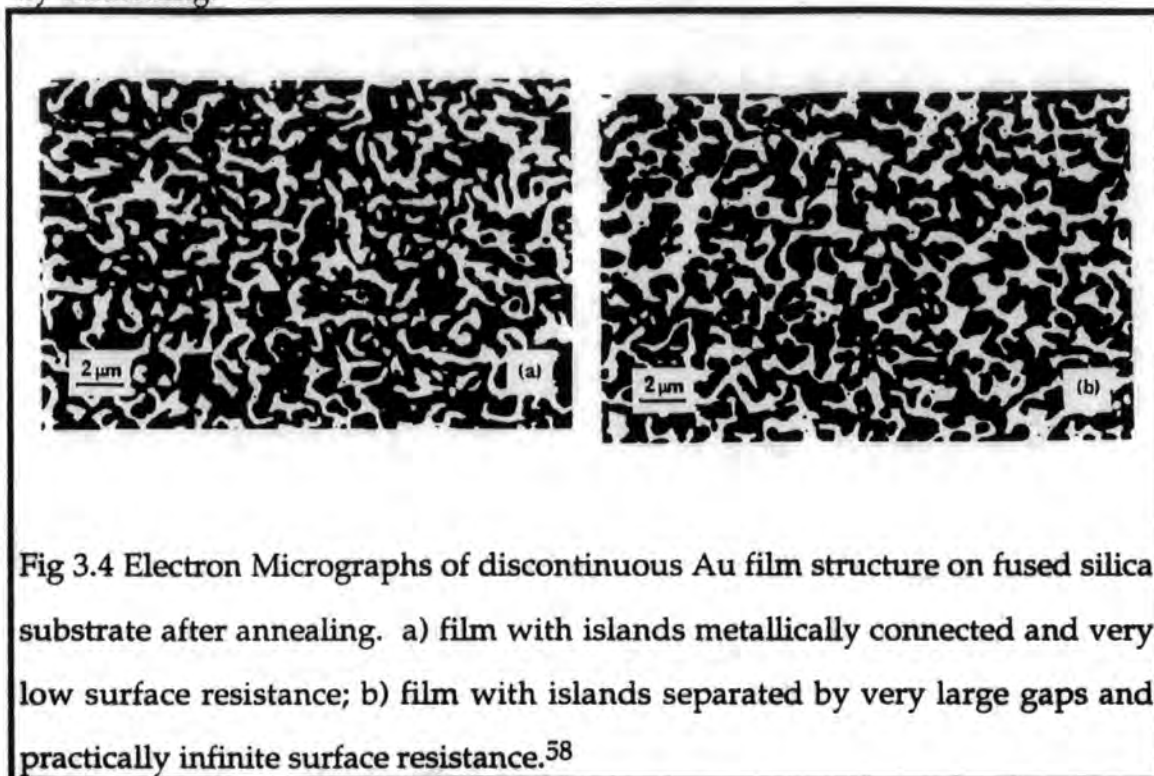


Fig 3.4 Electron Micrographs of discontinuous Au film structure on fused silica substrate after annealing. a) film with islands metallically connected and very low surface resistance; b) film with islands separated by very large gaps and practically infinite surface resistance.[58]

Typical results on the electrical conductivity versus temperature for gold films deposited on different types of substrates can be seen in fig. 5.
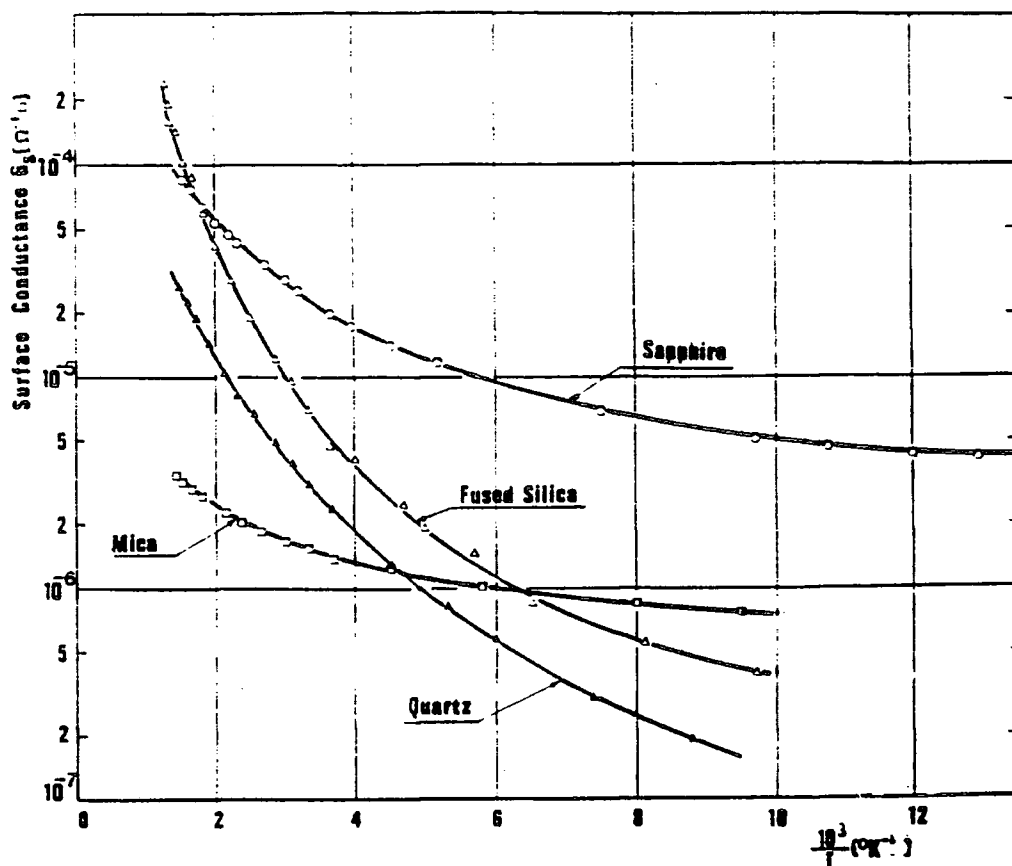
Fig 3.5 Electrical conductivity vs temperature for gold films deposited on different types of substrate.

From the above figure it should be noted that the temperature dependence is non-linear. (Other authors [53, 46] presumed a linear dependence because their temperature interval measurements were too small).

Gold on fused silica has a conductivity change which is about one order of magnitude greater than gold on sapphire for the same temperature interval of 600K. This is because of a difference in film structures.

The experimental data lead to the conclusion that the present theory of the electrical conductance behaviour versus temperature is confirmed over a large range of temperatures, provided that the thermionic effect is neglected. This fact is explained by observing that the mean free path of the electrons within

60

the substrate and near its surface is probably smaller than the gap width between the metal islands.

## 3.4 Conclusions

Several methods are used to deposit thin metallic films, and these include CVD, PVD, and Sol-gel techniques. The most common methods of depositing thin gold films are various PVD techniques, eg., evaporation, ion plating, and sputtering.

Discontinuous thin films have very important electrical properties and the most research in this field has been carried out on the formation of electrical properties of these films. However, complementary optical measurements have also been performed. The optical properties of these films are unique as there exists a large interface between the metallic clusters and the surrounding medium. The position and intensity of the optical absorption maximum are dependant on the metal volume fraction, the size and shape of the metallic grains, and the effect of disorder. Several models have been proposed to explain the optical properties of discontinuous metallic films.

The electrical properties and conduction mechanism of discontinuous thin films has never been satisfactorily explained. However, several models have been proposed. The most accurate of these models is that proposed by Barr & Finney, who calculated the tunnelling between two initially neutral islands with respect to the requirement that the tunnelling excess must be able to provide the electrostatic energy. The conduction mechanism in discontinuous gold films was proposed, by Despax et al, to be temperature dependant.

In the work described in this thesis, a method of deposition of a conducting gold film was established. The technique established is very different to the methods outlined at the beginning of this chapter. This method consisted of

the surface modification of spin coated gold (III) chloride film through the use of a hydrogen plasma.

## 3.5 References:

1. Ohring, M., *The Materials Science of Thin Films*, Academic Press, 1991

2. Vossen, J.L., Kern, W., *Thin Films Processes II*, Academic Press 1991

3. Klein, L., *Ann. Rev. Mater. Sci.*, **15** 227 (1985)

4. Colgate, S., et al, *J.Vac. Sci. Technol.* B9 (3) 1577 (1991)

5. Sugano,S., *Microcluster Physics*, Springer-Verlag 1991 Chapter 8

6. Klumb, A., Aita, C., *J. Vac. Sci. Technol.*,A7 1697 (1989)

7.Roy, R., Meissner, R.,*Thin Solid Films* **109**, 27, (1983)

8. H.Biederman, *Vacuum* **34**, 405, (1984)

9. Perrin, C., Despax, B., Kay, E., *J. Vac. Sci. Technol*, A4,46 (1986)

10. Kasai, P., Jones, P., *J.Phys.Chem.* **90** 2439 (1986)

11. McIntosh, P., Ozin, G., *Inorg. Chem.* **16** 51 (1977)

12.Harris, L., Beasley, J., *J.Opt. Soc. Am.* **42** 134 (1952)

13. Granquist, C., Hunderi, O., *Phys.Rev* . B16 3513 (1977)

14. Harris, L., McGinnies, R. , Siegel , B., *J. Opt. Soc.Am* . **38** 582 (1948)

15. McKenzie. D., *J. Opt. Soc. Am.* **66** 249 (1976)

16. T.Tagaki, D., Ymada, I., Sasek, A., *J. Vac. Sci. Technol.* **12** 1128 (1975)

17. Richtmeier, S., Parks, E., Liu, Y., Pobo, L., Riley, S., *J. Chem. Phys.*, **82** 359 (1985)

18. Whetten, R., Cox, D., Trevor, R., Kaldon, A., *J. Phys. Chem.*, **89** 566 (1985)

19. Moini, M., Eyler, J., *Chem. Phys. Lett.*, **137** 311 (1987)

20.Colgate, S., Simon, C., D'Agostino, R., *J. Vac. Sci. Technol.* , B9 1577 (1991)

21. Kay, E., Hecq , M., *J. Appl. Phys.*, **55** (2) 370 (1984)

22. Perry, A., Archer, N., *Mat Coating Technol.* , **4** 1-16 (1980)

23. Feuer, E., Suhr, H., *Appl. Phys.*, A44 171-5 (1987)

24. C.Brekel, A.Jansen, *J Cryst Growth* , **43** 488 (1978)

25. G.F.Sanick, J Hopkins, *Appl. Phys. Lett* ., **46** 1184-6 (1985)

26. T. Baum C Jones *J. Vac. Sci.Technol .*, B4 1187-91 (1986)

27. L. Martiniu, C Biederman *Vacuum* , 35 171-6 (1985)

28.Vezzoli, G., Chen, M.,  *Mat. Res. Soc. Symp. Proc.* , 286 (1993)

29. J Eden *Thin Film Processes 1*, Academic Press, 1990, page 478

30.Wang,C., Herron, *J. Phys. Chem .*, 95 525 1991

31. Blauner, P., Butt, Y., *J. Vac. Sci. Technol.*, B7 1816 (1989)

32. Biedermann, H, Holland L., *Nucl. Instr. and Methods* 212 497 (1983)

33. Gransquivst, C.G. hunderi, O., *Appl. Opt..* 20 26 (1981)

34. a) Maxwell-Garnett, C., *Philos. Trans. R. Soc. London,* 203 385 (1904)

b) Lafait, J., Berthier, S., Gadeene, M., Gadenne, P., *Mat. Res. Soc. Symp. Proc.,* 195 53 (1990)

35. Bruggemann, D.A., *Annalen der Physik, ,* 24 636 (1935)

36 Sheng, P., *Phys. Rev. Lett .,* 45 60 (1980)

37 Sheng, P., *Opt. & Laser Technol.,* 253 (1981)

38. Cohen, R. W., Couts, M.D. &Abeles, B., *Phys. Rev* B8, 3689 (1983)

39. Granquivst, C. G., Hunderi, O., *Solid State Commun.,* 19 939 (1976)

40. Y. Yagil P. Gadenne, G. Deutscher, *Phys. Rev. B* 46 (4) 2503 (1992)

41. Berthier,S., Lafait,J., *Thin Solid Films,* 25 171 (1985)

42. Yagil, Y., et al *Phys. Rev .B* 43 11 342 (1991)

43. Gejen, J., et al *Phys. Rev. Lett.* 50 77 (1983)

44. P. Gadenne, Y. Yagil, *J. Appl. Phys.* 66 3019 (1989)

45. Scot Ruska, W., *Microelectronic Processing,* McGraw Hill (1987) Chapter1.

46. Skofronick, G., Philips, M., *Appl. Phys Lett* 7 249 (1965)

47. Celasco, M., Maseoro, A., Paper 2 *Phys. Rev .* B 17 (6) 2564 (1978)

48. D'Agostino, R., *Plasma Deposition; Treatment and Etching of Polymers,* Academic Press, 1990

49. Perrin, J., Despax, B., Hanchett, V. and Kay, E., *J. Vac. Sci. Technol.* A4 46 (1986)

50. Kittel, C., *Introduction to Solid State Physics,* 6th Ed., Wiley, 1986

51. Lux J., *Mat. Sci .* 28 258 (1993)

52. Morris,J., Coutts, C., *Thin Solid Films* **47** 3 (1977)

53. Neugebauer, R., Webb, M., *Appl. Phys.* **33** 74 (1962)

54. Abeles, B., Dryer, J.E., *J. Vac. Sci. Technol.*, **10** 316 1976

55. Swanson, J.G., Campbell, *Thin Solid Films*, **1** 325 1967-1968

56 Hill, R.M., Kiernan, R., Stops, D.W., *Proc. R. Soc. London Ser. A*, **309** 397 (1969)

57. Raven, R., *Phys, Rev.* B **29** (11) 6218 (1984)

58. Celasco, M., Masoero, Paper 1 *Phys. Rev. B* **17** (6) 2553 (1978)

59. Canet, P. ,Laurent, C. , Despax,  B., *J. Appl. Phys.* **7** (26) 2423 (1992)

60. Redner, R., Mueller *Phys. Rev* . B **26** 5293 (1982)

61. Celasco, C., Fionilo, D., *Appl. Phys. Lett* . **26** 213 (1975)

# 4. Experimental: Initial Deposition and Analysis of AuCl₃.

## 4.1 Introduction

4.1.1 Introduction to the Project

4.1.2 AuCl3

## 4.2 Experimental Techniques

### 4.2.1 Spin Coating Techniques

*4.2.1.1 Results*

*4.2.1.2 Discussion*

### 4.2.2 Au (4f) XPS

*4.2.2.1 Pure Gold*

*4.2.2.2 (a) AuCl3 as received*

*4.2.3.2 (b) Peak fitted AuCl3*

## 4.3 References

## 4.1 Introduction

### 4.1.1 Introduction to the Project

The aim of the project outlined in this thesis was to develop a method for the deposition of conducting thin gold films. The proposed method was the following: $AuCl_3$ was dissolved in IPA, spin coated onto either a glass or nylon substrate, and this was then treated with a hydrogen plasma in order to remove chlorine.

In this chapter, the spin coating and analysis of $AuCl_3$ in IPA was examined. A Commax Precima Spin coating apparatus was used for the coating of the substrates. The deposited films were then characterised using a Cratos ES 200 X-ray photoelectron spectrometer with an unmonochromated source (Mg $k_{\alpha 1,2} = 1253.6 eV$). The spectrometer was calibrated with respect to the gold 4f 7/2 peak at 83.9 eV, full width at half maximum 1.2 eV.[1] Spectra were recorded in the C(1s), Au(4f), Cl(2p), O(1s), Si(2p), and N(1s) regions. Emitted core level electrons were collected at a 30° take off angle from the substrate normal with the cylindrical hemispherical analyser operating in the FRR mode (FRR = 22:1). Instrumentally determined sensitivity factors for unit stoichiometry were taken as C(1s) : Au(4f) : Cl(2p) : O(1s) : Si(2p) : N(1s) as 1.0 : 0.093 : 0.43 : 0.55 : 1.05 : 0.74. The absence of a Si (2p), N (1s) peak was indicative of complete coverage of the glass, nylon substrates respectively.

## 4.1.2 AuCl3

Gold (III) is the most common oxidation state of gold in compounds. Square planar four co-ordination is the most common structure of AuCl3.. Unhydrolysed AuCl3 forms a planar bridged dimer as is shown in fig. 4.1.
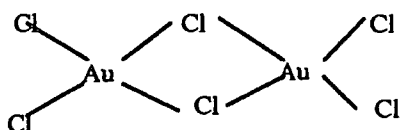


**Fig. 4.1** AuCl3 Planar Bridged Dimer.[2]

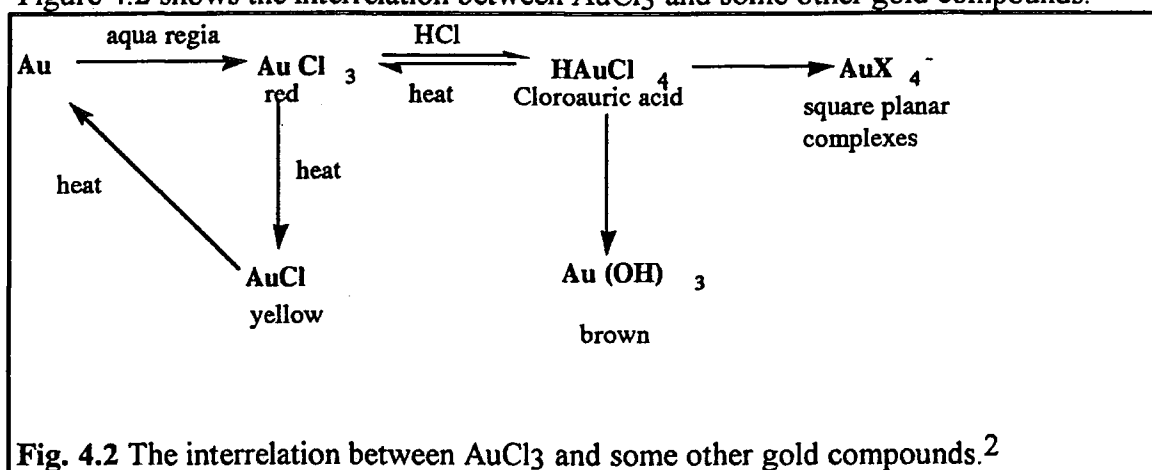Figure 4.2 shows the interrelation between AuCl3 and some other gold compounds.[2]



**Fig. 4.2** The interrelation between AuCl3 and some other gold compounds.[2]

## 4.2 Experimental Techniques

Gold (III) chloride (Au(III)Cl3, 99.99% from ABCR, Karlsruhe, Germany) was spin coated, from different concentrations of AuCl3 % wt/vol IPA (Analar IPA, 99.7%), on to two different substrates: nylon 6,6 (Lawson Mordon Flexible Ltd., 25μm biaxially orientated) and glass (Sodaware Ltd.) slides. Both substrates were cleaned twice with IPA in a sonic bath and dried in air, for 2 minutes at ambient temperature and pressure, before use. The % areas of the respective elements, determined from XPS analysis, on the surface of the clean nylon and glass slides are shown in Table A..

| Element | Glass | Nylon |
|---------|-------|-------|
| Chlorine | 0 | 0 |
| Gold | 0 | 0 |
| Carbon | 39.7±2.7 | 76.1±3.1 |
| Oxygen | 40.1±2.1 | 12.1±2.4 |
| Silicon | 19.8±1.2 | 0 |
| Nitrogen | 0 | 11.8±1.3 |

**Table A** XPS analysis of the clean surfaces of glass and nylon.

### 4.2.1 Spin Coating Techniques

#### *4.2.1.2 Introduction*

A Commax Precima Spin Coating Apparatus was used for the coating of two different substrates, nylon 6,6 and glass, with various $AuCl_3$ % wt/vol solutions (2, 10, 20, 30, 40, 50, 80 %). In order to obtain uniform coverage of the substrates, two different methods of spin coating were employed during the course of the work outlined in this thesis. These are described below and from now on will be referred to as technique 1 and technique 2. In all cases the substrates were washed twice in IPA in a sonic bath, dried (in air for 2 minutes at ambient temperature and pressure) and then stuck onto a spin plate using double sided adhesive tape. The substrate environment was then flushed for 30 seconds with nitrogen and the substrate was then coated, using either technique 1 or 2.

*Technique 1:*

The sample was spun for 60 seconds (speed 20,000 rpm). During this spin time the known % wt/vol solution was dropped (1 drop = 0.024 cc ± 0.004cc), using a pippette, onto the centre of the substrate.

*Technique 2:*

Using a pippette, the known % wt/vol solution was dropped (1 drop = 0.24 cc ± 0.004cc) onto the centre of the substrate, allowed to dry for 10 seconds, and this was spun for 20 seconds (speed 20,000 rpm). This step was carried out three times.

### 4.2.1.2 Results

The efficiencies of techniques 1 & 2 (as previously described), in producing a uniform film were examined using XPS. The results of these examinations are shown in the following pages. A key to the figure numbers, the corresponding % wt/vol solution, the technique used and the substrate employed,is given in Table B.

| $AuCl_3$ % wt/vol solution | Substrate | Technique employed | Figure Number |
|---|---|---|---|
| 2 | Glass | 1 | 4.3 |
| 2 | Glass | 2 | 4.4 |
| 2 | Nylon | 1 & 2 | 4.5 |
| 10 | Glass | 1 | 4.6 |
| 10 | Glass | 2 | 4.7 |
| 10 | Nylon | 1 & 2 | 4.8 |

**Table B:** The key to the Spin Coating Graphs.

The average errors bars (± Standard devation (S.D.)) for each element in the figures (4.3 to 4.8) are given in Table C.

| Element Fig. No. | Au | Cl | C | O | Si | N |
|---|---|---|---|---|---|---|
| Fig. 4.3 | ±1.31 | ±2.98 | ±1.47 | ±2.1 | ±0.97 | ±0 |
| Fig. 4.4 | ±0.94 | ±1.76 | ±2.13 | ±1.76 | ±0.83 | ±0 |
| Fig. 4.5 | ±0.73 | ±2.01 | ±2.59 | ±1.63 | ±0 | ±0.76 |
| Fig. 4.6 | ±1.19 | ±1.41 | ±1.71 | ±1.31 | ±1.03 | ±0 |
| Fig. 4.7 | ±1.27 | ±1.13 | ±1.43 | ±0.98 | ±1.41 | ±0 |
| Fig. 4.8 | ±0.89 | ±1.61 | ±.91 | ±1.13 | ±0 | ±1.03 |

**Table C:** The error s on the elements in figures 4.3 to 4.8
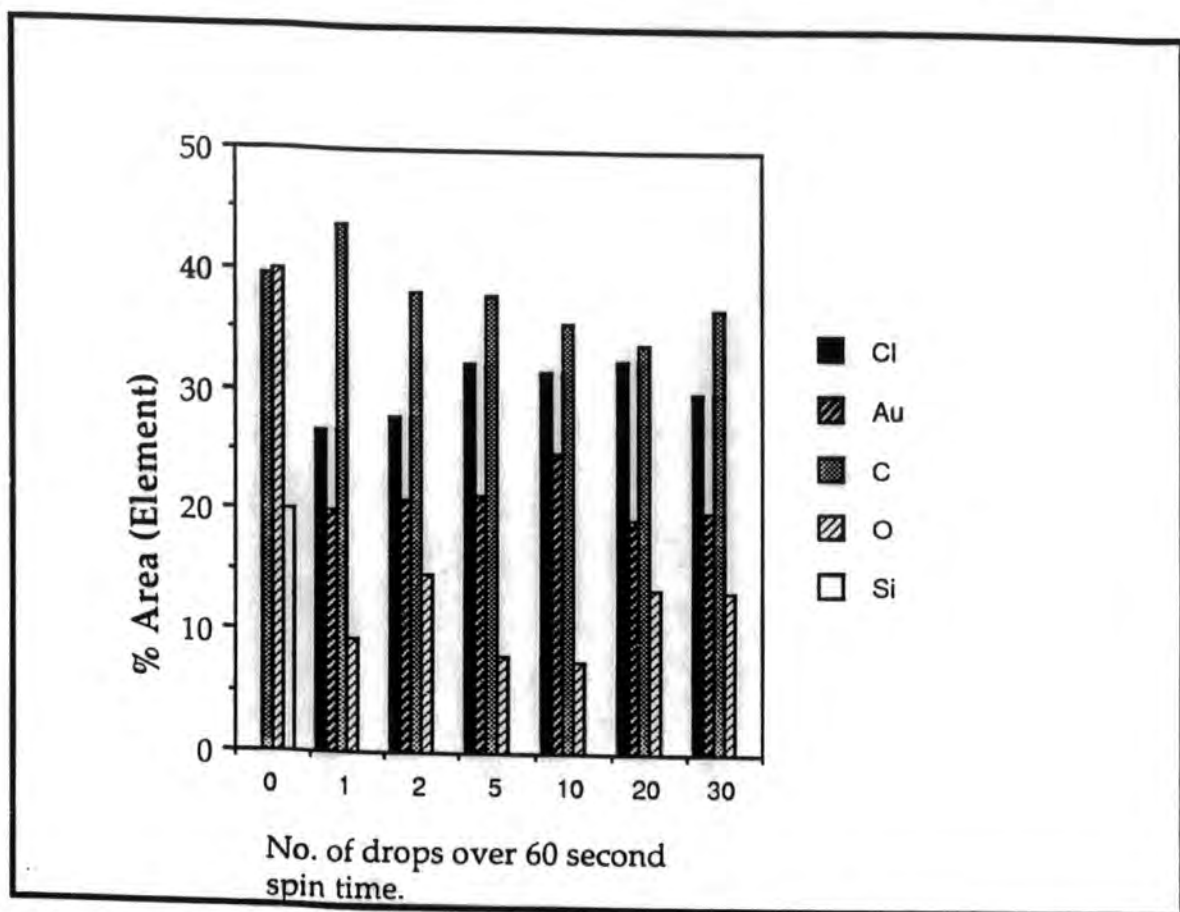
**Fig 4.3** 2% AuCl3 spin coated onto Glass using Technique 1
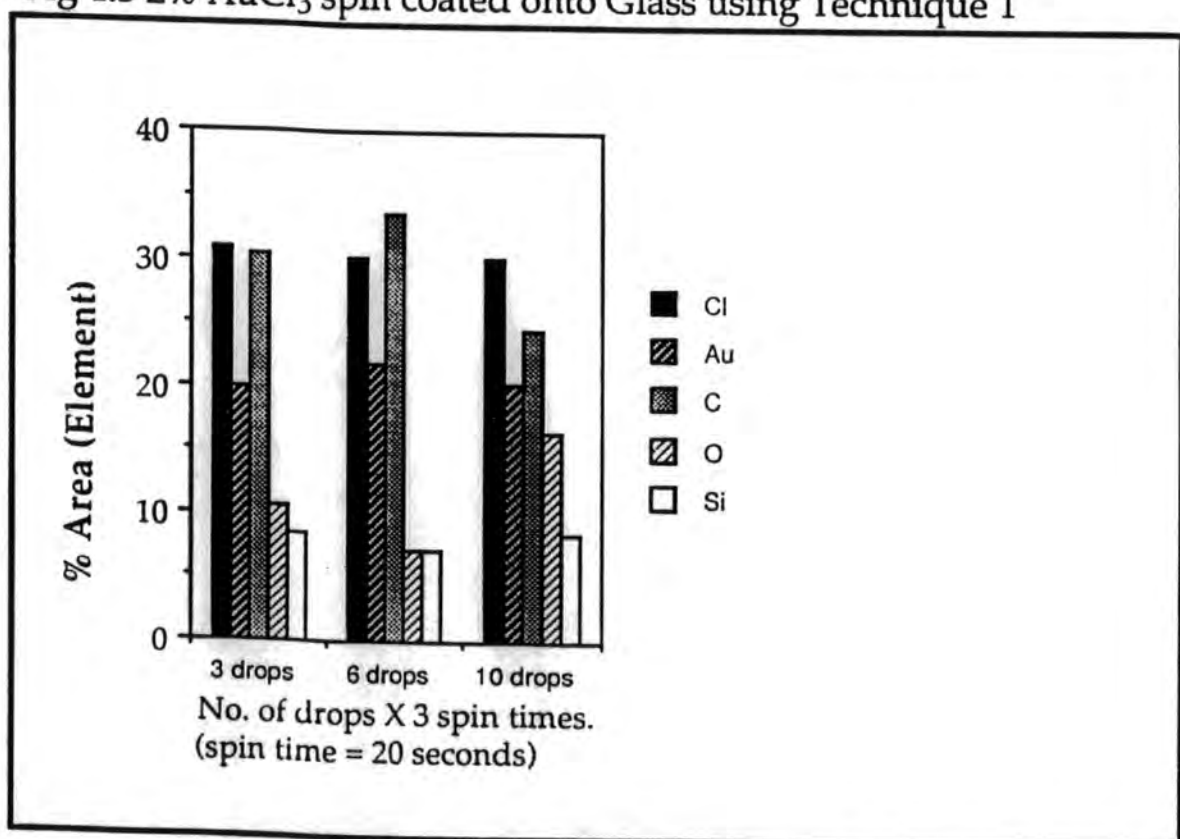


**Fig. 4.4.** 2% AuCl3 spin coated onto Glass using Technique 2
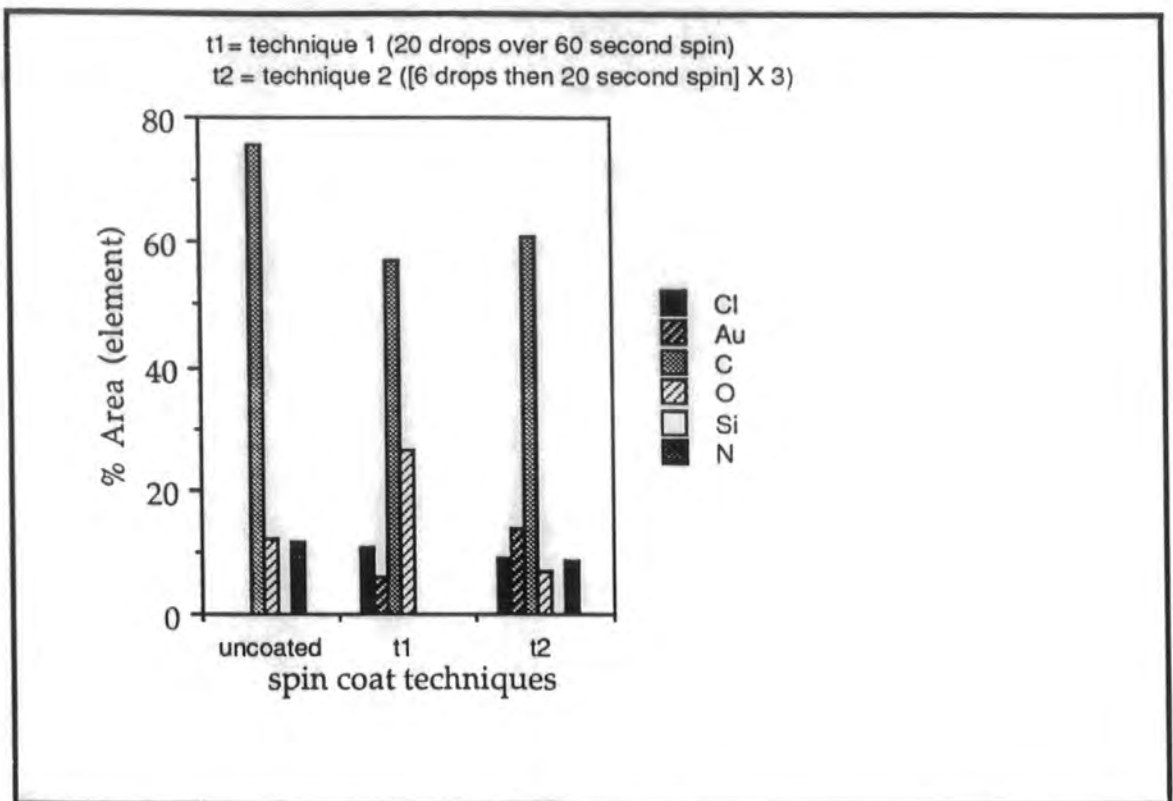
Fig. 4.5 2% AuCl3 spin coated onto Nylon using the Optima of Techniques 1 & 2
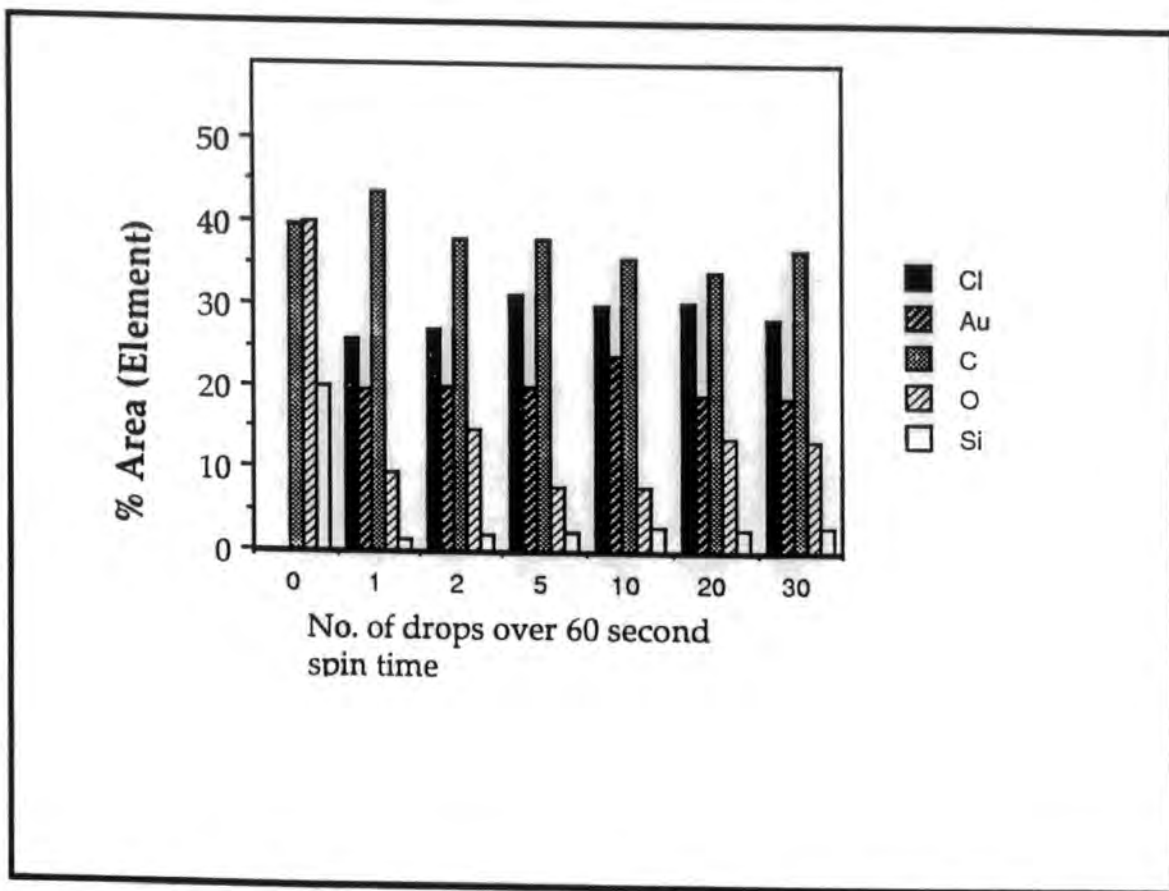
**Fig. 4.6** 10% AuCl₃ spin coated onto Glass using Technique 1.
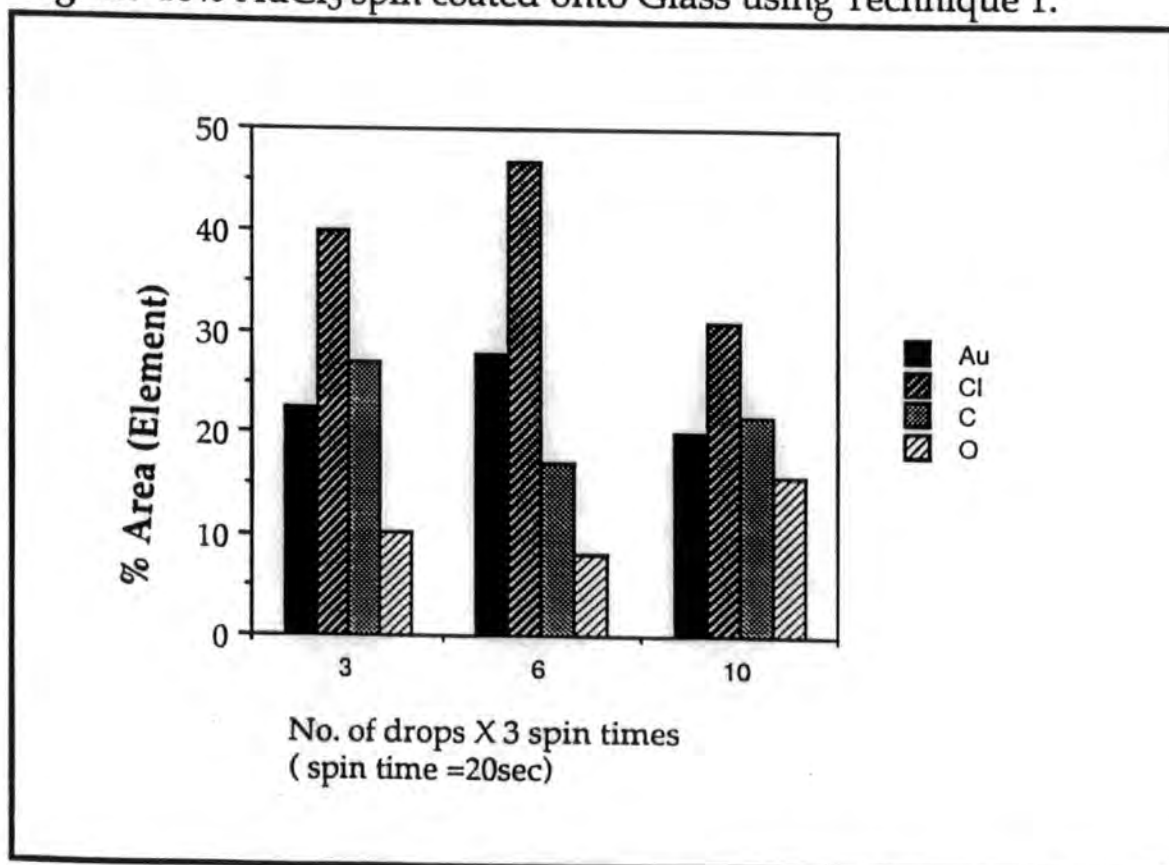


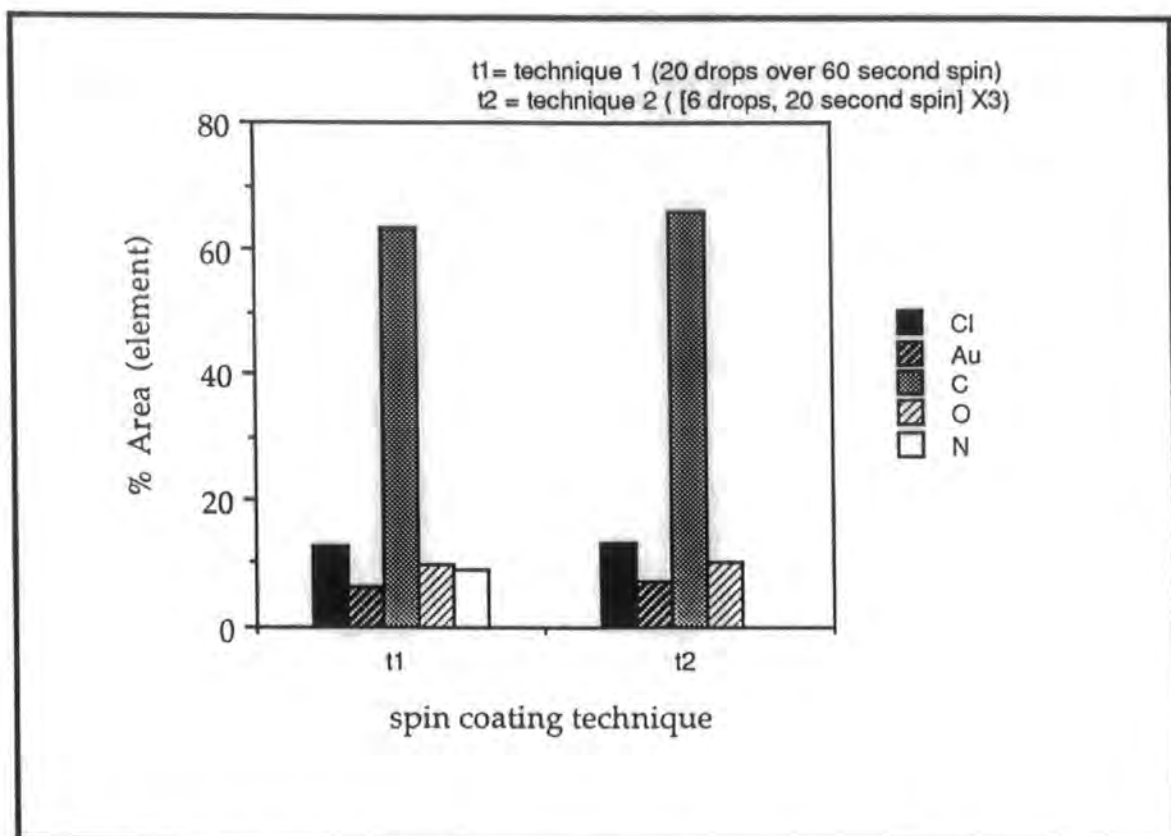**Fig. 4.7** 10% AuCl₃ spin coated onto Glass using Technique 2

**Fig 4.8** 10% AuCl₃ spin coated onto nylon using the Optima of Techniques 1 & 2

*4.3.1.2 Discussion*

In order to obtain uniform coverage of the glass and nylon substrates, two different techniques (1 & 2) of spin coating were employed. It was decided, from the XPS analysis ( figures 4.3, 4.6) that the optimum of **technique 1** was to drop 20 drops of the known % AuCl₃ in IPA onto the substrate during the 60 second spin time. Using this optimum, the XPS values for the % area of the elements on the surface of 2% AuCl₃ in IPA, spin coated onto glass were: C(1s) 35%, Au (4f) 20%, Cl (2p) 34%, O (1s) 15%. From figures 4.4 and 4.7, it was decided that the optimum of **technique** 2 was to drop 6 drops of known % wt/vol solution, allow this to dry for 10 seconds, and then to spin the substrate for 20 seconds and to repeat this step three times. The XPS values, using this optimum technique, for the % area of the elements on the surface of 10% AuCl₃

in IPA, spin coated onto glass, were C(1s) 17%, Au (4f) 30%, Cl (2p) 45%, O (1s) 8%. As stated before, the results for the higher % wt/vol AuCl3 (20, 30, 40, 50, 80) solutions were similiar to those for the 10% AuCl3 solutions spin coated onto glass. For example the XPS values for the % area of the elements on the surface of 50% AuCl3 in IPA, spin coated onto glass were: C(1s) 22%, Au (4f) 25%, Cl (2p) 46%, O (1s) 8%. From figures 4.3 to 4.8, it appeared that **technique 1** gave rise to uniform coverage, on both substrates, for the 2% AuCl3 in IPA (but not for 10 or higher % AuCl3 in IPA), and that **technique 2** gave rise to uniform coverage, on both substrates, for the 10 and higher % AuCl3 in IPA, (but not for 2% AuCl3 in IPA).

These results may be explained by the following: perhaps the efficiency of **technique 1** depends upon the presence of excess amounts of solvent to efficiently "carry" the solution over the substrate. **Technique 2**, however, has an extra parameter of "drying time" (of 10 seconds) as the solution is first dropped onto the substrate and then spun. Perhaps the resulting coverage from technique 2 is then a function of % AuCl3 present in the solution being dropped. As there are less solids (AuCl3) in the 2% AuCl3 in IPA solution than in the 10% and higher % AuCl3 in IPA solutions, that when the 2% AuCl3 solution on the substrate is spun, either the IPA is scattered off the substrate and voids are left in the film, or the IPA actually washes off the solution. However, the 10%, and higher AuCl3 solutions have enough AuCl3 species present to obtain uniform coverage. It is cited that using technique 2, the final film thickness is a function of initial solvent concentration and of rotational speed.[3]

From the above results, the following were proposed:
- Technique 1 is from now assumed to be the addition of 20 drops of 2% AuCl3 in IPA over the spin time of 60 seconds.

- Technique 2 is 6 drops of 10% or higher $AuCl_3$ % wgt/vol solutions on the centre of the substrate, which is dried in air for 10 seconds before being spun for 20 seconds. This step is repeated three times

The errors on the peak areas of the elements may be due to several factors, some of which are outlined below.

- The gold (III) chloride was first weighed on a Mettler weighing scales which has an error of 0.005mg.

- The weighed sample was then dissolved in IPA. The IPA was transferred to the sample bottle using a pippette, which has an error of 0.05ml.

- The sample was dropped onto the substrate using a pippette, and the error on the drop size was 0.004cc.

- The spin coater was used to spin the substrate and the speed of spinning had an error of 20 rpm.

### 4.3.2 Au (4f) XPS Analysis

*4.3.2.1 Pure Gold*

A pure gold sample (Goodfellows, 99.99%) was washed in nitric acid and was examined using XPS. A doublet was observed. The gold doublet arises from the removal of a 4f electron leaving the $4f_{7/2}$ and the $4f_{5/2}$ core states for which $L = 3$, $S = 1/2$, and $J = 5/2$ or $7/2$. The experimentally observed doublet had maxima at $83.9 \pm 0.04$ eV and $87.54 \pm 0.04$ eV respectively i.e. separated by $3.64 \pm 0.04$ eV (see fig. 4.10). The relative areas of the doublet were as A:B (see fig.4.10), 1:0.752, and the relative full widths at half maximum were as A:B, 1:1.05. The Au ($4f_{7/2}$) peak, i.e. peak A, at 83.9 eV is used as the reference point for the work discussed in this thesis. The literature values for the Au ($4f_{7/2}$) vary and these are discussed in Chapter 2 of this work.
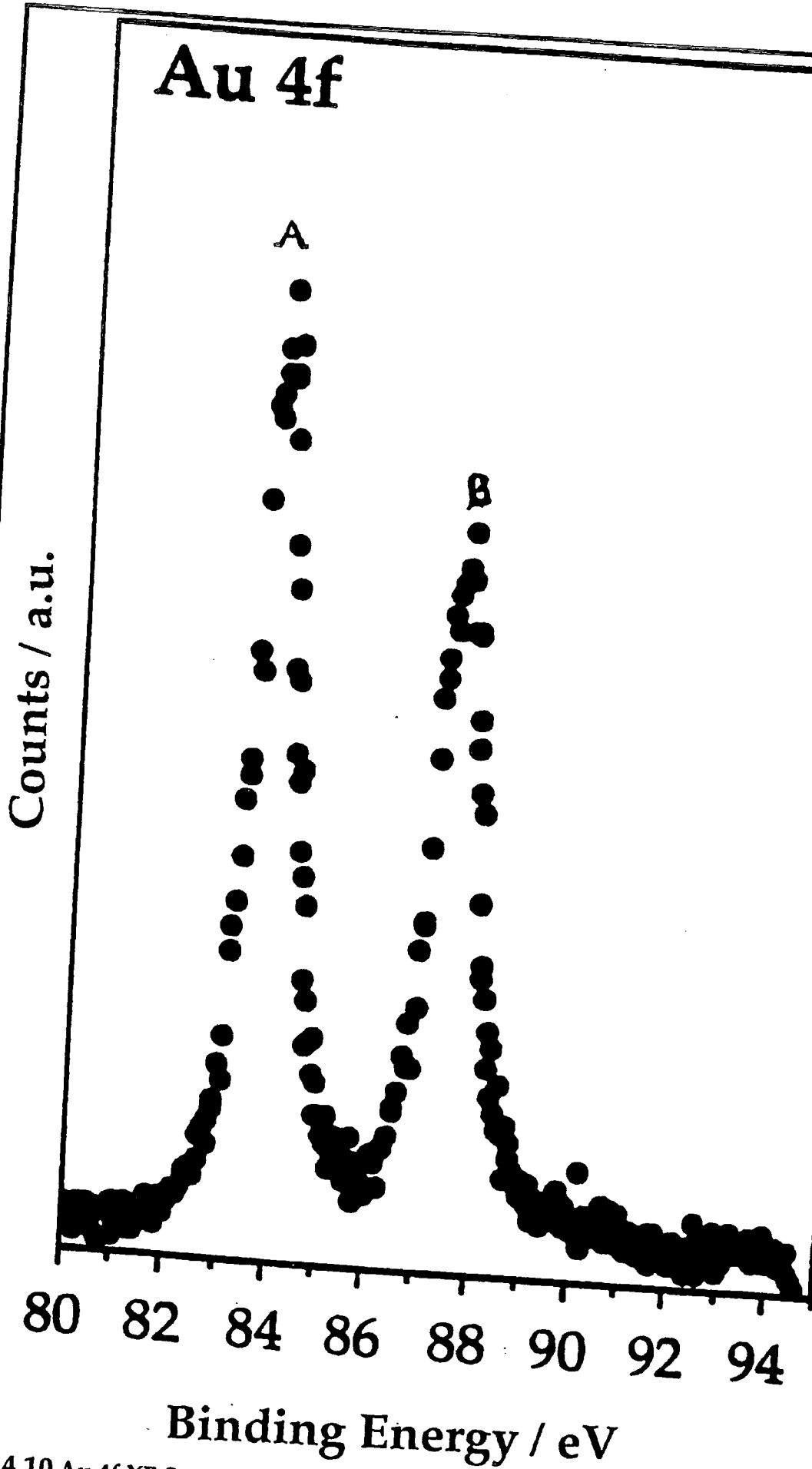
Fig 4.10 Au 4f XP Spetcra of Pure Au (Goodfellows, 99.99% purity)

77

*4.3.2.2 (a) Pure AuCl3 as received*

The AuCl$_3$ was dissolved in IPA, and with no further treatment, was examined by XPS. Three peaks were observed from the XPS analysis (see fig 4.10 [a]) and using a gaussian peak fitting program four peaks [Au (4f $_{7/2, 5/2}$) for both Au (0) ( Peaks A & C)and Au(III) (Peaks B & D)] of maxima 84.23 ± 0.03 (A), 87.4 ± 0.02 (B), 87.6 ± 0.05 (C), and 91.9 ± 0.03 (D) eV were established to be present (see fig 4.11[b]). This is due to the presence of both Au(0) and Au(III) in the original sample.
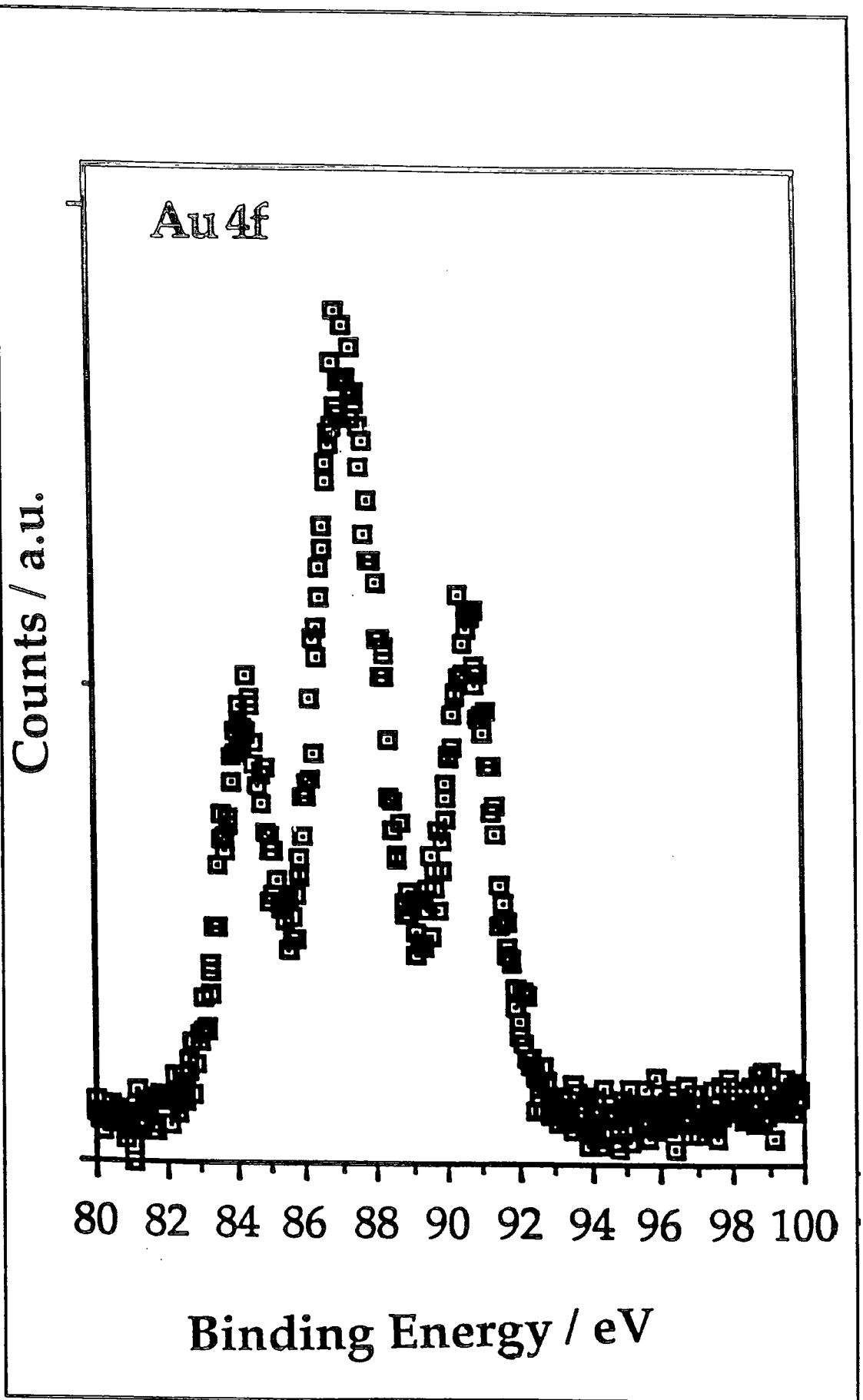
Fig. 4.11 (a) Au 4f XP spectra of AuCl3 as receieved

### 4.3.2.2 (b) Peak fitted AuCl₃

AuCl₃ in IPA with no further treatment was examined by XPS. This was peak fitted using a Gaussian fit program.



Fig 4.11 [b]  Peak fitted AuCl₃
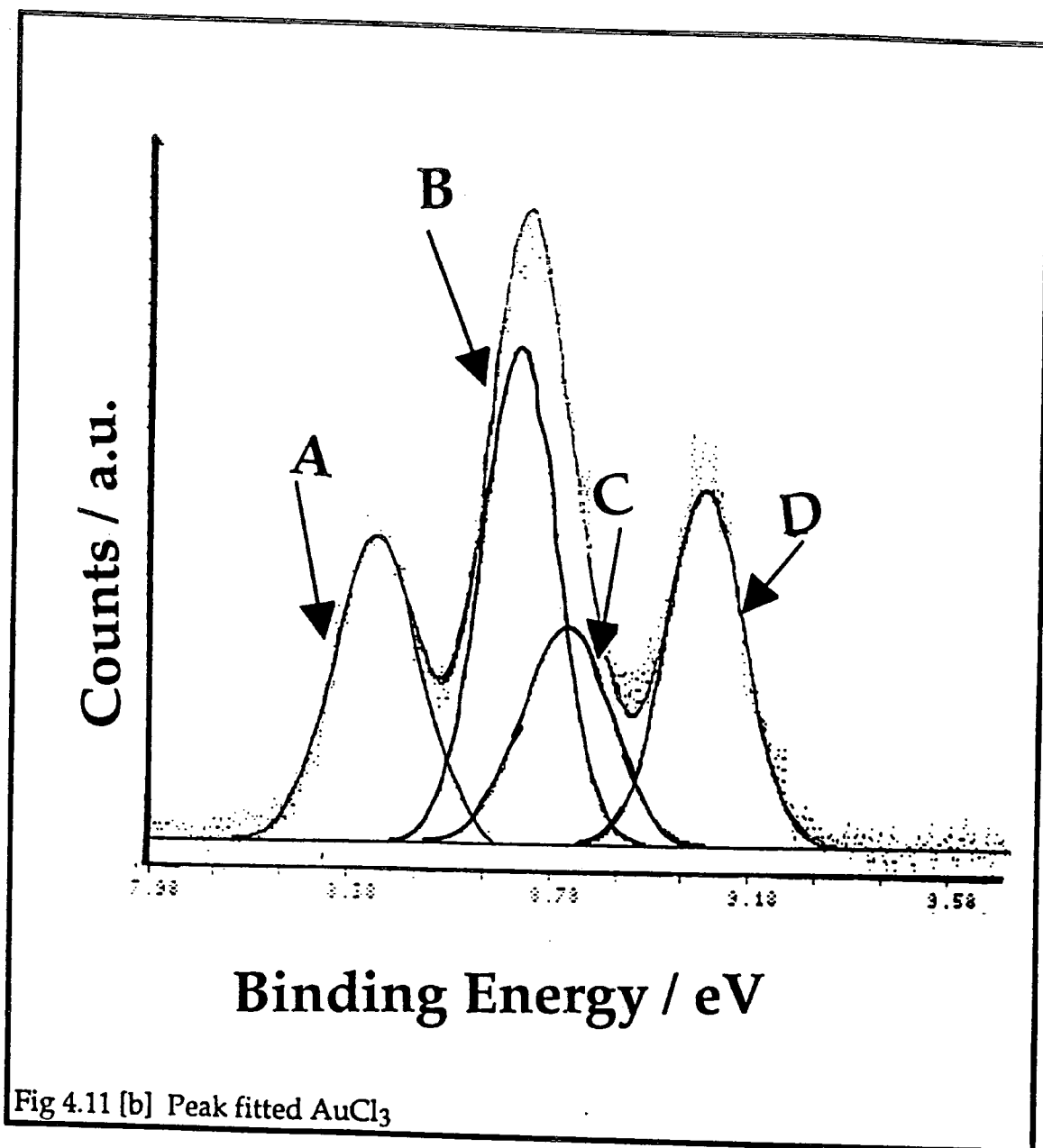
## 4.3 References

1.*Perkin & Elmer handbook of X-ray Photoelectron Spectroscopy*, (1989)

2.MacKay, R.M., MacKay, *Introduction to Modern Inorganic Chemistry*, Blackie 1989.

3.Yonkoski, R.K., Soane, D.S., *J. Appl. Phys.*, 72 (2) 725 (1992)

# 5. Hydrogen Plasma Treatments

## 5.1 Introduction

## 5.2 Experimental Design

### 5.2.1 Reactor Set-up

### 5.2.2 An Experimental Cycle

## 5.3 Glass Substrate

### 5.3.1 Variation in Concentration

*5.3.1.1 Elemental Analysis by XPS*

*5.3.1.2 Au Analysis by XPS*

*5.3.1.3 Discussion*

### 5.3.2 Treatment Time Variation, Power 5 Watts

*5..3.21 Elemental analysis by XPS*

*5.3.2.2 Au analysis by XPS*

*5.3.2.3 Discussion*

### 5.3.3 Power Variation, Treatment Time 10 minutes.

*5.3.3.1 Elemental analysis by XPS*

*5..3.3.2 Au analysis by XPS*

*5..3.3.3 Discussion*

## 5.4 Nylon Substrate

### 5.4.1 Power Variation, Treatment Time 1 minute.

*5..41.1 Elemental analysis by XPS*

*5.4.1.2 Au analysis by XPS*

*5.4.1.3 Discussion*

## 5.5 Conclusions & Further Work

## 5.1 Introduction

In the work discussed in this chapter, the reduction of gold (III) choride, spin coated onto either glass or nylon, using a hydrogen plasma of various powers and for various treatment times, was studied.

The plasma treated films were characterised using a Cratos ES 200 X-ray photoelectron spectrometer with an unmonochromated source (Mg $k_{\alpha 1,2}$= 1253.6eV). The spectrometer was calibrated with respect to the gold 4f 7/2 peak at 83.9 eV, full width at half maximum 1.2 eV.[1] Spectra were recorded in the C(1s), Au(4f), Cl(2p), O(1s), Si(2p), and N(1s) regions. Emitted core level electrons were collected at a 30° take off angle from the substrate normal with the cylindrical hemispherical analyser operating in the FRR mode (FRR = 22:1). Instrumentally determined sensitivity factors for unit stoichiometry were taken as C(1s) : Au(4f) : Cl(2p) : O(1s) : Si(2p) : N(1s) as 1.0 : 0.093 : 0.43 : 0.55 : 1.05 : 0.74. The abscence of a Si (2p), N (1s) peak was indicative of complete coverage of the glass, nylon substrates respectively.

## 5.2 Experimental

### 5.2.1 Reactor set-up

Glow discharge experiments were carried out in an electrodeless cylindrical glass reactor (4.5 cm internal diameter, 490cm$^3$ volume) enclosed in a Faraday cage.[1] This reactor was fitted with a gas (hydrogen) inlet, a pirani pressure gauge and a 47 dm$^3$min$^{-1}$ two stage rotary pump attached via a liquid nitrogen cold trap. A 13.56 MHz radio frequency (RF) source was inductively coupled to a copper coil (4mm tube diameter, 9 turns spanning 12 to 19.5 cm from the gas inlet) via a LC matching unit (figure 5.1).
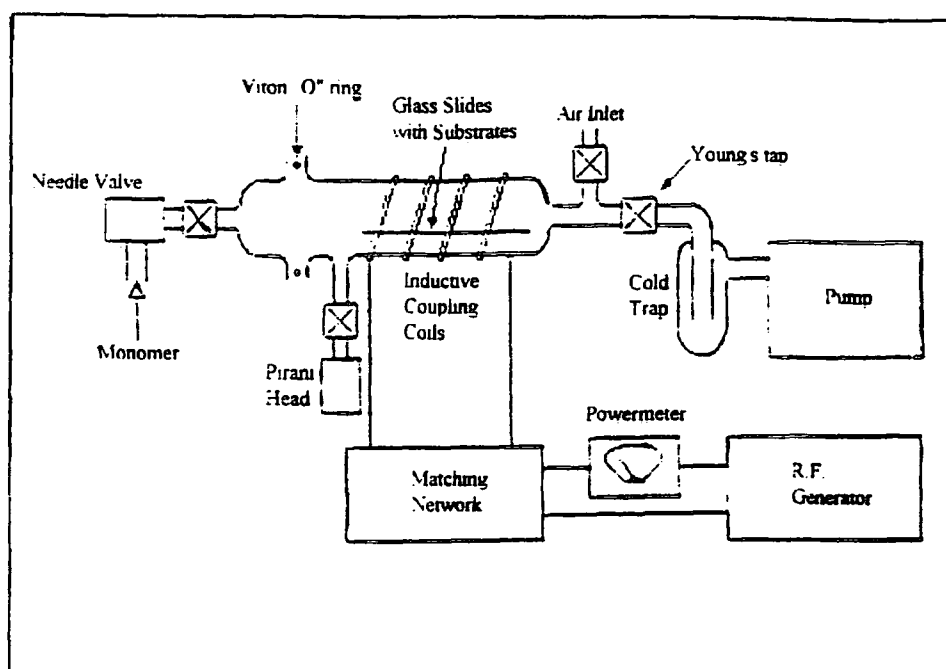
**Fig 5.1** The reactor set-up used in this work[1]

All the joints were grease free. The gas flow rate was controlled using a fine needle valve. All experiments were carried out using a continuous mass flow of hydrogen ($F_{H_2}$) which can be estimated from the following equations:

Assuming the gas inside the reactor behaves as a real gas,[2] then

$$m = (MV/RT)\, P \qquad\qquad (5.2.1.1)$$

where m is the mass of the gas inside the reactor, M is the molecular weight of the gas, V is the volume of the reactor, R is the universal gas constant (R = 82.0575 $cm^3 \cdot atm \cdot K^{-1} \cdot mol^{-1}$), T is the gas temperature, and P is the gas pressure.

In a reactor which is fed constantly by gas of a flow rate $F_g$, when one closes the outlet to the pump at a time t=0 (leaving the gas inlet open), $F_g$ is related to the increase in pressure according to the equation 5.2.1.2

$$F_g = dm/dt = (MV/RT)\ dp/dt\ ]_{t=0} \qquad (5.2.1.2)$$

If $dp/dt]_{t=0}$ as $\Delta P/\Delta t$ (i.e. the ratio of change in the pressure in the reactor and time spent for this change), this becomes equation 5.2.1.3

$$F_g = c(MV/RT)\Delta p/\Delta t \qquad (5.2.1.3)$$

Using the above equations, Fg can be estimated experimentally, by closing the outlet to the pump abruptly and measuring the increase in pressure , $\Delta p$, as well as its related time interval, $\Delta t$.

### 5.2.2 An Experimental Cycle

The following procedure outlines a complete experimental cycle of the work described in this thesis.

a)   A clean (i.e. scrubbed with detergent, washed with water,   rinsed with IPA and dried) glass reactor was cleaned further with an air plasma (30 minutes, 50 to 100 Watts, pressure 0.1Torr).

b)   The reactor was pumped down to 0.01 Torr and the leak rate estimated. This was always less than $2.6 \times 10^{-10}$ kg/s.[1]

c)   The reactor was then opened to air and the spin coated sample placed 7.5 cm from the gas inlet.

d)   In order to remove atmospheric oxygen from the plasma environment the reactor was pumped down to 0.01 Torr.

e) Hydrogen gas (supplied by BOC and used without further purification) was allowed into the reaction chamber (continuous flow), resulting in an increase of pressure to 0.1 Torr. The hydrogen flow rate was estimated to be $1.05 \times 10^{-9}$ kg/s. Hydrogen was allowed to flow through the reaction chamber for 5 minutes before the initiation of the glow discharge.

f) The glow discharge was initiated and allowed to run for the required time and power treatment. The RF gave rise to a lilac glow as is characteristic of hydrogen gas. In all cases the glow discharge extended through the length of the vertical coil region and for a substantial distance on either side of the sample position in the horizontal portion of the reactor.

g) After the glow discharge was extinguished, the hydrogen was allowed to flow through the reaction chamber for a further 5 minutes at a pressure of 0.1 torr.

h) The reactor was then pumped down to 0.01 torr and maintained at this pressure for 2 minutes.

i) The sample was then removed and analysed by XPS. Typically XPS analysis began approximately 10 minutes after plasma treatment and took 30 minutes to complete.
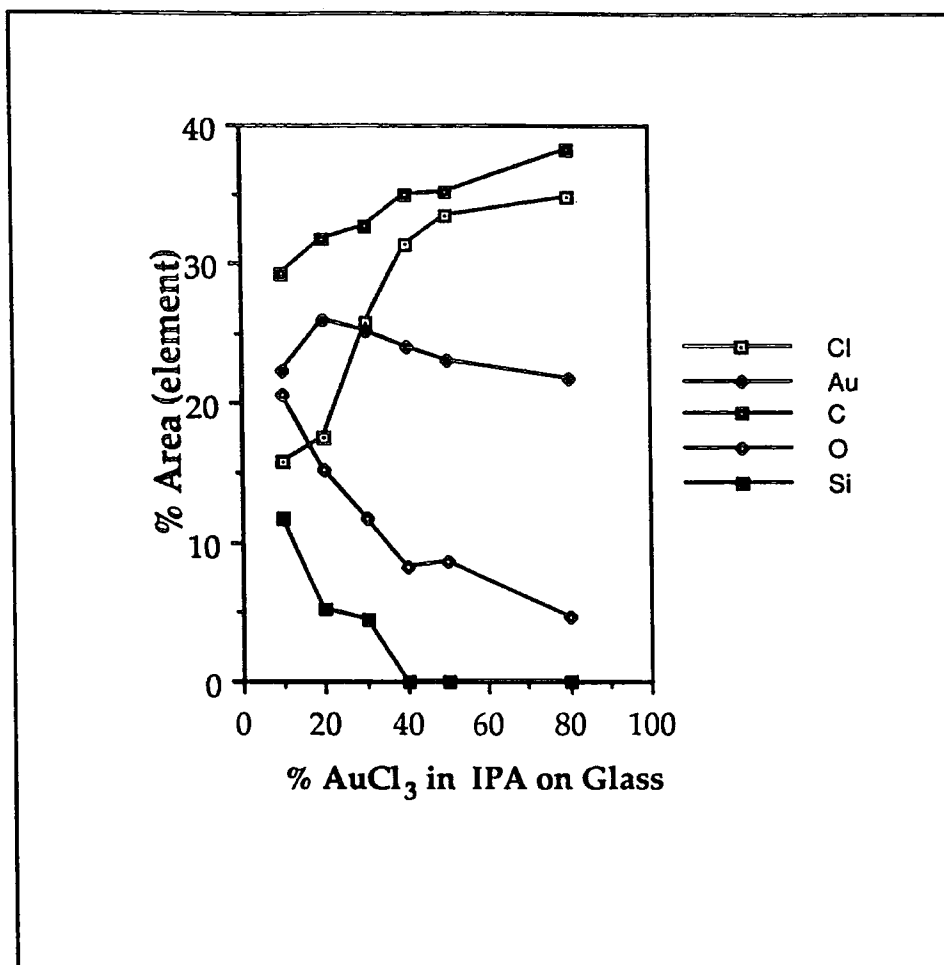
**Fig 5.2** AuCl₃ on Glass as a function of Concentration,Plasma Power 5 Watts, Treatment Time of 10 Minutes.

*5.3.2.2 Au 4f analysis.*

As discussed in section 4.3.1, pure Au, when examined by XPS, has 2 peaks with maxima at 83.9eV and 87.4eV, and that the untreated AuCl₃, when examined by XPS, has 4 peaks with maxima at 84.0eV, 87.4eV, 87.6eV and 91.1eV. Figure 5.3 shows that for a 2% wt/vol solution, treated for 10 minutes by a 5 Watt plasma, full reduction of the gold species (Au[III] to Au [0]) is obtained. Higher % wt/vol solutions, treated by the same plasma, show the presence both fully reduced gold, Au(0), and also some Au (III) species.
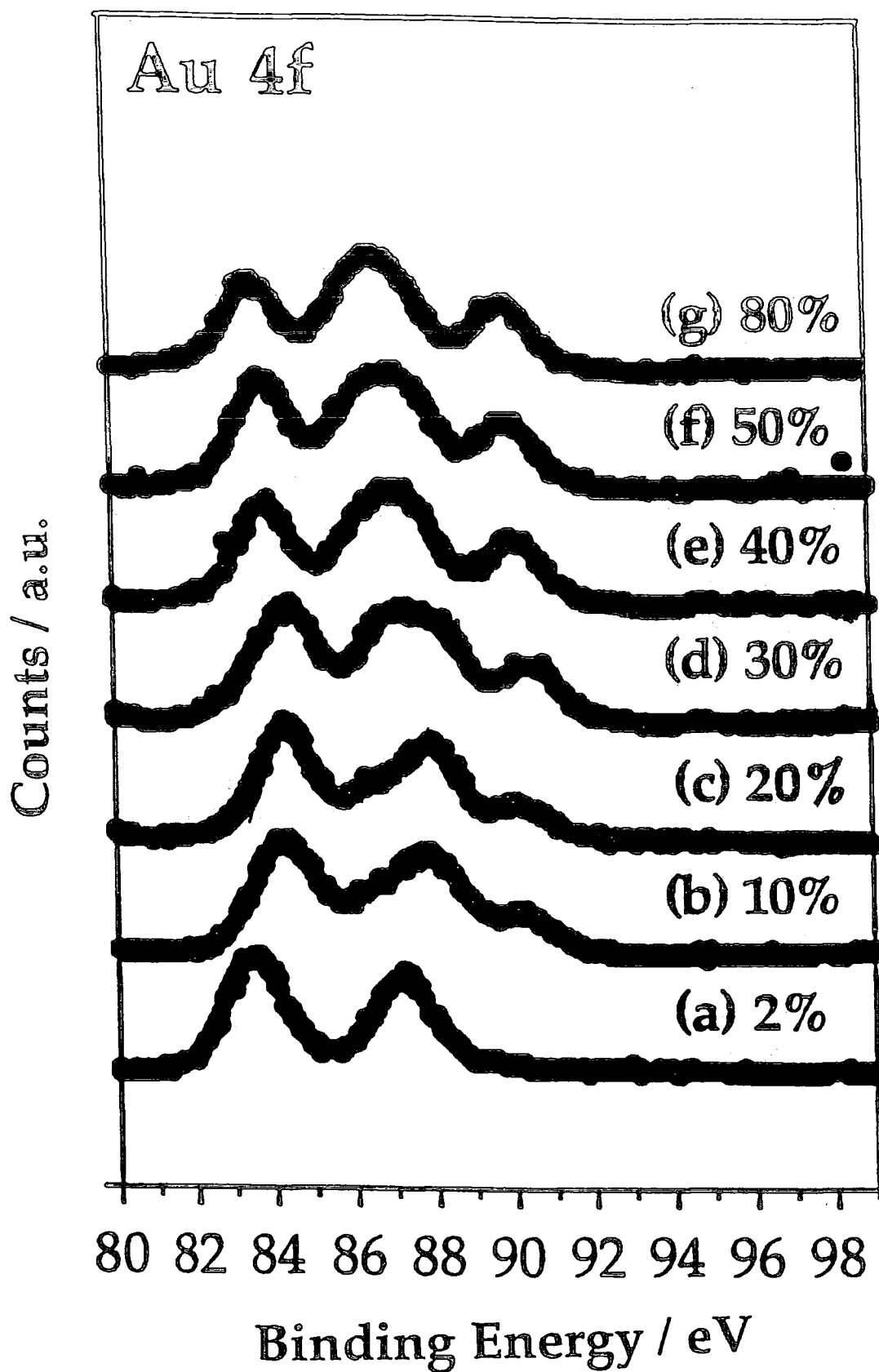
**Fig. 5.3** Au 4f XP Spectra of Plasma Treated AuCl₃ on Glass as a function of Concentration (Treatment time of 10 mins, Power of Watts).

*5.3.2.3 Discussion*

In this section, a 5 Watt hydrogen plasma was used to treat 2, 10, 20, 30, 40, 50 and 80 $AuCl_3$ % wgt/vol in IPA solutions, over a treatment time of 10 minutes.

The following trends were observed: with increasing concentration, the XPS Si (2p), O (1s) peak areas decrease, Au (4f) areas remain roughly constant, and Cl (2p) and C (1s) peak areas increase. The Au (4f) data show that only 2% $AuCl_3$ in IPA wgt/vol solution is reduced fully by a 5 Watt hydrogen plasma, treatment time 10 minutes. For higher concentrations, using this plasma treatment, the Au species present in the original solution are not reduced to Au(0).

As the concentration of the solution increases, so too does the film thickness. Based on this assumption it appears from these results, that with increasing film thickness, the hydrogen plasma only removes the chlorine species on the top layers (less than ca. 50Å) of the film, and not from deeper within the film. As the literature suggests that hydrogen plasmas can actually penetrate more than 100Å then perhaps the chlorine situated deeper in the film does react with the hydrogen plasma, but does not form a volatile hydride, perhaps it is 'trapped' as HCl within the film. Perhaps, however, the literature values do not apply to this system and the hydrogen plasma is incapable of penetrating more than ca. 50 Å of this surface.

From the above results the following was deduced:
- With increasing concentration, the film thickness increases.
- A 5 Watt hydrogen plasma only reacts with chlorine, to form a volatile hydride, to a certain depth of the film.

and the following was observed:
- 2% $AuCl_3$ in IPA is fully reduced by a 5 Watt hydrogen plasma for a treatment time of 10 minutes

- 2% AuCl$_3$ in IPA is fully reduced by a 5 Watt hydrogen plasma for a treatment time of 10 minutes

### 5.3.3 Treatment Time Variation, Power 5 Watts

A hydrogen plasma of 5 watts was used to treat 2, 10, and 50% AuCl$_3$ wt/vol solutions on glass, with various treatment times.

### *5.3.3.1 Elemental Analysis*

The elemental analysis of the 2, 10 and 50% AuCl$_3$ wt/vol solutions are shown in figures 5.4, 5.5, and 5.6 respectively. Generally, for all three % wt/vol solutions, as the treatment time increases, the O(1s) and Si(2p) areas increase and the C(1s) and Cl(2p) areas decrease. The Au(4f) areas remain roughly constant.

On comparison of the three graphs (5.4, 5.5, 5.6), the following trends were observed: for increasing concentration (i.e. 2 to 10 to 50%), Si (2p) areas decrease and increase with increasing treatment time. The XP C (1s) peak areas increase with increasing concentration and increasing treatment time. The XP O (1s) peak areas decrease with increasing concentration and with increasing treatment time. The XP Cl (2p) peak areas increase with increasing concentration but decrease with increasing treatment time. The XP Au (4f) peak areas remain roughly constant.

The average error bars for the respective concentrations on glass are given in table B.

| Element Conc. | Au | Cl | C | O | Si | N |
|---|---|---|---|---|---|---|
| 2% AuCl3 | ± 1.1 | ± 2.6 | ± 4.5 | ± 3.3 | ± 1.1 | ± 0 |
| 10% AuCl3 | ± 1.4 | ± 2.7 | ± 3.9 | ± 4.1 | ± 2.7 | ± 0 |
| 50% AuCl3 | ± 2.3 | ± 1.7 | ± 2.9 | ± 2.9 | ± 0.5 | ± 0 |

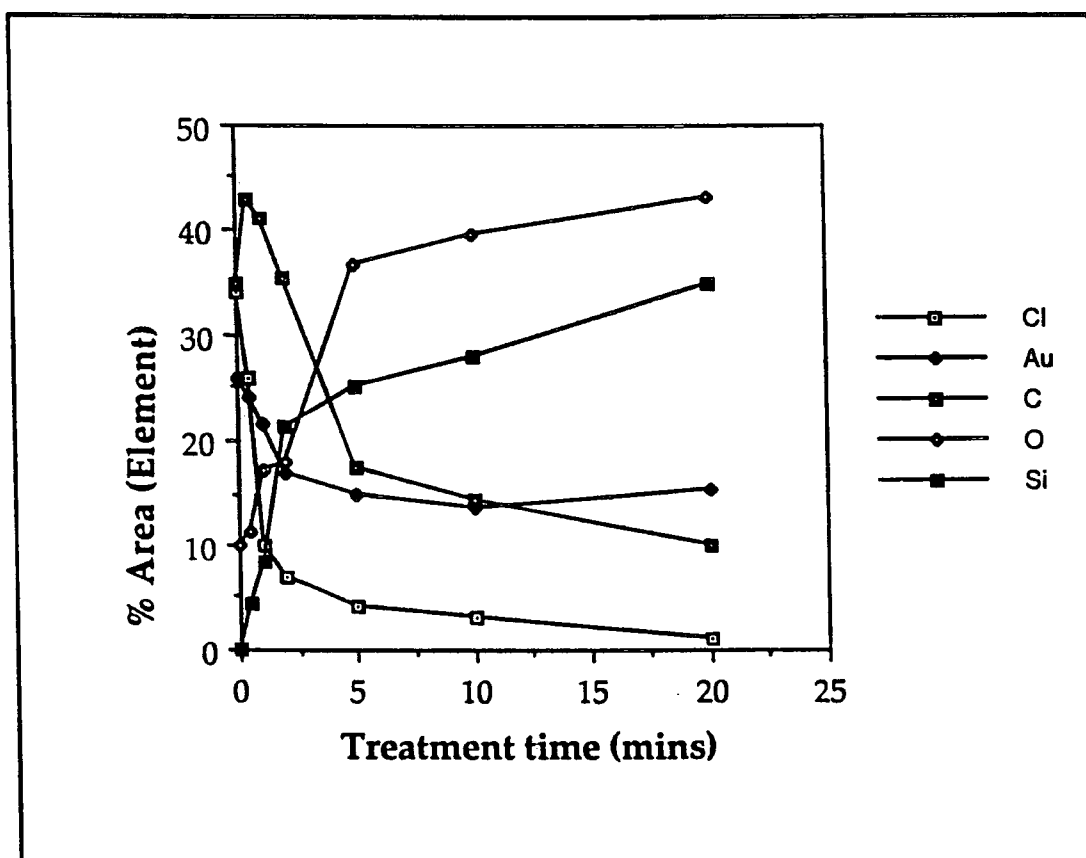Table B: The errors on the analysed elements as shown in figs 5.4, 5.5, 5.6.



**Fig. 5.4** 2% AuCl3 on Glass as a function of Treatment Time, Plasma Power of 5 Watts
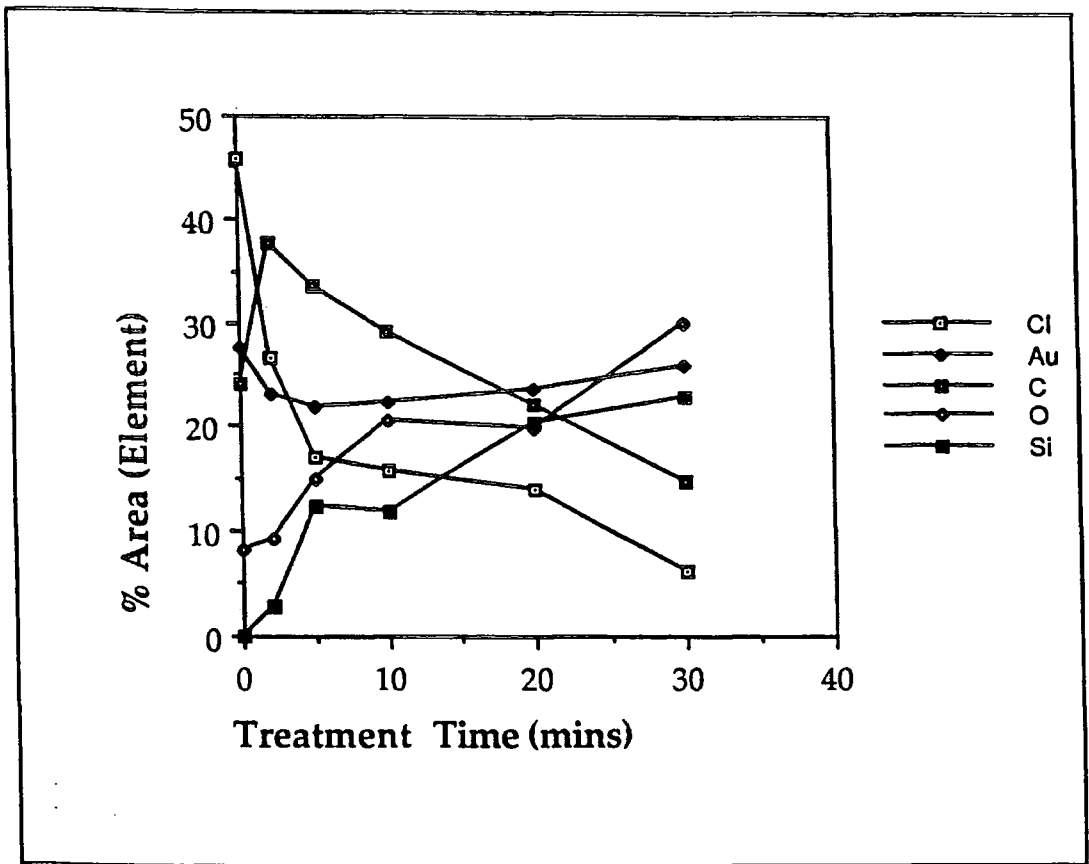
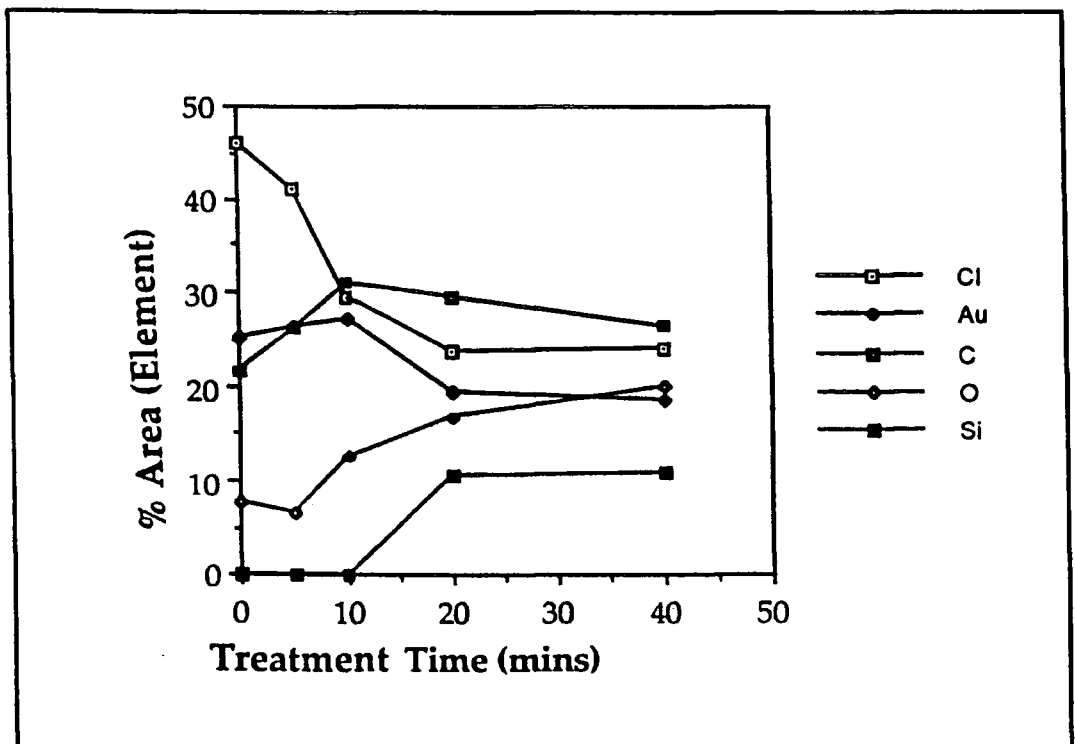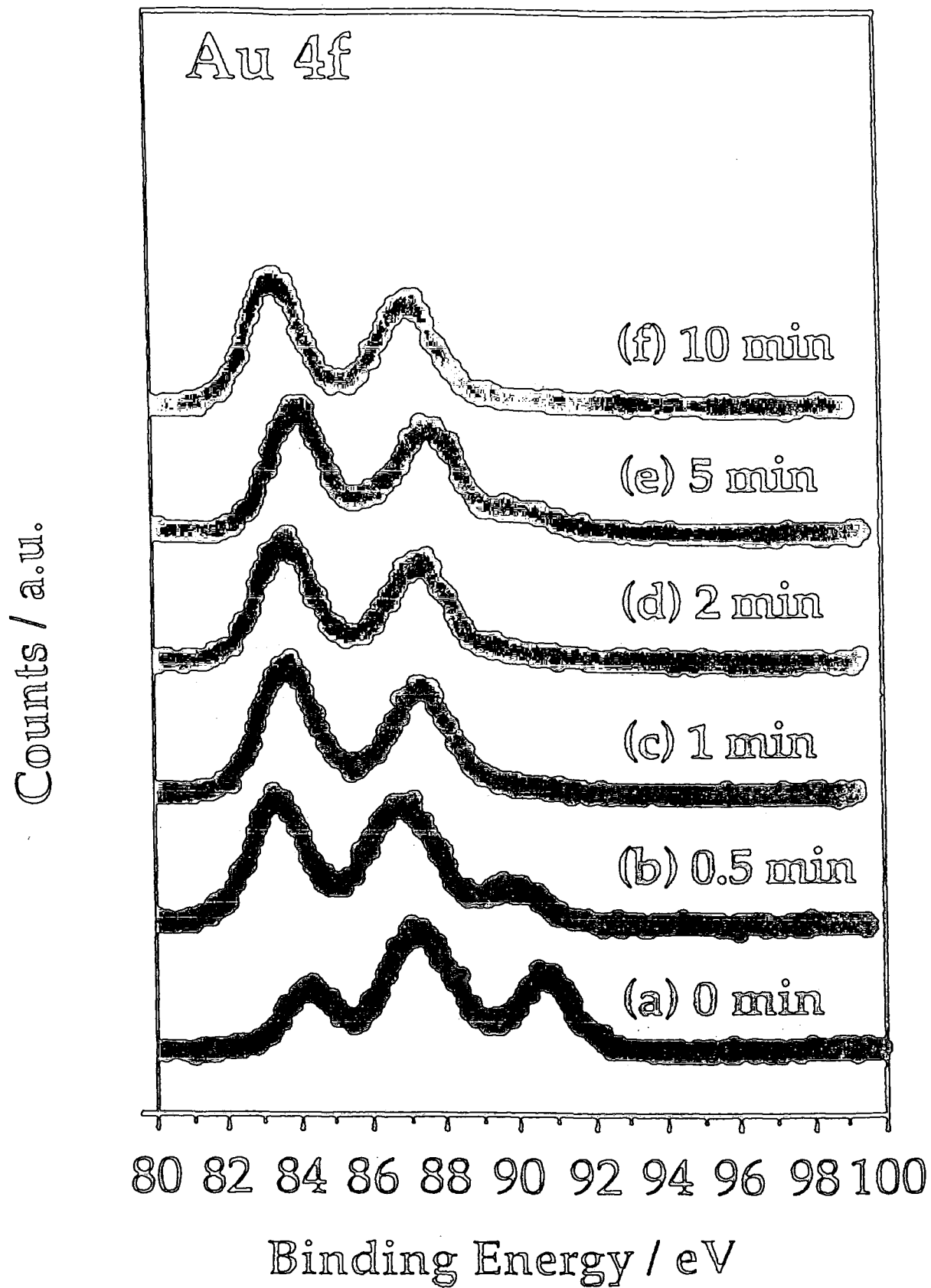**Fig. 5.5** 10% AuCl3 on Glass as a function of Treatment Time
Plasma of 5 Watts



**Fig. 5.6** 50% AuCl3 on Glass as a function of Treatment Tim‹
Plasma of 5 Watts

### 5.3.3.2 *Au(4f) analysis by XPS*

The Au (4f) graphs of 2, 10, 50 % AuCl3 wt/vol solutions, treated with a 5 Watt plasma for various treatment times, are shown in figures 5.7, 5.8, and 5.9 respectively. Full reduction of the gold species in a 2% AuCl3 solution occurs after a treatment time of 10 minutes, and for a 10% AuCl3 solution, after 30 minutes. Full reduction of the 50% AuCl3 is not observed, even after a 40 minute treatment time, as both Au(O) [Au (4f $_{7/2}$) at 83.9eV] and Au(III) [Au (4f $_{7/2}$) at eV] species are still present.

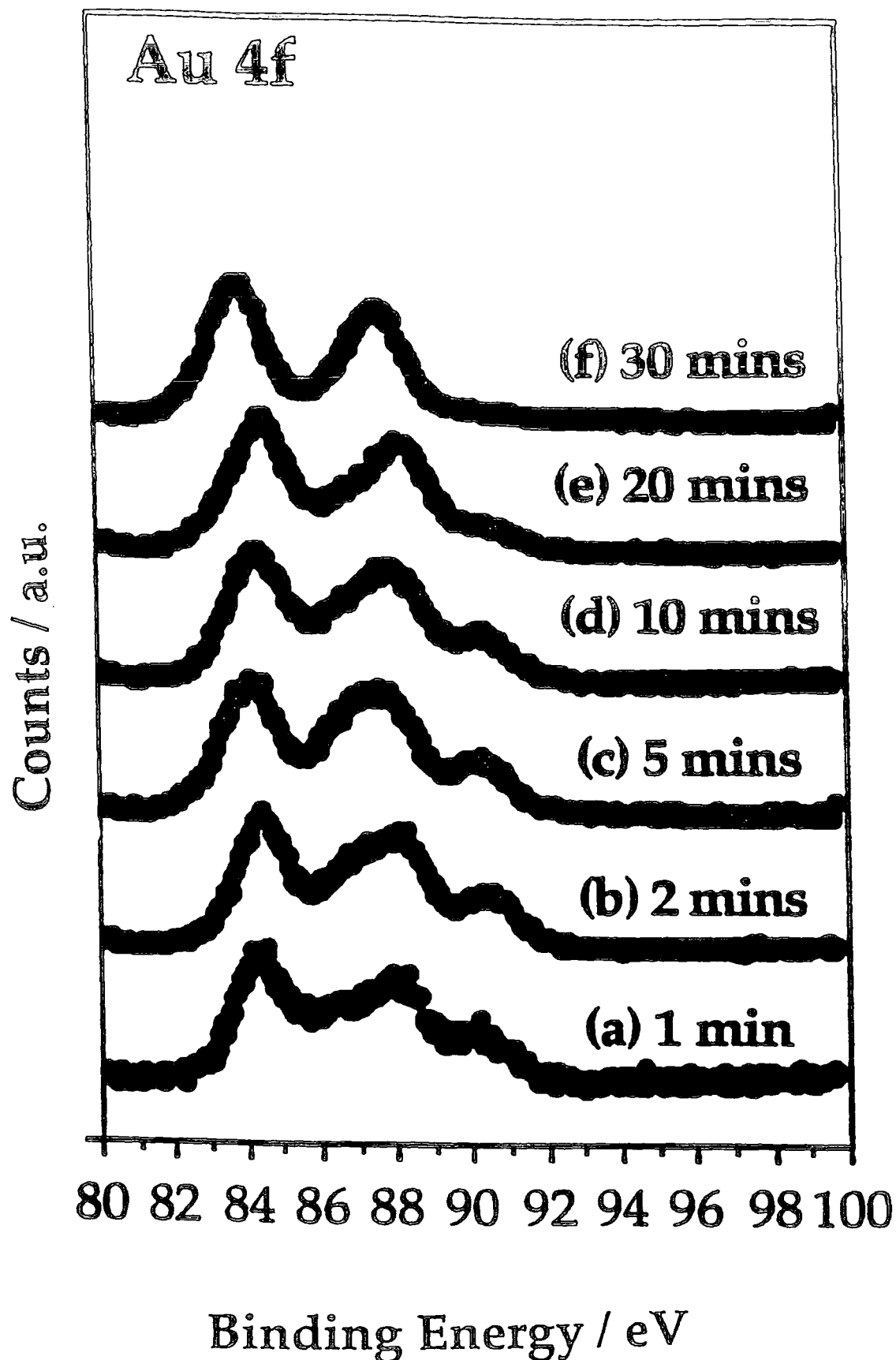Fig. 5.7 Au 4f Spectra of 2% AuCl₃ on Glass as a function of Treatment Time (Power 5 Watts)

Fig 5.8 Au 4f XPSpectra of 10% AuCl3 on Glass as a function of Treatment Time, Power of 5 Watts.
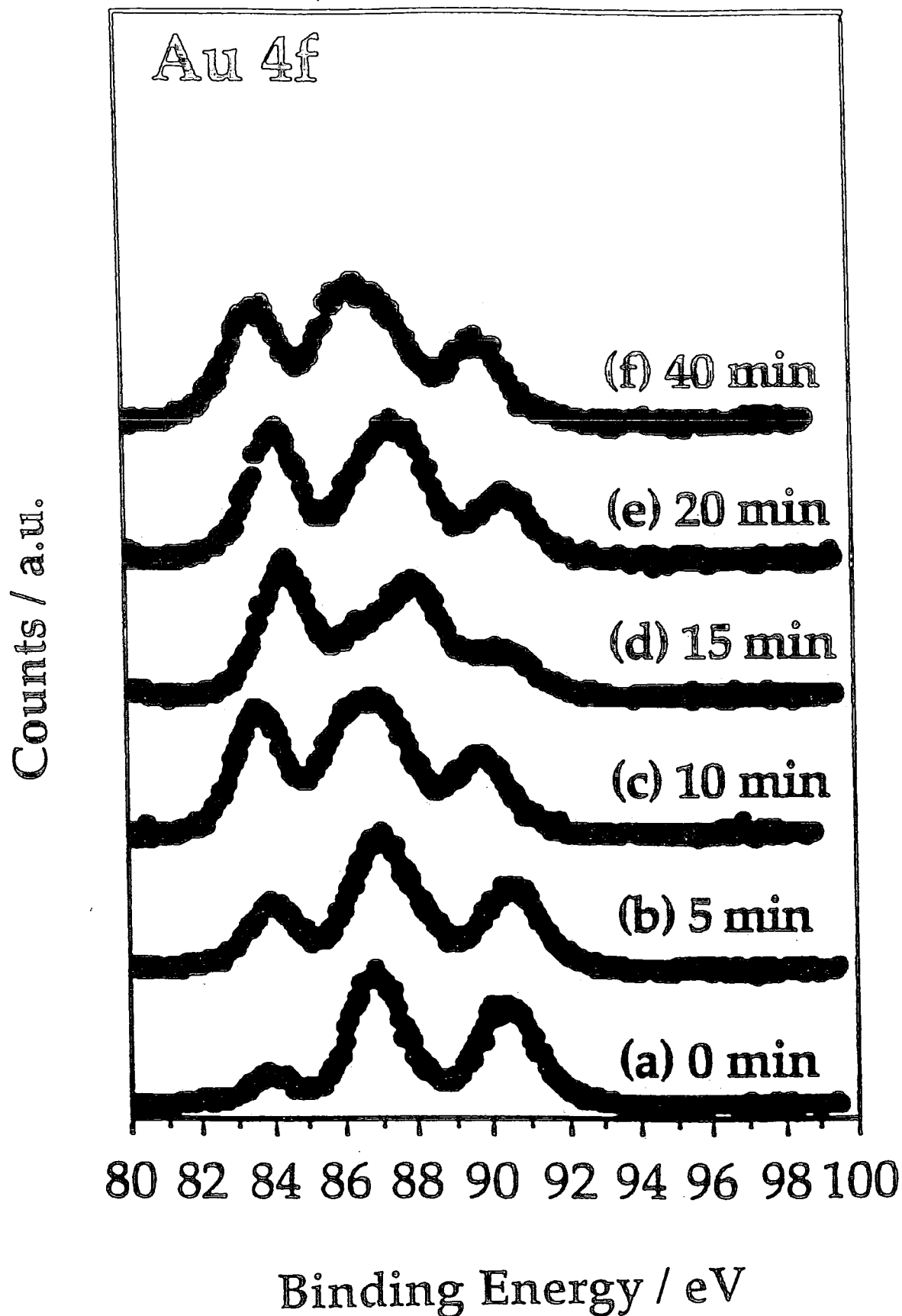
Fig. 5.9 Au 4f XP Spectra of 50% AuCl₃ on Glass as a function of Treatment Time, Power of 5 Watts

*5.3.3.3Conclusions*

A 5 Watt hydrogen plasma was used to treat 2, 10, and 50% AuCl₃ in IPA, with various treatment times.

With increasing treatment times the following trends were observed for 2, 10, and 50% (Figs 5.4, 5.5, 5.6 respectively) AuCl₃ in IPA on glass: the XPS Si (2p), and O (1s) peak areas increase, the Au (4f) areas remain roughly constant, and C (1s), and Cl (2p) peak areas decrease. These effects are most pronounced for 2% AuCl₃ solution, because this is assumed to be the least thick film. For 2% AuCl₃ in IPA, the XPS Cl (2p) peak area is reduced from 35% to 3% after 20 minutes treatment with a 5 Watt plasma, which shows that the hydrogen plasma effectively removes the chlorine species from the surface of the gold (III) chloride film. However, it seems that by effectively removing the chlorine species, voids are created in the film and the substrate is consequently exposed, as XP Si (2p) peaks were observed.

The XPS Au (4f) graphs (figs 5.7 to 5.9) show that using a 5 Watt plasma, full reduction, [Au (4f $_{7/2}$) is 83.9eV], of 2% AuCl₃ in IPA occurs after 10 minutes treament, of 10% AuCl₃ after 30 minutes, and of 50% AuCl₃ does not occur up to a treatment time of 40 minutes. This again demonstrates the fact that at short treatment times the hydrogen plasma reacts with the chlorine of the top layers of the AuCl₃ film to form a volatile hydride, and this is removed. This reaction of chlorine with hydrogen to form a volatile species, appears to be a fuction of time; as for longer treatment times, the hydrogen plasma is capable of removing the chlorine species situated at greater depth in the film.

The following deductions were made:

- With increasing treatment time, chlorine is removed from the surface of the film, and voids are left in the film, for plasma powers of 5 Watts. This is seen by the appearance of Xp Si (2p) peaks.

- The reaction of chlorine with a hydrogen plasma, to form a volatile hydride, is a function of treatment time.

### 5.3.4 Power Variation, Treatment Time 10 minutes.

A glass slide spin coated with 50% $AuCl_3$ in IPA was treated with a hydrogen plasma for 10 minutes, and the power was varied from 5 to 50 Watts.

### 5.3 .4.1 Elemental Analysis by XPS

As the power of the hydrogen plasma increases, the area of Cl (2p) decreases (see fig 5.10); for powers of 5, 10, and 50 Watts the areas of Cl (2p) are 30%, 21%, and 10% respectively. Similarly, with increasing power, the C(1s) also decreases from 30% at 10 Watts to 10% at 50 Watts. The Si (2p) and O (1s) areas, however, increase with increasing plasma powers, and for powers of 5, 10, and 50 Watts the areas of Si(2p) are 0%, 3% and 19% respectively, and the areas of O (1s) are 13% after 5 Watts and 27% after 50 Watts. The area of gold species remains relatively constant with increasing plasma powers. (fig. 5.10). The avarage standard deviationd for the analysed elements are shown in table C.

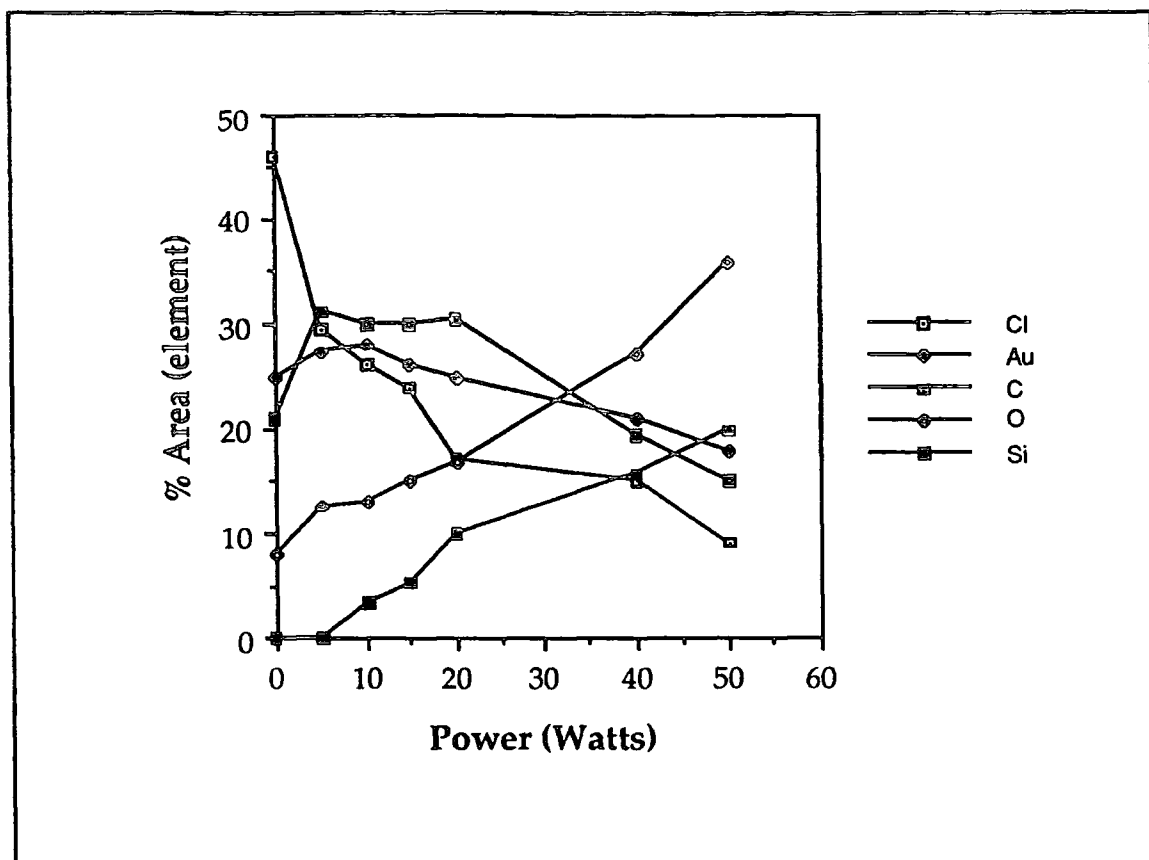| Element Conc. | Au | Cl | C | O | Si | N |
|---|---|---|---|---|---|---|
| 50% $AuCl_3$ | ± 1.9 | ± 1.7 | ± 2.5 | ± 2.4 | ± 0.9 | ± 0 |

**Table C**

**Fig. 5.10** 50% AuCl3 on Glass as a function of Power, Treatment Time of 10 mins.

*5.3.4.2 Au analysis by XPS*

The full reduction of Au(III) to Au (0) in a 50% AuCl3 solution is not observed for the above plasma treatments (fig 5.11). Even after 10 minutes treatment with a plasma of 50 Watts, both Au(0) and Au(III) are detected .
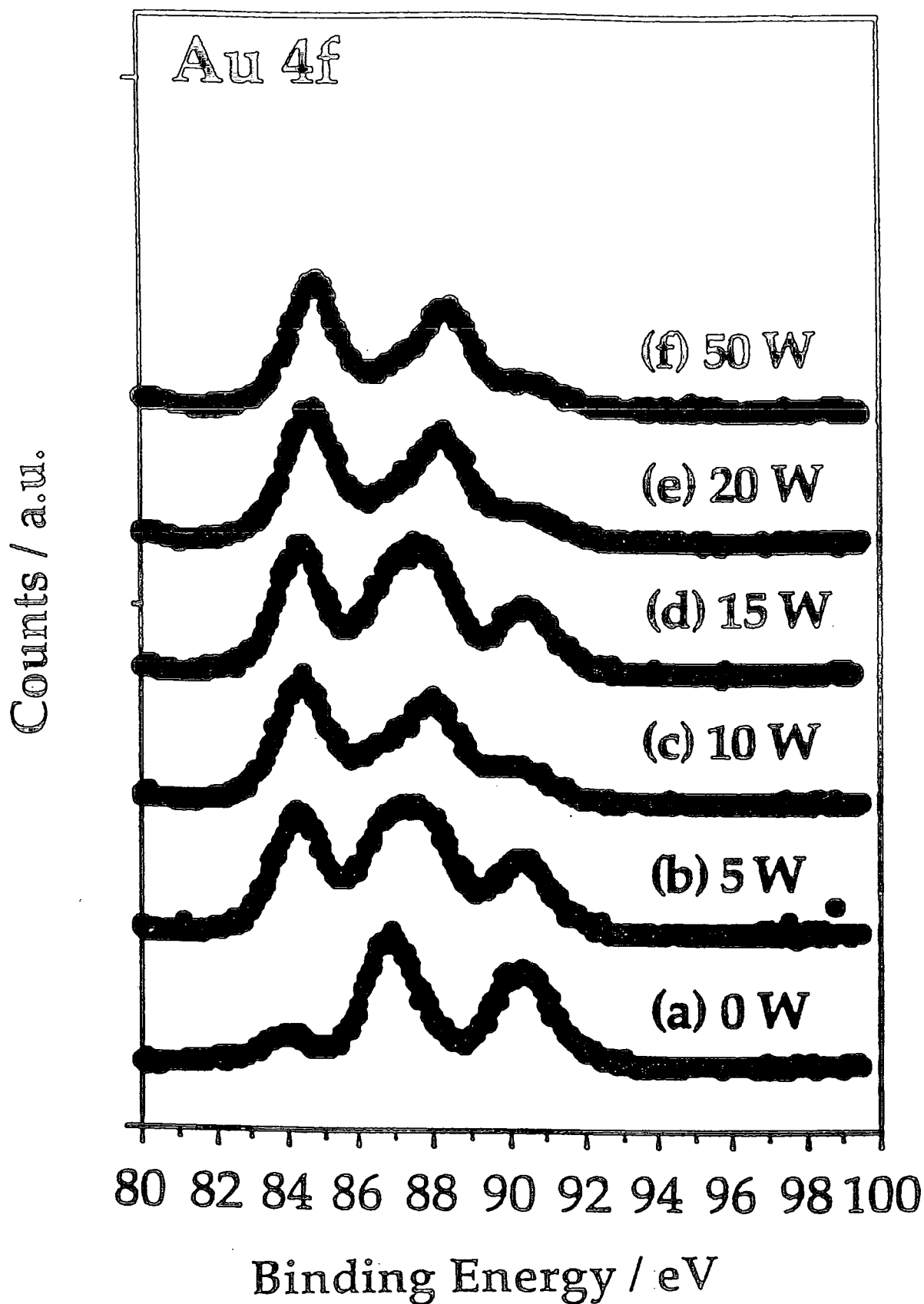
Fig. 5.11 Au 4f XP Spectra of 50% AuCl3 on Glass as a function of Power (Treatment Time of 10 mins)

*5.3.4.3 Discussion*

A glass slide spin coated with 50% $AuCl_3$ in IPA was treated with a hydrogen plasma for 10 minutes and the power was varied from 5 to 50 Watts. As the power of the hydogen plasma increased, the XPS Cl (2p), C (1s), and Au (4f) peak areas decreased, but the Si (2p) and O (1s) peak areas increased. Again, as the chlorine species are removed, the substrate is exposed. The XPS Au (4f) shows that as the power of the hydrogen plasma is increased, the more Au(III) is reduced to Au (0), however, a 50 Watt plasma, for 10 minutes, does not reduce the 50% $AuCl_3$ fully.

The following deductions were made:

. As the power of the hydrogen plasma is increased, the greater is the removal of chlorine species.

. The effect of power on the hydrogen plasma appears to be greater than the effect of treatement time on the hydrogen plasma with respect to the removal of chlorine species (compare figs 5.3 and 5.7 or 5.6 and 5.8).

## 5.4 Nylon Substrate.

### 5.4.1 Power Variation, Treatment Time 1 minute.

Hydrogen plasmas of powers of 5 to 100 Watts were used to treat 10 and 50% $AuCl_3$ wgt/volume solutions, spin coated onto nylon, over a treatment time of 1 minute.

*5.4.1.1 Elemental Analysis by XPS*

Generally for both % wt/vol solutions the following trends were observed: For increasing power the C(1s) and O(1s) areas remain roughly constant, the Cl(2p)

areas decrease and the Au(4f) areas increase. These results are shown graphically in figures 5.12 and 5.13.

With increasing power, the area of C(1s) remains roughly constant for both solutions. At powers of 10, 50 and 100 Watts the areas of C(1s) for the 10 % solution are 57, 51 and 54% respectively and for the 50% solution the areas of the C(1s) are 55, 47,and 50% respectively. The Au (4f) areas increase with increasing power for both solutions. The areas for the 10% solution are 20, 25 and 37% respectively; and for the 50% solution the areas are 27, 33, 34% respectively. Cl (2p) areas decrease with increasing power and are 12, 11, and 5% for the 10% solution and 14,8, and 7% for the 50% solution. O (1s) areas remain constant with increasing power, for both solutions. N(1s) areas drop from 7% to 0% for the 10% solution and remain at 0% for the 50% solution, with increasing power. The standard deviations of the analysed elements in figures 5.12 and 5.13 are shown in table D.

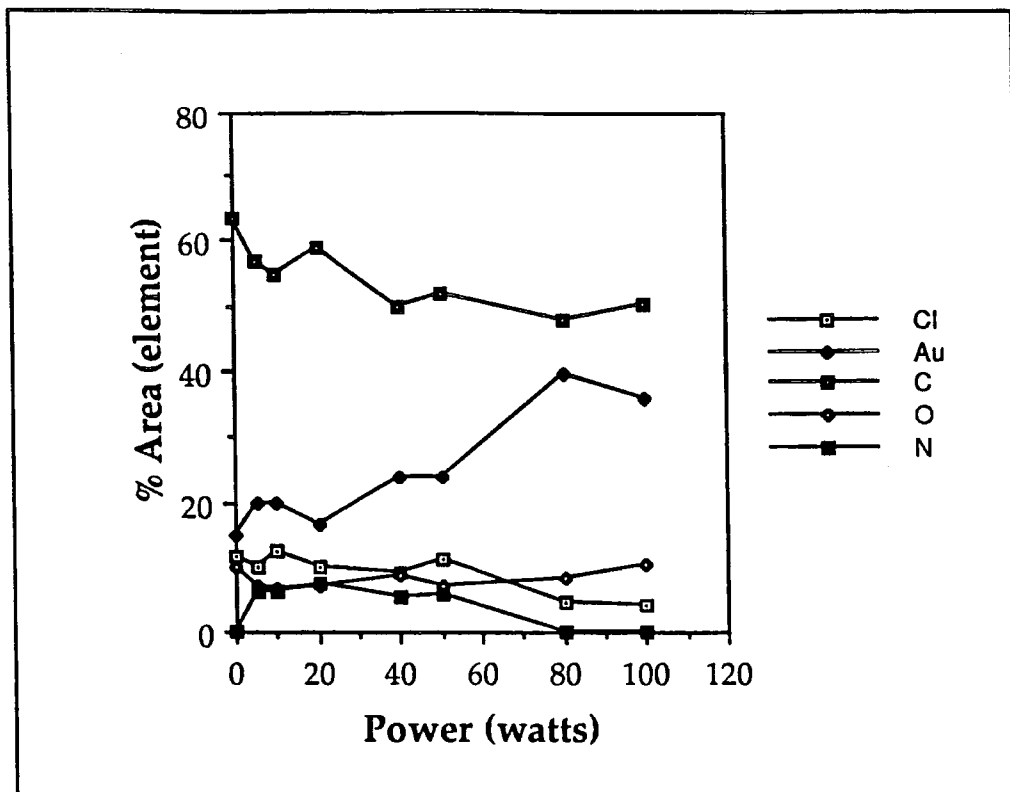| Element Conc. | Au | Cl | C | O | Si | N |
|---|---|---|---|---|---|---|
| 10% AuCl3 | ± 2.94 | ± 4.05 | ± 3.28 | ± 1.25 | ± 0 | ± 0.91 |
| 50% AuCl3 | ± 1.7 | ± 3.28 | ± 2.7 | ± 1.03 | ± 0 | ± 0.7 |

**Table D**

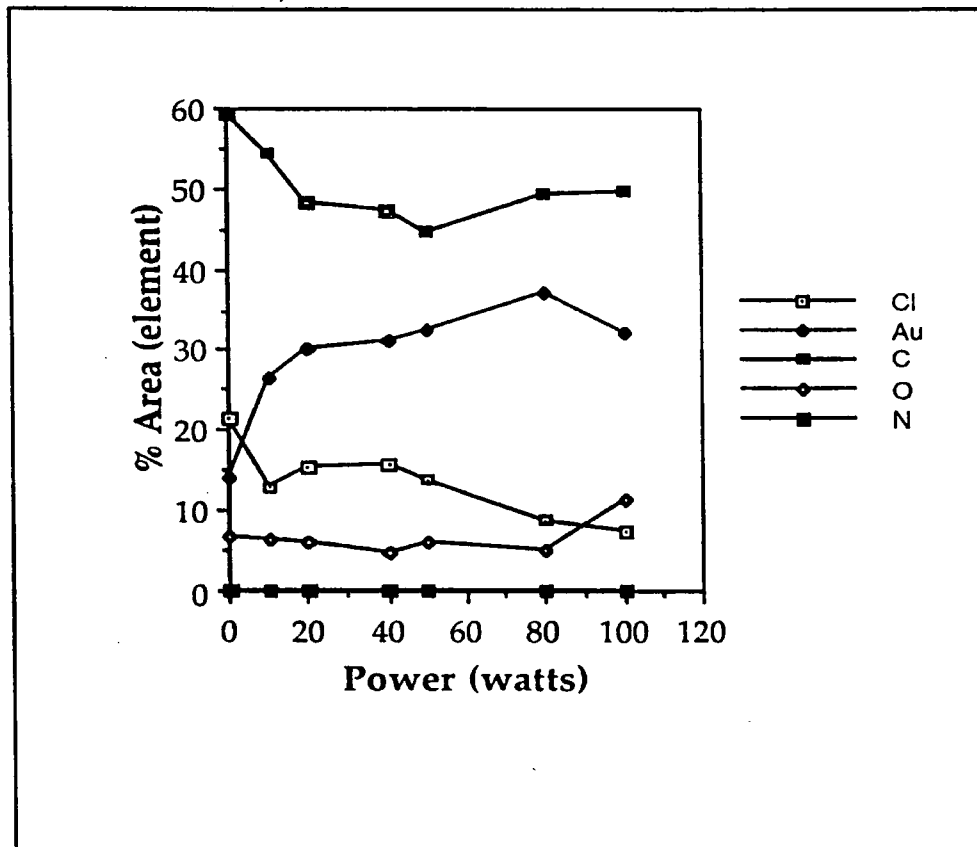**Fig. 5.12** 10% AuCl₃ on Nylon as a function of Power, (Treatment Time of 10 mins)



**Fig. 5.13** 50% AuCl₃ on Nylon as a function of Power (Treatment Time of 10 mins)

### 5.4.1.2 *Au analysis by XPS*

For treatment times of 1 minute, the Au (4f) XPS data show that full reduction of the gold species is observed for 10% $AuCl_3$ in IPA on nylon after a 40 Watt hydrogen plasma (see fig. 5.14) and for 50% $AuCl_3$ in IPA on nylon after a 80 Watt hydrogen plasma (see fig. 5.15).
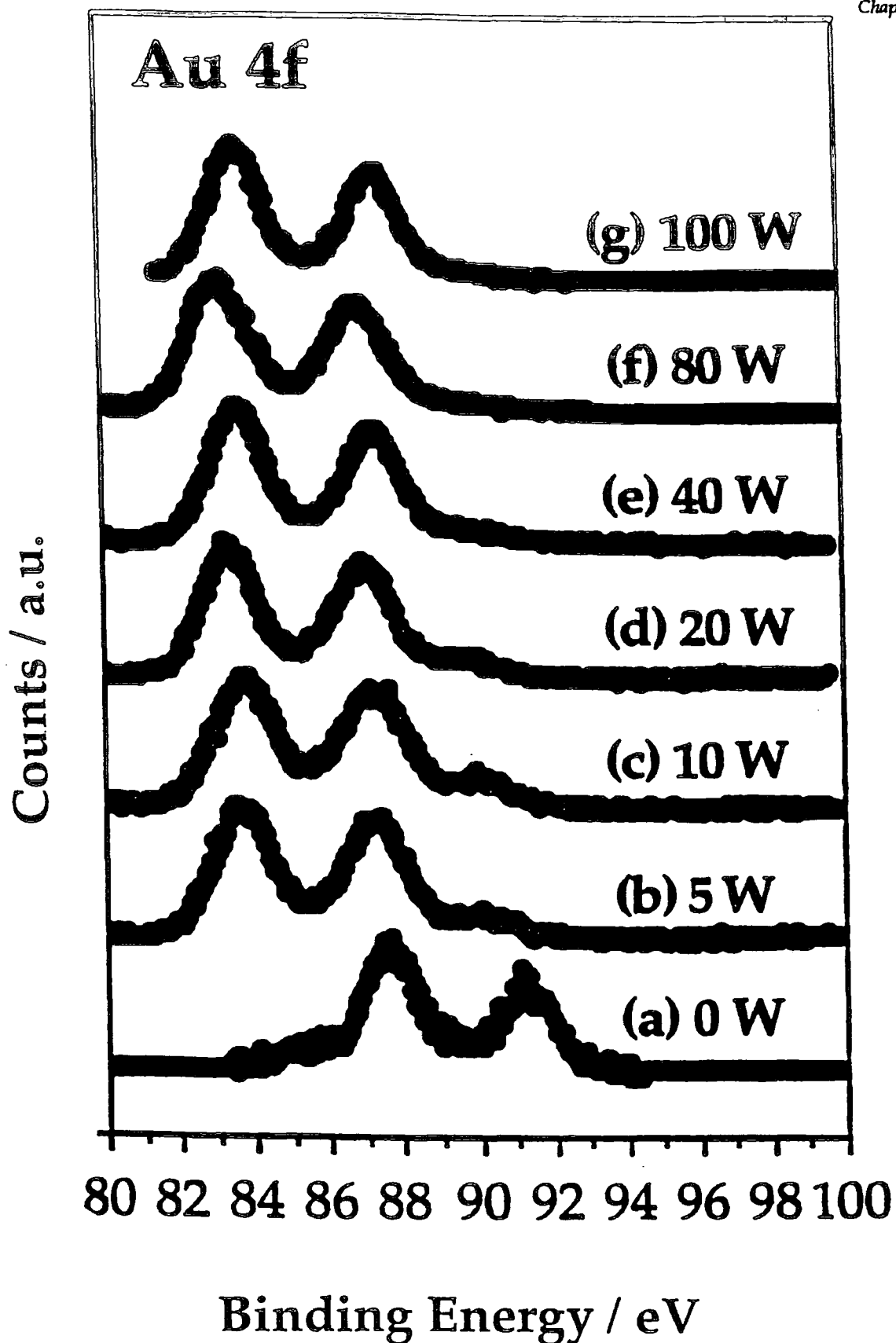
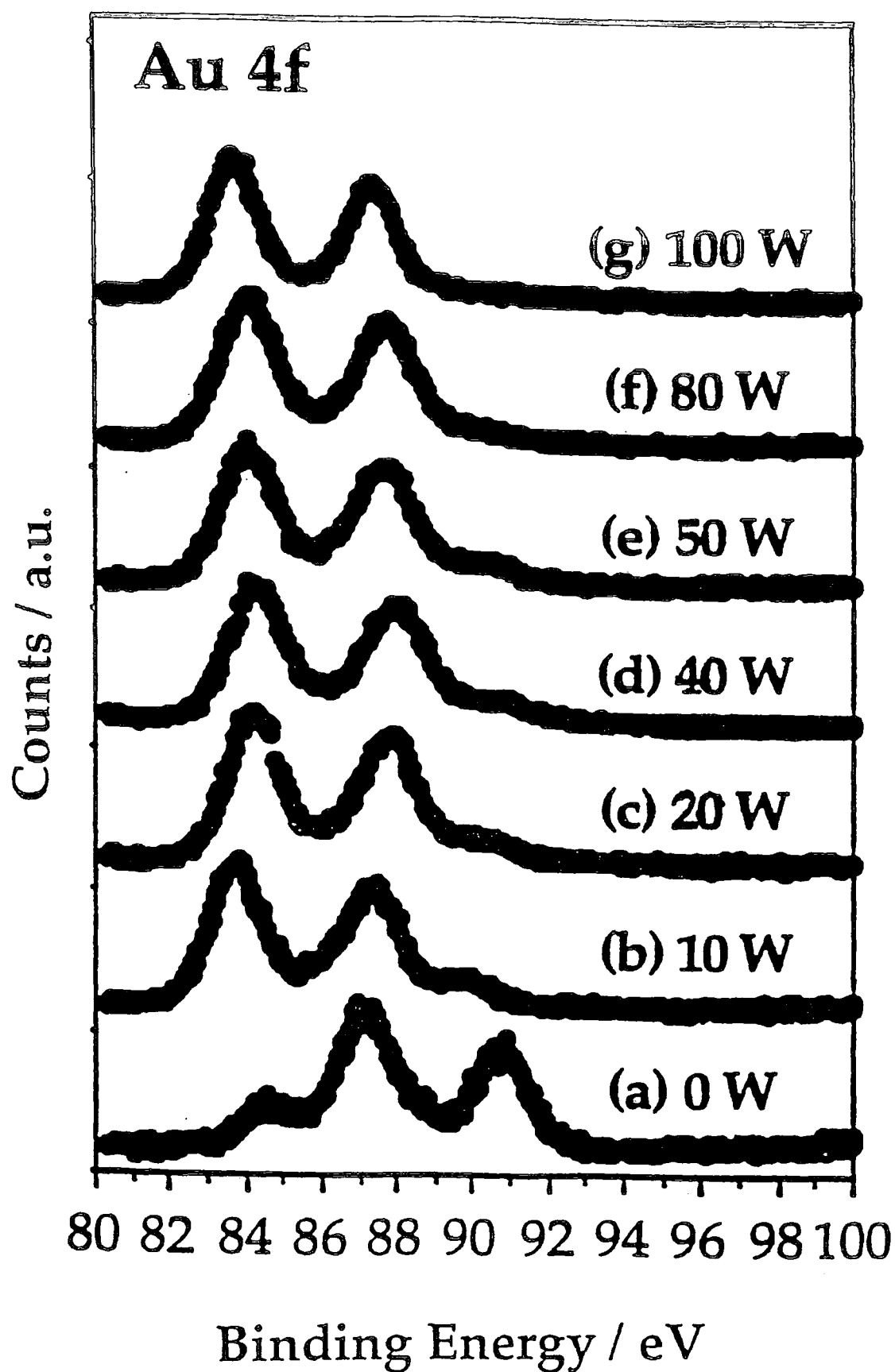Fig. 5.14 Au4f XP Spectra of 10% AuCl3 on Nylon as a function of Power, (Treatment Time of 1 min)

Fig. 5.15 Au4f XP Spectra of 50% AuCl3 on Nylon as a function of Power.

(Treatment Time of 1 min)

## 5.4.1.3 Discussion

Hydrogen plasmas of powers 5-100 Watts, and for treatment times of 1 minute, were used to treat 10 and 50 % $AuCl_3$ wgt/vol solutions, spin coated onto nylon.

With increasing power, it was observed that the XPS Au(4f) peak areas increase, the C(1s) and O (1s) areas remain roughly constant, and the Cl(2p) decrease. For the 10% $AuCl_3$, an XPS N (1s) peak was observed for hydrogen plasma powers of 5 to 50 Watts but not for 80 and 100 Watts. This means that the nylon was exposed for powers of 5 to 50 watts and then at higher powers the nylon becomes covered once again. As suggested before, as the hydrogen plasma removes chlorine, the substrate is exposed, but it appears that at high powers that the metal centres perhaps become ductile and spread across the substrate surface to give rise to uniform coverage. On treatment of the 50% $AuCl_3$ in IPA on nylon, the substrate is never exposed for the various power treatments.

The C(1s) peak areas are very high in comparison to those observed on glass. A different method was used to seal the nylon to the reaction plate in the reactor. This led to exposure of some double sided adhesive tape, and this may have reacted with the hydrogen plasma and some carbon and/or carbon products were deposited on the sample.

The XPS Au(4f) data show that full reduction of the 10% film arose after 40 Watt plasma treatment and for the 50% film after an 80 Watt treatment.

The following conclusions were drawn:
- $AuCl_3$ has better sticking probability to nylon than to glass
- At high plasma powers, the metal islands spread

## 5.5 Conclusions & Further Work

From this chapter the following conclusions were drawn: with increasing concentration, the thickness of the film increases, and the XPS C(1s) areas increase. The hydrogen plasma appears to remove some chlorine to a certain depth of the $AuCl_3$ surface. The effect of the hydrogen plasma may be limited by the diffusion of active $H^+/H\cdot$ into the inorganic film, or the hydrogen plasma reacts with the Cl species to form HCl and this remains in the film.

Future work to be done on this:

· Depth profiling to determine the depth of chlorine removal, and to identify the chlorine species below the surface layer (this may not give rise to conclusive results as relatively small differences in the binding energies of the various chlorine environments exist)

· The thickness should be measured to confirm the statement that thickness is a function of concentration.

· Different reducing gases could be used

· Different Au precursors could be used, perhaps with F ligands as these are very reactive.

From this chapter, it has been seen that both increased time and increased power affect the depth of chlorine removal by the hydrogen plasma. This could be confirmed by carrying out a depth profile study of some of the resultant films. Increased plasma power seems to have greater effect than increased treatment times.

Also, the film appears to adhere better to the nylon substrate than to a glass substrate, as for example, the nylon substrate is not exposed at all for 50% $AuCl_3$ (fig 5.10), for plasma powers of 5-100 Watts, but for 50% $AuCl_3$ on a

glass substrate, XPS Si (2p) peaks are observed even for a 5 Watt plasma of treatment time 10 minutes (see fig. 5.3).

The metal centres (gold islands) appear to become ductile and 'spread' over the substrate surface when treated with high plasma powers, to give rise to a uniform coverage. This could be confirmed by analysis using atomic force microscopy.

Finally, using a multimeter, it was observed that 50% $AuCl_3$ in IPA, when treated with a 100 Watt hydrogen plasma, gave rise to a conducting film (Resistivity of ca. 8-10 $\Omega$). More accurate conductance measurements can be carried out to optimise this aspect of the continuous gold film.

The errors on the peak areas of the elements are probably due to those already outlined in chapter 4, p.76.
In addition to these, as the spin coated films were treated with a hydrogen plasma, then there is also an error due to the reactor and power supply.

## 5.6 References

1. Fonseca, J.L.F., Phd thesis, University of Durham, 1994.
2. Ehrlich, C.D., Basford, J.A., J. Vac. Sci. Technol., A10 1 1992.

# 6 Summary

## 6.1 Introduction

## 6.2 Plasma Chemistry

## 6.3 XPS as an Analysis Tool

## 6.4 Thin Metallic Films

## 6.5 Deposition and Analysis of AuCl3 in IPA

## 6.6 Hydrogen Plasma Treatments

## 6.7 Proposed Future Experimental Work

## 6. Summary

### 6.1 Introduction

Plasmas, which are also referred to as the fourth state of matter, find more and more applications in everyday usage. One of the regions of greatest interest to plasma chemistry is that of glow discharge plasmas. One of the biggest advantages of this technique is that these plasmas can be used to modify temperature sensitive substrates.

During the last thirty years, in the electronics industry, there has been increasing interest in the use of partially ionised plasmas for the processing of surfaces. A large amount of work has been carried out on plasma etching using halogen plasmas. However, halogen plasmas cause both handling and environmental problems and as a result hydrogen plasmas are often used as a substitute.

In the work outlined in this thesis, a hydrogen plasma was generated at 0.1 torr, using an RF power supply, in order to modify the surfaces of gold (III) chloride films. It has been postulated that if hydrogen atoms will react with a material in a plasma to form a volatile compound (eg. HCl), then the surface will be modified. The aim of this work was to create a conducting gold film, by removal of the chlorine species from the original spin coated film, through use of a hydrogen plasma.

### 6.2 Plasma Chemistry

In chapter 1 of this thesis, an introduction to general plasma chemistry was given. The types of plasmas that exist, specifically glow discharge plasmas, and the types of electric fields used to generate glow discharge plasmas were discussed. The topic of surface modification using glow discharge plasmas and specifically hydrogen plasma as a surface modifier was then explained.

112

Generally, the greatest field of interest to the plasma chemist is that of glow discharge plasmas. Surface modification using glow discharge plasmas is very important in the electronics industry. A lot of work in this field has been carried out using halogen plasmas. However, due to increasing environmental and handling problems created from the use of halogen plasmas, there has been growing interest in the use of hydrogen plasmas as surface modification plasmas. It has been postulated that if hydrogen atoms react with a material in the plasma to form a volatile compound (eg. HCl) then the surface will be modified.

### 6.3 XPS as an Analysis Tool

In chapter 2, XPS as an analysis tool, the instrumentation required, and spectral interpretation was explained. Finally, examples of XP spectra from the literature were given. The elements shown in these literature examples were the elements analysed experimentally (see chapters 4 & 5) by the author.

### 6.4 Thin Metallic Films

Several methods are used to deposit thin metallic films, and these include CVD, PVD, and sol-gel techniques. The most common methods of depositing thin gold films are various PVD techniques, eg., evaporation, ion plating, and sputtering.

Discontinuous thin films have very important electrical properties and the most research in this field has been carried out on the formation of electrical properties of these films. However, complementary optical measurements have also been performed. The optical properties of these films are unique as there exists a large interface between the metallic clusters and the surrounding medium. The position and intensity of the optical absorption maximum are dependant on the metal volume fraction, the size and shape of the metallic

grains, and the effect of disorder. Several models have been proposed to explain the optical properties of discontinuous metallic films.

The electrical properties and conduction mechanism of discontinuous thin films has never been satisfactorily explained. However, several models have been proposed. The most accurate of these models is that proposed by Barr & Finney, who calculated the tunnelling between two initially neutral islands with respect to the requirement that the tunnelling excess must be able to provide the electrostatic energy. The conduction mechanism in discontinuous gold films was proposed, by Despax et al, to be temperature dependant.

### 6.5 Deposition and Analysis of AuCl3 in IPA

In this chapter, the spin coating and analysis of AuCl3 in IPA was examined. A Commax Precima Spin coating apparatus was used for the coating of the substrates. The deposited films were then characterised using a Cratos ES 200 X-ray photoelectron spectrometer with an unmonochromated source (Mg $k_{\alpha 1,2}$= 1253.6eV). The aim of the spin coating examination was to obtain uniform films of AuCl3 on both glass and nylon. In order to obtain uniform coverage of the glass and nylon substrates, two different techniques (1 & 2) of spin coating were employed.·

From the results shown in this chapter, the following techniques were proposed:

- Technique 1 was assumed to be the addition of 20 drops of 2% AuCl3 in IPA over the spin time of 60 seconds.

  Technique 2 was 6 drops of 10% or higher AuCl3 % wgt/vol solutions on the centre of the substrate, which is dried in air for 10 seconds before being spun for 20 seconds. This step is repeated three times

114

In order to understand the XPS analysis of the received $AuCl_3$ (ABCR, 99.99%), a pure gold sample (Goodfellows, 99.99%) was examined using XPS. A doublet was observed. The gold doublet arises from the removal of a 4f electron leaving the $4f_{7/2}$ and the $4f_{5/2}$ core states for which L = 3, S =1/2, and J = 5/2 or 7/2. The experimentally observed doublet had maxima at 83.9 ± 0.04 eV and 87.54 ± 0.04 eV respectively i.e. separated by 3.64 ± 0.04 eV (see fig. 4.10). The relative areas of the doublet were as A:B (see fig.4.10), 1:0.752, and the relative full widths at half maximum were as A:B, 1:1.05. The Au ($4f_{7/2}$) peak, i.e. peak A, at 83.9 eV is used as the reference point for the work discussed in this thesis.

This was then used to analyse the received $AuCl_3$. The $AuCl_3$ was dissolved in IPA, and with no further treatment, was examined by XPS. Three peaks were observed from the XPS analysis (as is shown in fig 4.10 [a]) and using a gaussian peak fitting program four peaks [Au ($4f_{7/2, 5/2}$) for both Au (0) (Peaks A & C)and Au(III) (Peaks B & D)] of maxima 84.23 ± 0.03 (A), 87.4 ± 0.02 (B), 87.6 ± 0.05 (C), and 91.9 ± 0.03 (D) eV were established to be present (shown in fig 4.11[b]). This is due to the presence of both Au(0) and Au(III) in the original sample.

## 6.6 Hydrogen Plasma Treatments

From this chapter, the following conclusions were drawn: with increasing concentration, the thickness of the film increases. The hydrogen plasma appears to remove some chlorine to a certain depth of the $AuCl_3$ surface. The effect of the hydrogen plasma may be limited by the diffusion of active $H^+/H\cdot$ into the inorganic film, or the hydrogen plasma reacts with the Cl species to form HCl and this remains in the film. This chlorine removal is a function of both plasma power and treatment time.

From this work, it has been seen that both increased time and increased power affect the depth of chlorine removal by the hydrogen plasma. This could be confirmed by carrying out a depth profile study of some of the resultant films. Increased plasma power seems to have greater effect than increased treatment times.

Also, the film appears to adhere better to the nylon substrate than to a glass substrate, as for example, the nylon substrate is not exposed at all for 50% $AuCl_3$ (see fig 5.10), for plasma powers of 5-100 Watts, but for 50% $AuCl_3$ on a glass substrate, XPS Si (2p) peaks are observed even for a 5 Watt plasma of treatment time 10 minutes (see fig. 5.3).

It apopears that the metal centres (gold islands) become ductile and 'spread' over the substrate surface when treated with high plasma powers, to give rise to a uniform coverage. This could be confirmed by analysis using atomic force microscopy.

Finally, using a multimeter, it was observed that 50% $AuCl_3$ in IPA, when treated with a 100 Watt hydrogen plasma, gave rise to a conducting film . More accurate conductance measurements can be carried out to optimise this aspect of the continuous gold film.

## 6.7 Proposed Future Experimental Work:

Based on the results from chapters 4 and 5, the author proposes that the following work should be carried out.

- Depth profiling to determine the depth of chlorine removal, and to identify the chlorine species below the surface layer.

- The thickness of the film should be measured to confirm the statement that thickness is a function of concentration.

- Different reducing gases could be used

- Different Au precursors could be used, perhaps with F ligands as these are very reactive.

- Atomic Force Microscopy could be carried out to compare the surfaces before and after hydrogen plasma treatment.

- The conductance of the resulting gold films should be examined.